University of North Dakota
UND Scholarly Commons

Theses and Dissertations | Theses, Dissertations, and Senior Projects

2008

Molecular Characterization of Dopamine Transporter Phosphorylation and Regulation

Balachandra Kumar Gorentla

Follow this and additional works at: https://commons.und.edu/theses

 Part of the Psychology Commons

Recommended Citation

Gorentla, Balachandra Kumar, "Molecular Characterization of Dopamine Transporter Phosphorylation and Regulation" (2008). *Theses and Dissertations*. 705.
https://commons.und.edu/theses/705

This Dissertation is brought to you for free and open access by the Theses, Dissertations, and Senior Projects at UND Scholarly Commons. It has been accepted for inclusion in Theses and Dissertations by an authorized administrator of UND Scholarly Commons. For more information, please contact zeineb.yousif@library.und.edu.

MOLECULAR CHARACTERIZATION OF DOPAMINE TRANSPORTER PHOSPHORYLATION AND REGULATION

By

Balachandra Kumar Gorentla
Bachelor of Science, Sri Venkateswara University, India 1995
Master of Science, Sri Venkateswara University, India 1999

A Dissertation

Submitted to the Graduate Faculty

of the

University of North Dakota

in partial fulfillment of the requirements

for the degree of

Doctor of Philosophy

Grand Forks, North Dakota
August
2008

This dissertation, submitted by Balachandra Kumar Gorentla in partial fulfillment of the requirements for the Degree of Doctor of Philosophy from the University of North Dakota, has been read by the Faculty Advisory Committee under whom the work has been done and is hereby approved.

Chairperson

This dissertation meets the standards for appearance, conforms to the style and format requirements of the Graduate School of the University of North Dakota, and is hereby approved.

Dean of the Graduate School

July 18, 2008
Date

PERMISSION

Title Molecular Characterization of Dopamine Transporter Phosphorylation and Regulation

Department Biochemistry and Molecular Biology

Degree Doctor of Philosophy

In presenting this dissertation in partial fulfillment of the requirements for a graduate degree from the University of North Dakota, I agree that the library of this University shall make it freely available for inspection. I further agree that permission for extensive copying for scholarly purposes may be granted by the professor who supervised my dissertation work or in her absence, by the chairperson of the department or the dean of the Graduate School. It is understood that any copying or publication or other use of this dissertation or part thereof for financial gain shall not be allowed without my written permission. It is also understood that due recognition shall be given to me and to the University of North Dakota in any scholarly use which may be made of any material in my dissertation.

Signature _____

Date 7/15/2008

TABLE OF CONTENTS

LIST OF FIGURES

LIST OF TABLES

ABBREVIATIONS

5-HT	5-hydroxytryptamine/serotonin
6-OHDA	6-hydroxydopamine
AD	Alzheimer's disease
ADHD	attention deficit hyperactivity disorder
AMPH	amphetamine
ANOVA	analysis of variance
BCA	Bicinchonic acid
BSA	bovine serum albumin
CaMK II	calmodulin dependent protein kinase II
CBD	chitin binding domain
CDAT	recombinantly expressed carboxy-terminus cytosolic tail domain of rat DAT
CFT	2β-carbomethoxy-3β-(4-fluorophenyl)tropane
CKII	casein kinase II
CNS	central nervous system
DA	dopamine
DAT	dopamine transporter
DAG	diacylglycerol
DOPS	1,2-Dioleoyl-sn-Glycero-3-[Phospho-L-Serine]
DMSO	dimethyl sulfoxide
DNA	deoxyribonucleic acid
DTT	dithiothreitol
EDTA	ethylene diamine tetra acetic acid
EL	extracellular loop
ERK1/2	extracellular regulated protein kinase 1/2
FRET	fluorescence resonance energy transfer
GABA	gamma-aminobutyric acid
GAT	GABA transporter
GBR 12909	1-[2-[bis(4-fluorophenyl)methoxy]ethyl]-4-3-(phenylpropyl)piperazine
GSK-3β	glycogen synthase kinase-3β
hDAT	human dopamine transporter
HEK 293 cell	human embryonic kidney -293 cells
HEPES	4-(2-hydroxyethyl)-10 piperazine ethane sulfonic acid
IL	intracellular loop
JNK2	c-Jun N-terminal kinase 2
KDa	kilodaltons
KRH	Krebs-Ringers HEPES
$LeuT_{Aa}$	leucine transporter from *aquifex aeolicus*

LLC-PK$_1$ cell	lewis lung carcinoma porcine kidney cell
MAB	monoclonal antibody
MAPK	mitogen activatated protein kianse
METH	methamphetamine
MPP^+	1-methyl-4-phenylpyridinium
MPTP	1-methyl-4-phenyl-1,2,3,6-tetrahydropyridin
NDAT	recombinantly expressed amino-terminus cytosolic tail domain of rat DAT
NE	norepinephrine
NET	norepinephrine transporter
NSS	neurotransmitter:sodium symporter
OA	okadaic acid
OAG	1-oleoyl-2-acetyl-sn-glycerol
PCR	polymerase chain reaction
PD	Parkinson's disease
PI3K	phosphatidylinositol 3-kinase
PICK1	protein interacting kinases C-kinase
PKA	cyclic AMP dependent protein kinase
PKC	protein kinase C
PKG	protein kinase G
PMA	phorbol 12-myristate 13- acetate
PP1	protein phosphatase 1
PP2A	protein phosphatase 2A
PP2B	protein phosphatase 2B
PVDF	polyvinylidene fluoride
RACK1	receptor for activated C-kinase
ROS	reaction oxygen species
rDAT	rat dopamine transporter
RTI82	3β-(p-chlorophenyl)tropane-2-β-carboxylic acid, 4`-azido-3`-iodophenylethyl ester
SDS-PAGE	sodium dodecyl sulphate-polyacrylamide gel electrophoresis
SERT	serotonin transporter
SN	substantia nigra
TH	tyrosine hydroxylase
TM	transmembrane domain
UV	ultraviolet
VTA	ventral tegmental area

ACKNOWLEDGEMENTS

I would like to start by thanking Dr.Roxanne Vaughan. She gave me a lot of support and encouragement for successful completion of my graduate study in her lab. As a mentor, Dr.Vaughan was always open for teaching and guiding critical aspects of scientific skills and for brain storming scientific discussions. I learned scientific thinking and attitude from you which made a foundation to build my career.

I would like acknowledge everyone in the department of Biochemistry and Molecular Biology for helping me to complete my graduate study. I would also like to thank friends that made in UND, especially Chandra Sekhar Bathula for spiritual and moral support. I enjoyed your friendship and I can't forget your support and help in all aspects of my stay in UND. I want to thank all of my friends out-side of UND, especially Dr.Reddy Peera Kommaddi for sharing my thoughts and helping in crucial moments. I also would like acknowledge Dr.James D Foster for helping me in the lab and out side the lab.

Finally, I want to thank my family for continuous support and encouragement in each and every aspect of my life. I am grateful forever to my parents, brothers, sister, brother-in-law for making me to belive my self. My brother Chandra Sekhar Gorentla influenced my thinking that driven me to stand sturdy in difficult times of life. I want to thank my better half and wife Aruna for believing my abilities and for encouraging me in difficult situations to strengthen

my confidence. Inspite of my late working hours, Aruna has been extremly cooperative and very patient to support my graduate study with unconditional love. Thank you all and I am forever indebted to you.

This dissertation is dedicated

to my beloved parents,

Gorentla Venkata Ramanaiah and Gorentla Rama Subbamma

ABSTRACT

The dopamine transporter (DAT) is a presynaptic membrane phosphoprotein that terminates dopaminergic synaptic transmission by clearing dopamine (DA) back into presynaptic neuron by a reuptake process. DAT is also a molecular target for psychostimulants such as cocaine, amphetamine (AMPH) and methamphetamine (METH) that increase DA synaptic levels either by blocking reuptake or by inducing DA efflux. DAT phosphorylation and transport down regulation are best demonstrated with the treatment of Protein kinase C (PKC) activators such as (phorbol 12-myristate 13- acetate) PMA. Serine(s) and threonine(s) are known to be involved in DAT phosphorylation.

Pretreatment with psychostimulant substrates such as AMPH and METH have been shown to regulate DAT phosphorylation and DA transport activity. Here we have examined the effects of DA, cocaine and various other psychoactive transport blockers on DAT phosphorylation and regulation in rDAT expressing LLC-PK$_1$ cells by using $^{32}PO_4$ metabolic labeling and [^{3}H] DA uptake assays. Pretreatment with cocaine or methylphenidate (MPH) had no effect on basal or PMA stimulated DAT phosphorylation and DA transport. GBR 12909 suppressed PMA-induced DAT phosphorylation and internalization. Treatment with DA did not affect DAT phosphorylation while inducing PKC mediated DA transport down regulation. These results provide information on the potential for endogenous and psychoactive compounds to modulate DAT

CHAPTER I

INTRODUCTION

Synaptic Transmission

Billions of neurons in the human nervous system communicate with each other to orchestrate complex behaviors, perceptions, reflexes, instincts, emotions, thinking and learning. Mostly, the communication occurs between neurons or between neuron and muscle through specialized junctions called "synapses" and the process by which one neuron communicates with other neuron is called "synaptic transmission".

Synaptic transmission is initiated with a wave of depolarization along the axon called an action potential. Because the action potential cannot be propagated directly between the cells that are separated by a synaptic cleft, chemical messengers "neurotransmitters" are employed to communicate between one cell and the next. The synaptic transmission process includes the following events, namely the fusion of neurotransmitter containing synaptic vesicles with presynaptic plasma membrane, release of neurotransmitters into synaptic cleft, activation of post synaptic receptors and sequestration of released neurotransmitters.

Neurotransmitters are synthesized in the neuronal cell body and packaged into synaptic vesicles. The packaged vesicles are vectorially directed towards the presynaptic membrane and docked to specific regions of membrane called

active zones. The docked vesicle undergoes maturation by a process called priming that enables the membrane fusion of vesicles. When an action potential reaches the nerve terminal, it induces the opening of voltage gated Ca^{2+} channels which leads to rapid influx of Ca^{2+} into the cell. This leads to a spike in local intracellular Ca^{2+} levels and triggers the membrane fusion of synaptic vesicles and results in exocytosis of neurotransmitters into the synaptic space [1-3].

The neurotransmitters released into synapse are readily available for the activation of the postsynaptic receptors that further stimulate depolarization in the postsynaptic neuron. In order to terminate synaptic transmission effectively, the released neurotransmitters must be degraded by specific enzymes or re-accumulated into the presynaptic neurons or glial cells through specific membrane transporter proteins.

The Dopaminergic System

The dopaminergic system refers to the dopaminergic neurons that synthesize and release the neurotransmitter dopamine (DA). The dopaminergic system is involved in cognition, motor activity, and reward. Disorders associated with DA are attention deficit hyperactivity disorder (ADHD), motor/movement disorders such as Parkinson disease, addiction, schizophrenia, paranoia and autism [4]. In brain, dopaminergic neurons primarily originate from three areas that include the ventral tegmental area (VTA) of the mid brain, the substantia nigra pars compacta and the arcuate nucleus of the hypothalamus.

Figure 1. The Dopaminergic System. Dopaminergic system representing the dopaminergic neurons that primarily originate from the ventral tegmental area (VTA) of mid brain, the substantia nigra pars compacta and the arcuate nucleus of the hypothalamus. Neurons from these areas project axons to many areas of brain such as the cerebral cortex especially to frontal lobes, the striatum, and the median eminence or infundibular region.

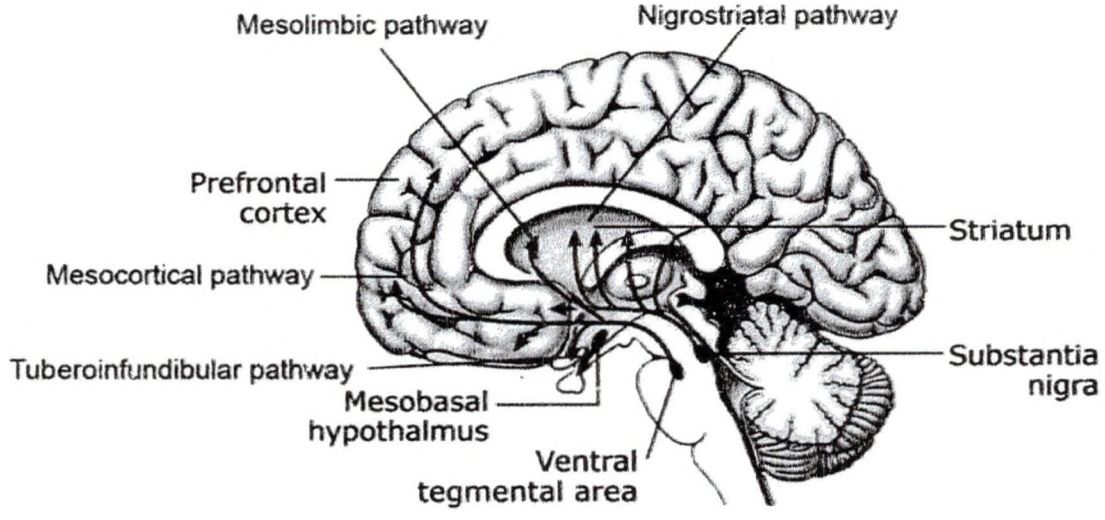

Image courtesy of Benjamin Cummings/ Pearson Education: Human physiology, 3rd edition, Figure 9.19c, with permission

Figure 1. The Dopaminergic System

Neurons from these areas project axons to many areas of brain with four neural pathways namely the Mesocortical, Mesolimbic, Nigrostriatal, and Tuberoinfundibular pathways (Figure 1). The mesocortical pathway originates from the VTA and spreads to the frontal lobes of cerebrum and is implicated in motivation and emotional response. The mesolimbic pathway links the VTA and nucleus accumbens that is located in the striatum and is associated with reward circuits. Therefore, this pathway has been implicated in drug addiction process [5]. The nigrostriatal pathway connects the substantia nigra with the striatum and is particularly important in motor control. The degeneration of these neurons leads to Parkinson disease. The tuberoinfundibular pathway contains neurons of the arcuate nucleus and projects into the median eminence (the 'infundibular region'). This pathway is known to regulate the secretion of prolactin from the anterior pituitary gland.

Metabolism of Dopamine

Dopamine, norepinephrine (NE) and epinephrine belong to the group of catecholamine neurotransmitters. Catecholamines act as neuromodulators and/or hormones in the central nervous system (CNS). NE is a biologically derived product of DA and acts as a precursor for epinephrine biosynthesis. Tyrosine, a precursor for biosynthesis of all catecholamines, is converted to 3, 4-dihydroxy-L-phenylalanine (L-DOPA) by a rate limiting enzyme tyrosine hydroxylase (TH). TH is present in all catecholamine synthesizing cells and catalyzes the addition of a hydroxyl group to the meta-position of tyrosine. The

conversion of L-DOPA to DA is the final step of the catecholamine biosynthetic pathway in dopaminergic neurons, which is catalyzed by DOPA decarboxylase.

DA is synthesized in the cytosol and is present in low concentrations (μM range). The uptake of monoamines from the cytoplasm into vesicles is mediated by vesicular monoamine transporter 2 (VMAT2) along with an ATPase-generated proton gradient. Additionally, this mechanism concentrates intra-vesicular DA up to 0.5 M. During synaptic transmission, these vesicles release DA into the synaptic cleft by exocytosis. Termination of DA synaptic transmission occurs through rapid reuptake of DA by a membrane bound carrier or transporter protein, the dopamine transporter (DAT), present on presynaptic membrane. DA is taken up into the cytosol and transported back into vesicles via VMAT2 for another round of exocytosis. During this process, some of the cytosolically located free DA molecules are catabolized into 4-Hydroxy-3-methoxy-phenylacetic acid or homovanillic acid (HVA) by monoamine oxidase (MAO) and catechol-O-methyltransferase (COMT). Accumulation of HVA in the striatum is used as a biomarker to assess the progression of PD.

The reuptake of catecholamines was first described by Axelrod *et al* (1960) with usage of radiolabeled NE [6]. Synpatosomal accumulation of radiolabeled NE in the presence of catecholamine catabolic blockers, has demonstrated the first evidence of catecholamine uptake [7]. In contrast, cocaine treatment decreased the accumulation of radioactive NE suggesting that this transport is carrier mediated event [8]. Subsequent experiments have shown that

the uptake process is Na^+ and Cl^--dependent and exhibits Michaelis-Menten saturation kinetics [6, 9].

Cloning of DAT

Until 1990, synaptosomal preparations and/or *Xenopus laevis* oocytes injected with substantia nigra mRNA were used to study DAT or other neurotransmitter transporters [10]. Kanner *et al* (1990) were the first to clone the gamma-amino butyric acid (GABA) neurotransmitter transporter 1 (GAT1/SLCA1) using the purified protein sequence and characterize GABA transport by expressing GAT1 in a heterologous system [11]. The adoption of expression cloning strategy is expedited the cloning and characterization of the norepinephrine transporter (NET/SLCA2) [12], DAT (SLCA3) [13, 14] and serotonin transporter (SERT/ SLCA4) [15]. Based on cDNA sequence homology, DAT belongs to a Na^+ and Cl^- - dependent solute carrier (SLC 6) family of plasma membrane neurotransmitter transporters that also includes GAT 1, NET, SERT, and the glycine transporter (GLYT) [16]. The SLC6 family of transporters requires Na^+ in order to generate the electrochemical gradient and to drive transport of the neurotransmitters against their concentration gradient [17, 18].

DAT Structure

DAT contains 619 amino acids in rat (rDAT) and 620 amino acids in human (hDAT). The predicted topology indicated that DAT has twelve transmembrane domains (TMs) that are connected by intracellular (ILs) and extracellular loops (ELs) and N- and C-cytosolic tail domains (Figure 2). TMs are presumed to form a pore for substrate translocation. A large extracellular loop 2

Figure 2. Schematic Diagram of rDAT. This is a predicted topological representation of rat DAT structure. The structure of rDAT contains twelve TMs, and cytosolically located N- and C-terminal tail domains. A large extracellular loop is present between TMs 3 and 4 with four glycosylation sites. Multiple serines (S), threonines (T) and tyrosines (Y) that may be involved in phosphorylation are shown in red, green and yellow respectively. The region highlighted with blue on the N-terminal cytosolic tail represents epitope 16 that was used for preparation of antibodies.

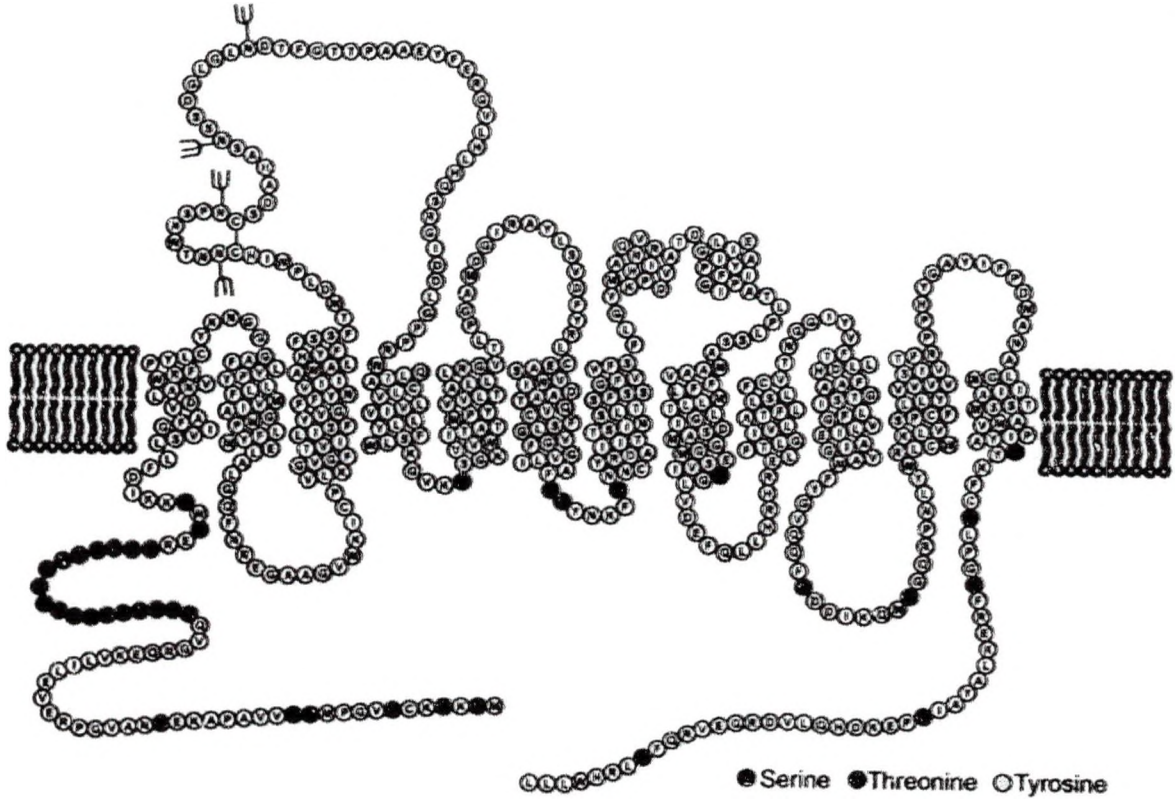

Figure 2. Schematic Diagram of rDAT.

(EL2) connects TMs 3 and 4 and its glycosylation is required for proper surface expression and DA transport activity [19]. In addition to glycosylation, DAT is also known to undergo a variety of post translational modifications including phosphorylation and ubiquitylation on cytosolic tail domains. The N- and C-terminal tail domains and ILs are rich with multiple potential phosphorylation sites [20].

Molecular Properties of DAT

A large body of evidence concluded that neurotransmitter transporters terminate synaptic transmission. DA uptake was demonstrated 35 years ago [8], but the development of specific radiolabeled ligands in 1980's [26, 27] and cloning of DAT in 1990's have expedited the current understanding of DAT physiology.

DAT transports the substrate DA inwardly against a concentration gradient using the driving force of Na^+ across the membrane. Two sodium ions and one chloride ion are co-transported along with one molecule of DA and make this process electrogenic [21] . The mechanism of DA translocation is proposed to occur through a cascade of conformational changes in DAT that allows the binding site to be alternatively accessible to extracellular or intracellular sides of the membrane [17]. This process keeps the DAT in an open conformation towards the extracellular side and in a closed conformation on the intracellular side. Binding of DA and ions to DAT induces a conformational change that results in a closed state on extracellular side and an open state on intracellular side. Following the release of DA and ions into the cytosol, DAT resets to an

open conformation on the extracellular side for a new transport cycle. In addition to forward transport, DAT can transport DA in the reverse direction (i.e., into the extracellular space) under some circumstances, such as following exposure to amphetamines [22].

Lack of three dimensional structure of DAT has limited the information about binding sites of DA, Na^+, Cl^- and transport blockers and conformations attained during substrate translocation and binding of transport blockers. Recently, Gouaux *et al* (2005) have crystallized and elucidated the structure of a leucine transporter derived from *Aquifex aeolicus* (Leu T_{Aa}) that shares ~ 20% sequence identity with DAT and other SLC6 family transporters [23]. In spite of low sequence identity with DAT and other neurotransmitter transporters, a high resolution Leu T_{Aa} crystal structure has advanced the understanding of the structural basis of the transport mechanism. TMs1 and 5 and TMs 6 and10 in Leu T_{Aa} crystal structure exist as two superimposable internal structural repeats by rotation in the plane of membrane. These superimposable internal repeats interact with one another to form a permeation pathway. During this process, TM 1 and TM 6 form the binding sites for substrate and Na^+.

Many electrophysiological studies have revealed that DAT can mediate macroscopic ionic currents, which are not stoichiometrically linked to substrate movement [21, 24-26], and is a common property of ion channels. The transport current is elicited by DA and other substrates, which can be blocked by non substrate blockers. Additionally, a tonic leak conductance generates steady-state current, which is not coupled by substrates, but can be blocked by substrates

and cocaine like drugs [25, 27]. Therefore physiological properties of DAT include the termination of neurotransmission by rapid reuptake of extracellular DA, reverse transport, and channel like properties [28].

Oligomerization of DAT

Experiments involving chemical crosslinking, mutagenesis, coimmunoprecipitation, and fluorescence resonance energy transfer (FRET) have demonstrated that DATs exist as oligomeric complexes [29-31]. The mutation of cysteine-243 in TM 4 and cysteine-306 in TM 6 results in decreased crosslinking ability of DAT suggesting that the interface of TM 4 and 6 may be involved in DAT oligomerization [31, 32]. The co-expression of non-functional cytosolic tail DAT mutant constructs with Wt DAT decreases the transport activity and surface expression of DAT. This dominant negative effect on transport activity was rescued by mutating a leucine zipper motif present in TM 2. These results indicate that the leucine zipper motif is important for oligomerization of DAT, and oligomerization is necessary for DAT surface expression and DA transport activity [29].

The substrate bound crystal structure of Leu T negates the possibility of formation of TM 4 and TM 6 interface during oligomerization, because these domains are deeply buried in this conformation. However, this interface may exist in conformations where DAT is not bound with substrates or blockers. Treatment with the substrates DA or AMPH reduced the cross linking ability of surface DAT demonstrating that substrates dissociate oligomerization of DAT [33].

Pharmacology of DAT

Dopamine is a neurochemical mediator of critical functions such as movement, emotion and reward. Abnormal levels of DA are associated with a variety of pathological conditions and pharmacological treatments. DAT is a very important target for pharmacological or recreational psychoactive drugs (Figure 3).

Psychostimulant Substrates

The term amphetamines represents both AMPH and methamphetamine (METH) which are potent psychomotor stimulants originally developed to treat asthma, sleep disorders (narcolepsy) and hyperactivity. They stimulate the CNS and sympathetic division of the peripheral nervous system and increase the synaptic levels of DA and NE. The reinforcing properties produced by amphetamines are linked to the elevation of extracellular DA levels suggesting that AMPH or its derivatives promote nonvesicular release of DA into the synapse through DAT [34-36]. AMPH is a non physiological substrate for DAT and chemically acts as a lipophilic weak base. The entry of AMPH into synaptic vesicles leads to collapse of the vesicular pH gradients followed by redistribution of DA from synaptic vesicle into the cytosol [37]. METH has been shown to produce faster and longer-lasting effects than AMPH in comparable concentrations possibly due to its higher hydrophobicity.

AMPH induced DA efflux is thought to occur by an exchange diffusion model [38]. This model is based on an alternating access model of DA uptake. In the alternating access model, binding of cargo (DA, Na^+, and Cl^-) to an

extracellularly oriented transporter induces a conformational rearrangement to an intracellularly oriented transporter. This leads to release of cargo into the cytosol, thereby completing the transport process. DA efflux induced by AMPH is believed to result from the ability of AMPH to reverse this inward transport process, in that the inward transport of AMPH by DAT increases the number of "inward-facing" transporter binding sites and thereby increases the rate of outward transport of DA through an exchange process [39]. Therefore this process increases extracellular DA levels that in turn enhances the synaptic activity of postsynaptic receptors and eventually leads to positive reinforcement. For example, Khoshbouei *et al.* (2004) [40] recently reported that DAT N-terminal phosphorylation plays a critical role in AMPH-induced DA efflux but not in DA uptake. These data suggest that AMPH-induced DA efflux mediated by the reversal of DAT is more complex than a simple exchange process [28].

Neurotoxins

In addition to psychostimulant drugs, DAT is also a target for neurotoxins that exert degenerative effects on DA systems such as the pathogenesis of Parkinson's disease. Neurotoxins such as 6-hydroxydopamine (6-OHDA) and 1-methyl-4-phenyl-1, 2, 3, 6-tetrahydropyridine (MPTP) chemically damage dopaminergic neurons *in vivo* [41, 42] and have been shown to produce Parkinson disease symptoms in animal models [43]. 6-OHDA is a hydroxylated analogue of natural substrate DA. MPTP is a contaminant produced during the synthesis of MPPP (1-methyl-4-phenyl-4-propionoxypiperidine), an opioid analgesic drug. Following entry into living organism, MPTP will be converted into

neurotoxic metabolite 1-methyl-4-phenylpyridinium (MPP^+) that produces toxic effects on cell. So MPP^+ and 6-OHDA are selectively accumulated in dopaminergic neurons through DAT and increase the formation of reactive oxygen species. Reactive oxygen species inhibit the function of mitochondrial complex I that further leads to mitochondrial dysfunction and cell death [44, 45].

Uptake Blockers

Cocaine

Cocaine is a psychostimulant drug and it produces a wide range of emotional experiences and reinforcement properties in users. Cocaine occurs naturally as an alkaloid in the leaves of coca (*Erythroxylon coca*) and has been federally classified as schedule II controlled substance drug due to its exceptional potential for abuse. Although cocaine possession, cultivation, and distribution is illegal for non-medicinal and non-government sanctioned purposes, it has been used world wide in many cultural, social and personal settings.

Cocaine is a powerful reinforcer and this property is believed to contribute to cocaine abuse and dependence [46, 47]. The reinforcement properties of cocaine have been demonstrated in humans and animal models by self administration and other behavioral techniques. Various neurochemical and neuroanatomical studies have shown that dopaminergic mesolimbocortical neurons are important for the reinforcing properties of cocaine [48]. Ligand binding studies have identified the DAT as one of the major cocaine receptors in brain [47]. The inhibitory potencies of cocaine and related compounds for DAT have shown a correlation with behavioral potencies obtained from drug

Figure 3. DAT Substrates, Neurotoxins and Psychostimulant Blockers. Representative chemical structures of (A) Psychostimulant Substrates (B) Neurotoxins (C) Psychostimulant blockers and (D) Psychoactive Therapeutic Agents.

(A)

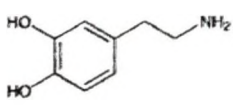

Dopamine

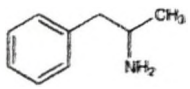

AMPH

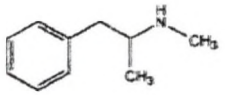

METH

(B)

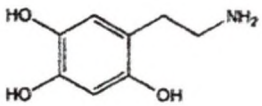

6-OHDA

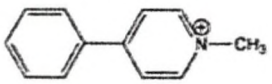

MPP+

(C)

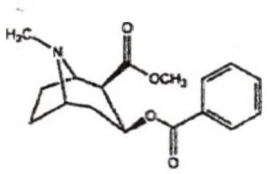

Cocaine

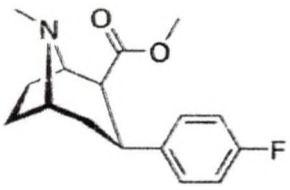

β-CFT

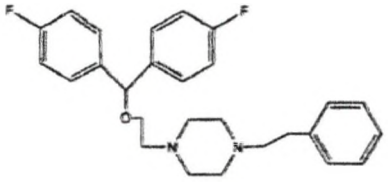

GBR 12909

(D)

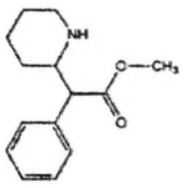

Methylphenidate

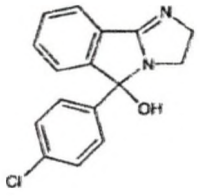

Mazindol

Figure 3. (A) DAT substrates, (B) Neurotoxins and (C, D) Psychostimulant Blockers.

reinforcement studies [47]. Additionally, microdialysis studies have shown that cocaine treatment increases extracellular DA levels in the limbic area reconfirming that DAT is major site of action for cocaine (reviewed in [46]).

GBR 12909

GBR 12909 (1-{2-[bis-(4-fluorophenyl) methoxy] ethyl]-4-(3-phenylpropyl) piperazine) is a noncompetitive, potent and selective inhibitor of DA uptake [49]. This compound was developed as a therapeutic for drug abuse to produce minimal or no euphoria, which may reduce abuse potential and dependence. GBR 12909 has been demonstrated to possess a different pharmacological and behavioral profile compared to cocaine [50]. When compared to cocaine, GBR 12909 has much higher affinity for DAT [51]. The oral administration of GBR 12909 in normal human volunteers has shown a non stimulant profile that is different from the cocaine induced profile [52]. These properties have promoted GBR 12909 for preclinical and phase I clinical trials as a potential therapeutic agent for cocaine abuse [53, 54].

Mazindol

Mazindol is a tricyclic compound and has been used as an appetite suppressant for treatment of exogenous or short term obesity and as an orphan drug for the treatment of Duchenne muscular dystrophy. It stimulates the CNS to increase heart rate and blood pressure, and decrease appetite. The mechanism of mazindol action is not known, however it act as a reuptake inhibitor for monoamine transmitters [55]. Mazindol was found to be non-addictive and it did

not produce euphoria in clinical trials [56] But in monkeys, a subset of all tested had shown the self-administration behavior [57].

Methylphenidate

Methylphenidate (MPH) is a generic therapeutic stimulant prescribed for ADHD. It is also used for daytime drowsiness symptoms of narcolepsy and chronic fatigue syndrome. MPH acts on the CNS to reduce impulsive behavior and induce attention on work and other tasks [58]. The mode of MPH action in ADHD diagnosed individuals is not well understood. MPH blocks the transport activity of DAT and NET and increases synaptic dopamine levels that in turn stimulate the under activated brain regions [59].

Regulation of DA Transport and DAT Phosphorylation

The cloning of DAT and identification of the crystal structure for a DAT homologue has provided the basis for current understanding of DAT structure and function. The cloning of DAT made it possible to characterize DA transport activity, DA efflux and mechanisms that regulate uptake or efflux. DAT functions are regulated by protein kinases, protein phosphatases, and protein- protein interactions.

Protein Kinases

The presence of multiple potential phosphorylation sites on cytosolic tails and ILs of DAT suggested that protein kinases can regulate DAT function (Figure 4). DA transport activity can be regulated by multiple signaling pathways, protein kinase A (PKA), protein kinase C (PKC), protein kinase G (PKG), calcium/calmodulin dependent protein kinase (CaMK II) and mitogen activated

Figure 4. Cytosolic Tail Domains of DAT Showing the Putative Phosphorylation Sites for Various Protein Kinases. (A) N-terminal cytosolic tail domain (B) C-terminal cytosolic tail domain of DAT showing enlarged S/T sites. Some of the S/T sites are enclosed in boxes that represent the consensus recognition motives for various protein kinases. Color of stars on the top of the box denotes the kinase specificity. (PKC = Red, PKA = Blue, CaMKII = Black, CKII = yellow, ERK1/2 = Green)

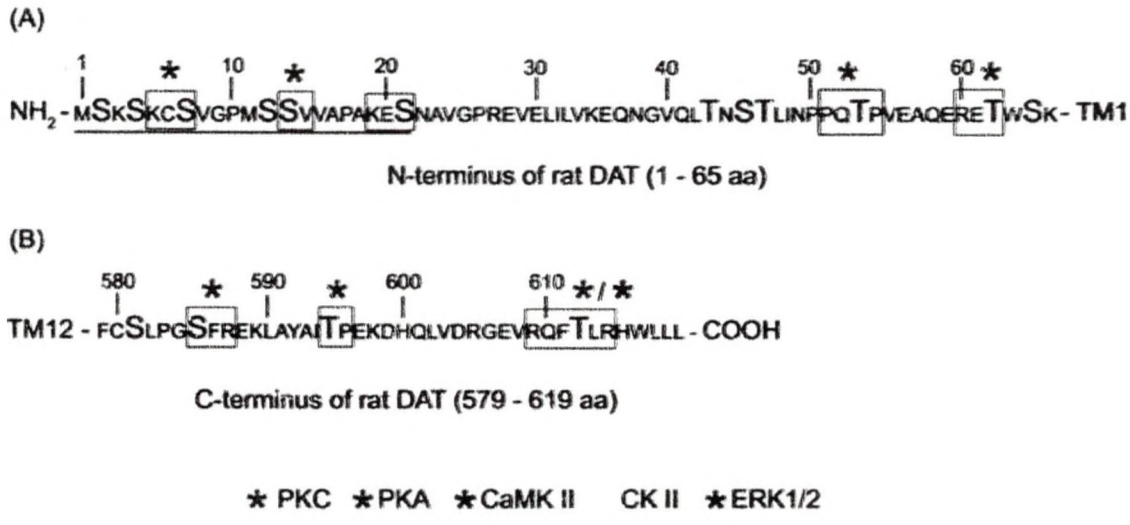

Figure 4. Cytosolic Tail Domains of DAT Showing the Putative Phosphorylation Sites.

protein kinases (MAPK's) [21, 60-62]. The down-regulation of transport activity has been well demonstrated by PKC activators in both striatal synaptosomes and heterologously expressing cells. Activation of PKC leads to decreased transport V_{max} with no change in K_m for DA. This decreased DA transport has been demonstrated to occur through trafficking dependent and independent mechanisms. The trafficking dependent mechanism involves the dynamin-dependent and clathrin-mediated endocytosis of DAT following the treatment with PKC activators leading to decreased surface expression. DATs present in detergent-resistant membrane raft populations are regulated by cholesterol dependent non-trafficking regulatory mechanisms. These studies suggest that multiple regulatory mechanisms are involved in regulation of DA transport activity.

Vaughan *et al* (1997) identified DAT phosphorylation both in rat striatum [63] and in cell lines [64] and this identification shed light on the possible role of phosphorylation in the regulation of DA transport. *In vivo* ^{32}P metabolic labeling followed by phosphoamino acid analysis of DAT has demonstrated that serine(s) (Ser) and threonine(s) (Thr) are involved in both basal and PMA stimulated DAT phosphorylation [65]. The combination of *in vitro* proteolysis followed by phospho-peptide mapping demonstrated an N-terminal cluster of Ser(s) as the major site(s) of DAT phosphorylation. The truncation of the first 21 amino acids in DAT (Δ 21) leads to the loss of DAT phosphorylation while retaining PMA induced DA transport down regulation demonstrating that N-terminal phosphorylation is not required for down-regulation of DA transport activity [66].

Various studies have shown roles for other protein kinases including PKA, CaMK II and the extracellular signal regulated kinase (ERK) family of MAPKs on DAT phosphorylation and regulation, but far less is known about their role in DAT properties compared to PKC. Treatment of cells with PKA activators such as 8-bromo-cAMP [67] and forskolin did not affect DA transport activity and DAT phosphorylation [63]. Although chemically synthesized N-terminus of DAT comprising of 1-27 aminoacid peptide has been shown act as *in vitro* substrate for CaMKII, phosphorylation sites involved in this process are not known [68]. In vivo pharmacological studies have shown that CaMKII regulates the DA transport activity [67]. *In vitro* studies have Acute treatment of synaptosomes or cells with phosphatidylinositol (PI) 3-kinase (PI3 Kinase) inhibitor decreased [^{3}H]DA uptake and DAT surface expression, presenting a role of PI3 kinase in regulation of DAT function [69].

Moron *et al* (2003) have shown that the blockade of ERK activation using MAPK kinase (MEK) inhibitors U0126 or PD98059 resulted in decreased [^{3}H] DA transport V_{max} and surface expression of DAT [70]. Further, the transient transfection of a constitutively active MEK mutant increased DA uptake. Collectively, these results suggest that the activation of ERKs regulate DAT surface expression and DA transport activity. Interestingly, MEK inhibitors suppressed basal DAT phosphorylation without affecting PMA stimulated phosphorylation [71], showing that ERK regulates the constitutive phosphorylation of DAT.

Protein Phosphatases

In addition to protein kinases, protein phosphatases are also known to affect DA transport and DAT phosphorylation. The treatment of synaptosomes with pharmacological protein phosphatase inhibitor, okadaic acid (OA) increased DAT phosphorylation and decreased DA transport activity [63]. Treatment of striatal homogenates with purified protein phosphatases 1 (PP1) and 2A (PP2A) leads to dephosphorylation of DATs [72]. These studies have suggested that DAT undergoes dephosphorylation and phosphorylation in native conditions. However the underlying mechanisms involved in this process are not known.

DAT-Protein Interactions

Increasing evidence suggests that DATs are regulated through protein-protein interactions. Over the past few years, different proteins have been identified that interact with cytosolic domains of DAT. These DAT- protein interactions were shown to play a role in trafficking, subcellular distribution, compartmentalizaiton of DAT, and DA forward and reverse transport activity. The list of interactive proteins include receptor for activated C kinase-1 (RACK1), syntaxin [73], CaMKII [68], PKC-β [74] and protein phosphatase PP2A [75]. Various methods were followed to identify these interacting proteins such as yeast two-hybrid (Y2H) system, GST pull downs, and co-immunoprecipitation. Interestingly, many of these proteins were also shown to interact with other members of SLC6 transporter family [76-79].

The C-terminal tail of DAT acts as binding partner for CaMKII and this binding interaction has been shown to play a role in AMPH-induced DA efflux

through N-terminal DAT phosphorylation [68]. The amino terminus of DAT has been reported to interact with a PKC substrate RACK1 and syntaxin, a member of the soluble N-ethylmaleimide-sensitive factor attachment protein receptor (SNARE) family [73]. The functional analysis of RACK1 binding has yet to be ascertained. Syntaxin is also shown to interact with both GAT1 and NET and negatively regulate their transport activities [78, 80]. Based on the shared protein sequence homology with NET, it can be presumed that DAT-syntaxin interaction may exert similar effects on DAT functional properties. Based on involvement of PKC in DAT functional and other properties, it can be assumed that PKC may interact with DAT. Recently; PKC-β has been shown to interact with DAT and regulate the amphetamine induced DA efflux [74].

In addition to protein kinases, protein phosphatases were also shown to regulate the DAT phosphorylation and regulation. Co-immunoprecipitation studies have shown that DAT forms a protein complex with protein phosphatase 2Ac [75] and this result suggests that protein phosphatases may regulate DAT phosphorylation or function via protein-protein interaction.

Effects of Substrates and DA Efflux

The physiological substrate DA and psychostimulant substrates AMPH and METH induce DA transport down regulation and internalization of DAT in both synaptosomes and cell lines [81-83]. In addition to transport down regulation, pretreatment with AMPH or METH, but not DA induced DA efflux through DAT. Inclusion of bisindolylmaleimide (BIM), a general PKC inhibitor [84, 85] or a PKC-β specific inhibitor LY379196 [74], blocked the AMPH- or METH-

induced transport down regulation and DA efflux suggesting that AMPH- or METH-induced down regulation or DA efflux occurs via PKC dependent mechanisms. Additionally, the treatment of cells or striatal tissue with AMPH or METH increased DAT phosphorylation.

Interestingly, the truncation of the first 22 amino acids on the DAT N-terminal tail (Δ 22) abolished METH induced DA efflux and DAT phosphorylation while not affecting the functional down regulation of DAT [85]. Additionally, the simultaneous mutation of five Ser→ alanine (Ala) (S2, S4, S7, S12, and S13) on the N-terminal tail of DAT produced an 3/A background mutant that displayed impaired DA efflux similar to Δ 22 mutant [40]. In contrast, the individual mutation of A→ aspartate (Asp) on the S/A background mutant at 7 or 12 restored the significant amount of wild type DA efflux. These results suggest that N-terminal phosphorylation possibly at S7 or S12 is essential for AMPH-induced DA efflux. CaMKII has been shown to induce DA efflux [86]. The combination of biochemical and electrophysiological studies has shown that the binding of CaMKII to the C-terminus of DAT is important for regulation of AMPH-induced DA efflux [68].

In most of these studies, psychoactive drugs were examined in isolation for their effects on DAT phosphorylation or regulation, and less has been done to examine drug effects in combination with PKC activators to investigate potential biochemical interactions of the processes.

Effects of Uptake Blockers

Compounds used to treat neurological disorders or that lead to drug addiction including cocaine, 2β-carbomethoxy-3β-(4-fluorophenyl) tropane (β-CFT), GBR 12909, mazindol, and MPH can bind to DAT and inhibit substrate transport. Various studies have examined the effects of cocaine on DAT regulation and showed conflicting results. Pretreatment of cells with cocaine had no effect on [^{3}H] DA uptake or surface expression [82, 83] while others have reported increased DAT surface expression and transport activity [87]. In contrast to psychostimulant substrates, cocaine has been reported to suppress PMA-induced DAT phosphorylation [88].

The present studies were focused on examining the effects of DA and uptake blockers such as cocaine, 2β-carbomethoxy-3β-(4-fluorophenyl) tropane (β-CFT), GBR 12909, mazindol, and MPH on PKC dependent and independent properties of DAT using rDAT expressing LLC-PK$_1$ cells. These studies are expected to identify the effects of drugs on DAT phosphorylation and DA transport activity, which potentially may be involved in differential behavioral responses that are regulated by DAT phosphorylation and drug pretreatments. These studies also compare the previously known effects of other monoamine transmitters on cognate transporter regulation or phosphorylation.

Although PMA treatment increased N-terminal DAT phosphorylation, it is not known if PKC is directly involved in this process. Additionally, the N-terminal tail of DAT contains multiple phosphorylation sites for various protein kinases, but it is not known if these protein kinases regulate the N-terminal phosphorylation.

Previous studies have shown that phosphorylation of DAT occurs on Ser(s) and Thr(s) *in vivo*; however, the sites involved in this process are not known. Therefore, the other section of present studies is designed to investigate the ability of serine/threonine protein kinases to phosphorylate a recombinantly expressed cytosolic N-terminal tail of DAT that may represent the N-terminus of *in vivo* DAT. The results of these studies will help in identifying the sites, protein kinases or protein phosphatases involved in N-terminal phosphorylation of DAT. Further, the correlation of obtained results with known *in vivo* findings will increase the understanding of DAT phosphorylation and its role in DAT function.

CHAPTER II

MATERIALS AND METHODS

Materials

Animals

Male Sprague Dawley rats (175-300 grams) were obtained from Charles River Laboratories (Wilmington, MA) and were maintained in compliance with the guidelines established by the University of North Dakota Institutional Animal Care and Use committee and the National Institutes of Health.

Reagents

Radiolabeled inorganic phosphate ($H_3[^{32}P]O_4$) and [γ-^{32}P] ATP (7000 Ci/mmol) were purchased from MP Biomedicals (Irvine, CA). [^3H] dopamine (45Ci/mmol), Protein A sepharose beads, High and Low range Rainbow molecular weight markers were obtained from GE Healthcare Life Sciences (Piscatway, NJ). (-)-Cocaine, 2β-carbomethoxy-3β-(4-fluorophenyl) tropane (β-CFT), mazindol, methylphenidate (MPH), GBR 12909, dopamine and sulpride were from Sigma-Aldrich (St.Louis, MO). PMA, Bisindolylmaleimide I (BIM), OA, OAG, PKC classical isoforms (α, βI, βII, and γ) (Specific activity for PKC isoforms: One unit is defined as the amount of enzyme that will transfer 1.0 n mol of phosphate to histone H1 per minute at 30°C, pH 7.4), PKA, PKG, CaMK II, ERK1/2, p38 kinase, JNK, GSK-3β, Akt, Cdk-5 (Specific activity: One unit is

defined as the amount of enzyme that will transfer 1.0 p mol of phosphate to the synthetic substrate GRTGRRNSI per minute at 30°C, pH 7.4), protein phosphatases (PP1, PP2A, and PP2B) (Specific activity for PP1 and PP2A: One unit is defined as the amount of enzyme that will hydrolyze 1.0 n mol of [^{32}P] inorganic phosphate from ^{32}P-labeled phosphorylase per min; specific activity for PP2B: One unit is defined as the amount of enzyme that will release 1.0 p mol of phosphate from the RII phosphopeptide substrate per min at 30°C) and Endoproteinase Asp-N were from Calbiochem/EMD Biosciences (La Jolla, CA). EZ-Link Sulfo-NHS-LC-Biotin and Immobilized Neutravidin beads were from Pierce Biotechnology (Rockford, IL). Complete Mini Protease Inhibitor was purchased from Roche Applied Science (Indianapolis, IN). IMPACT-CN kit (Intein expression vectors etc.), all restriction enzymes and modifying enzymes were obtained from New England Biolabs (Ipswitch, MA). Site directed mutagenesis QuickChange® kit was purchased from Stratagene (La Jolla, CA). Synthesized oligonucleotides were from MWG Biotech, Inc (High Point, NC). Isopropyl β-D-1-thiogalactopyranoside (IPTG) and all other fine chemicals were purchased from Sigma-Aldrich (St.Louis, MO) or Fischer Scientific (Pittsburg, PA).

Equipment

Centrifuges

The Beckman J6-MI swinging bucket rotor was used to prepare the cross-linked Protein A Sepharose beads and to pellet the cell lines. Beckman Avanti J-25, 16.250 and 25.50 rotors were used for harvesting E.coli cells for both protein and plasmid isolation purposes. Refrigerated Beckman Microfuge R or a bench

top Microfuge 18 were used for general lab procedures and immunoprecipitations.

Electrophoresis, Electroelution and Dialysis

Bio-Rad Mini-Protean III electrophoresis apparatus and Bio-Rad Mini trans blot electrophoresis transfer cell were used for SDS-PAGE gel electrophoresis and protein transfers, respectively. Gibco/BRL Life Technologies 250 EX power supply was used to control electrophoresis and protein transfer.

Phosphorylated proteins were electroeluted from gel-slices using Bio-Rad electroeluter Model 422 containing 3.5 kDa filter membranes. Electroeluted proteins or recombinantly expressed proteins were dialyzed using Pierce Slide A-Lyzer® 10 kDa or 2 kDa Cassettes respectively.

TLC electrophoresis

Hunter Thin Layer Peptide Mapping Electrophoresis System, CE (HTLE-7002) was used for two dimensional phosphoamino acid analysis.

Spectroscopy

A Beckman DU 640 spectrophotometer was used to quantify plasmid DNA and Molecular Devices Spectra Max 190 plate reader was used to quantify protein using the Bicinchonic acid (BCA) method. Radioactive incorporation in phosphorylated protein samples and in dopamine uptake assays was analyzed using Packard 1900 CA or Beckman LS6500 liquid scintillation counters.

Cell Culture, Molecular Biology and Miscellaneous

Mammalian cell lines were maintained in Nuair 2700-30 water-jacketed CO_2 incubator and handled in sterile Nuair Class II type A/B3 laminar flow hood.

A Mastercycler personal thermal cycler from Eppendorf was used for all Polymerase Chain Reaction (PCR) experiments. Bio-Rad Gel Dryer Model 583 was used to dry the SDS-PAGE gels.

Methods

Metabolic Phosphorylation of DAT

LLC-PK$_1$ Cells Expressing rDAT

Prior to labeling the rDAT expressing LLC-PK$_1$ cells, cells were preincubated in phosphate free medium for 30 min. $H_3[^{32}P]O_4$ was added to a final concentration of 0.5 mCi/ml and incubated for 2 h at 37°C. Test compounds were applied to cells for 30 min. PMA treatments to cells were performed as positive controls in parallel. Cells were washed three times with 1 ml of ice cold sucrose phosphate buffer (SP) consisting of 0.32 M sucrose and 10 mM sodium phosphate, pH 7.4, and lysed on ice for 15 min with 500 µl RIPA buffer. Lysates were centrifuged at 20,000 × g for 20 min at 4°C. The resultant supernatant was again centrifuged at 100,000 × g for 1 h. The supernatant was collected and immunoprecipitated with DAT specific antibodies. The immunoprecipitates were separated by SDS-PAGE and phosphorylated DATs were detected by autoradiography. Equal exposure times were followed for all autoradiographs to compare and analyze the phosphorylation intensities.

Rat Striatum

Male Sprague-Dawley rats (175-300 g) were decapitated and the striata were rapidly removed and weighed. The tissue was sliced into 350 µm slices using a McElvain Tissue Chopper, and equivalent amounts of tissue (4-8 slices)

were placed into wells of a 12-well culture plate containing oxygenated Krebs-bicarbonate buffer (KBB) consisting of 25 mM $NaHCO_3$, 125 mM NaCl, 5 mM KCl, 1.5 mM $CaCl_2$, 5 mM $MgSO_4$, and 10 mM glucose, pH 7.3. Slices were preincubated for 30 min at 30°C, with shaking at 105 rpm, followed by exchange with fresh buffer containing 1 mCi/ml $H_3[^{32}P]O_4$, and continued incubation with shaking at 30°C for 90-120 min. Oxygen (95% O_2, 5% CO_2) was gently blown across the top of the plate during the incubation, and test compounds were added for the final 30 min. Test compounds (OA, and OAG) were dissolved at high concentrations in dimethyl sulfoxide (DMSO) followed by dilution in the incubation mixture to a final DMSO concentration of 0.1%. At the end of labeling, tissue slices were transferred to a microcentrifuge tube and centrifuged at 4°C at 800 × g for 4 min. The supernatant fractions were removed, and 1 ml of ice-cold KBB was added to the slices. The tissue was disrupted by four passages through a 26-gauge needle; samples were centrifuged at 10,000 × g for 10 min at 4°C, and the supernatant fractions were removed from the sedimented membranes. For analyzing the DAT phosphorylation, the sedimented membranes were solubilized with 0.5% SDS sample buffer (60 mM Tris pH 6.9, 0.5% SDS, 10% Glycerol, 100 mM DTT) at 50 mg/ml original wet weight. The samples were centrifuged at 20,000 × g for 30 min to remove the insoluble material and soluble fraction was used for immunoprecipitation with DAT antibody 16 followed by SDS-PAGE and autoradiography. For *in situ* proteolysis sedimented membranes were resuspended in 50 mM Tris-HCl, pH 8.0, at 50 mg/ml original wet weight.

[^{3}H] DA Uptake Assay

Dopamine uptake assays were performed in rDAT expressing LLC-PK_1 cells. Cells were washed twice with 1 ml of Krebs-Ringer HEPES (KRH) buffer (25 mM HEPES, 125 mM NaCl, 4.8 mM KCl, 1.2 mM KH_2PO_4, 1.3 mM $CaCl_2$, 1.2 mM $MgSO_4$, 5.6 mM glucose, pH 7.4). Triplicate wells were pretreated at 37°C for 30 min or other indicated times with 1 ml KRH containing vehicle, DA, drugs, BIM, or PMA prior to assay for transport. Test compounds (DA, (−)-cocaine, β-CFT, mazindol, MPH) were prepared in deionized water, GBR 12909 was solubilized in ethanol and diluted with buffer, and PMA and BIM were prepared at high concentration in DMSO followed by dilution to a final DMSO concentration of 0.1–0.5%. For these initial experiments, saturating concentrations of uptake blockers were used. At the end of the pretreatments, cells were placed on ice to minimize potential reversal of treatment effects and rapidly washed three times with 1 ml ice-cold KRH to remove the drugs prior to assay for DA transport. Uptake was initiated by adding 10 µl of a 100× DA stock solution to bring the final concentrations of [^{3}H] DA to 10 nM and total DA to 3 µM. 100 µM (−)-cocaine was used to determine Non-specific uptake and was subtracted from total uptake values to obtain the specific uptake. Uptake assays were carried out at 37°C for 8 min and terminated by rapidly washing the wells three times with 1 ml ice-cold KRH. Cells were solubilized in 500 µl of RIPA buffer consisting of 1% Triton X-100, 1% sodium deoxycholate, 0.1% SDS, 150 mM NaCl, 10 mM sodium phosphate, 2 mM EDTA, 50 mM sodium fluoride, 0.2 mM sodium vanadate, 1 µM okadaic acid and one Complete Mini® Protease

Inhibitor Cocktail. Lysates were measured for incorporated radioactivity using a Packard 1900CA liquid scintillation counter at 62% efficiency.

Photoaffinity Labeling

Wild type rDAT expressing LLC-PK_1 cells were split into 6 well plates and were grown to 90-95% of confluence. Cells were washed twice with ice-cold KRH buffer and incubated with 5nM [^{125}I] RTI82 radioactive ligand, cocaine analogue on ice for 1h. Following the incubation, the lid of petri-dish was removed and the cells were exposed to UV light (254 nm) for 45 sec. Cells were washed with ice-cold KRH two times and solubilized with 500µl of RIPA containing Complete Mini® Protease Inhibitor Cocktail. The cell lysate was centrifuged at 20,000 × g for 30 min at 4°C. The soluble fraction extract was immunoprecipitated and used as a control for metabolic phosphorylation experiments.

Recombinant Cloning of Cytosolic Tails of DAT

Fusion protein expression plasmids pTYB2 or pTYB12 obtained from NEB were used to clone and express DAT cytosolic tail fusion proteins in E.coli. These plasmids allowed fusion of tag consisting of the intein and the chitin binding domain (CBD), to either the C-terminus (pTYB2) or the N-terminus (pTYB12) of the target protein. In the presence of thiols, such as DTT, the intein undergoes specific self-cleavage which releases the target protein from the chitin-bound intein tag. Customized oligonucleotide primers containing restriction sites were designed and obtained from MWG biotech to amplify the open reading frame encoding the rat N-terminal cytosolic tail (NDAT) (amino acids 1–65) and

C-terminal cytosolic tail (CDAT) (amino acids 579–619) domains of DAT using PCR.

Cloning of NDAT

The open reading frame sequence of ~210 nucleotides corresponding to NDAT were amplified from the cDNA sequence of rDAT using sense primer 5`-GTCCATATGAGTAAGAGCAAATGCTCCG-3` (containing Nde I site) and antisense primer 5`-CAGCCCGGGCTTGCTCCAGGTCTCCCGCTCT-3` (containing Sma I site). The amplified sequence was purified and the identity of the sequence was verified by DNA sequencing (Alpha Biolabs, CA) and was subcloned into pTYB2 plasmid that produces an N-terminal tag to NDAT after expression. 2 µg of amplified PCR product or 250 ng of pTYB1 plasmid was subjected to sequential double digestion, first with 10U of Sma I at 25°C for 3 h and then with 10U of Nde I at 37°C in NEB buffer 4 overnight. After completion of the reaction, the pTYB2 plasmid mixture was dephosphorylated using 5U of Antarctic phosphatase (NEB) at 37°C to prevent the recircularization of the plasmid. The reaction products of both samples were purified using Min-Elute purification kit and eluted into DNase free water. Ligation was performed by adding 1:3 molar ratios of linearized pTYB2 plasmid and PCR product to the ligation reaction mixture consisting of ligation buffer and 10U of T4 DNA ligase at 16°C overnight. Nova Blue™ (Novagen) competent cells were transformed with 2 µl of ligation reaction mix and were grown on LB agar petri-dishes containing 100 µg/ml of carbenecillin overnight at 37°C to screen for recombinant plasmid. The putative colonies were randomly selected and regrown in LB medium overnight

to prepare plasmids as described below. The integration of insert and identity of the sequence of the purified plasmid was verified by DNA sequencing. The recombinant plasmid (NDAT-pTYB1) was used to transform the T7 express® E. coli cells (NEB) to express the fusion protein.

Cloning of CDAT

The open reading frame sequence of ~135 nucleotides corresponding to CDAT were amplified from the cDNA sequence of rDAT using sense primer 5`-GTACAGAATGCTTTCTGCAGCCTGCCGGGGT-3` (Bsm I) and antisense primer 5`-GGGCCCCTCGAGTTACAGCAACAGCCAGTGACGC-3` (Xho I). The amplified product was purified and the identity of the sequence was verified by DNA sequencing (Alpha Biolabs, CA) and was subcloned into pTYB12 plasmid that produces a C-terminal tag to CDAT after expression. 2 µg of amplified PCR product or 250 ng of pTYB12 plasmid was subjected to sequential double digestion, first with 20U of Bsm I at 65°C for 4h and then with 10U of Xho I at 37°C in NEB buffer 2 and 100 µg/ml of BSA overnight. After completion of the reaction, pTYB12 plasmid mixture was dephosphorylated using 5U of Antarctic phosphatase (NEB) at 37°C to prevent the recircularization of the plasmid. The reaction products of both samples were purified using Min-Elute purification kit and eluted into DNase free water. Ligation was performed by adding 1:10 molar ratios of linearized pTYB12 plasmid and PCR product to the ligation reaction mixture consisting of ligation buffer and 10U of T4 DNA ligase at 16°C overnight. Nova Blue™ competent cells were transformed with 2 µl of ligation reaction mix and were grown on LB agar petri-dishes containing 100 µg/ml of carbenecillin

overnight to screen for recombinant plasmid. The putative colonies were randomly selected and sub-cultured in LB medium overnight to prepare the plasmid as described below. The integration of insert and the identity of the sequence of the purified plasmids were verified by DNA sequencing. The recombinant plasmid (CDAT-pTYB12) was used to transform the T7 express™ E. coli cells (NEB) to express the fusion protein.

Site-directed Mutagenesis

Mutant NDAT or rDAT expressing constructs containing threonine (T) substituted to alanine (A) were produced from pTYB2-NDAT and pcDNA- rDAT constructs using the Stratagene QuikChange® kit (La Jolla, CA). The oligonucleotide primers utilized to mutate codons were designed by using "The QuikChange® Primer Design Program" (http://www.stratagene.com) and synthesized by MWG Biotech. The QuikChange mutagenesis reaction was performed by sequential addition of reaction components mentioned below in Table 1 and by PCR. The PCR parameters were programmed in a thermocycler machine as mentioned in Table 2. Following the PCR reaction, 10U of Dpn I was added to the reaction mix and incubated at 37°C for 1 h to digest the template DNA. Nova Blue™ competent cells were transformed with 2 µl of reaction mix and grown on LB agar petri-dishes containing 100 µg/ml of carbenecillin overnight. Transformed bacterial colonies were randomly selected and sub-cultured in LB medium overnight to prepare the plasmid as described below. The purified plasmids were sequenced for accuracy of mutagenesis (Alpha biolabs,

CA), and were used to transform or transfect T7 express™ E.coli as described below.

Table 1. Quick Change® Reaction Mixture

Vol (µl)	Reagent
5	10X Reaction buffer (100 mM KCl, 100 mM $(NH_4)_2SO_4$, 200 mM Tris-HCl pH8.8, 20 mM $MgSO_4$, 1% Triton®, 1mg/ml nuclease-free BSA)
20	Template DNA (5ng/µl)
1.25	Forward oligonucleotide primer (125ng)
1.25	Reverse oligonucleotide primer (125ng)
1	dNTP mix
21.5	Nuclease free water
50	Final Volume

Table 2. Quick Change® Thermal Cycling Parameters

Segment	Cycles	Temperature	Time
1	1	95°C	30 sec
2	16	95°C 55°C 68°C	30sec 1min 8min

Bacterial Transformation and Plasmid Preparation

Nova Blue™ singles (Calbiochem) and T7 express™ competent cells (NEB) aliquots were transformed with 1-2 µl of plasmid DNA or ligation mix or PCR mix according the standard procedures described by the manufacturer. The LB agar petri-dish containing 100 µg/ml of carbenecillin was spread with transformed bacterial suspension and was incubated at 37°C overnight.

Transformed bacterial colonies were randomly selected from the LB agar petri-dish and were sub-cultured in glucose M9Y medium supplemented with 100 µg/ml of carbenecillin at 30°C in a shaking incubator at 200 rpm for ≥ 16 h. The bacterial cells were harvested from medium by centrifugation at 5000 × g for

10min at 4°C. The plasmid was isolated by using Pure Yield® plasmid Midi prep system (Promega) or GenElute™ Plasmid Miniprep Kit (Sigma). The isolated plasmid was electrophoresed on a 1% agarose gel containing 0.5 µg/ml ethidium bromide and separated plasmids were visualized by using GrabIT annotating grabber 2.04.6 (UVP Inc, Upland, CA). The quality and quantity of plasmid DNA was assessed using Beckman DU 640 spectrophotometer. The following formula was used to calculate conc. of DNA; [DNA µg/ml] = A_{260} (50) (dilution factor).

Expression and Purification of NDAT or CDAT

To express NDAT- CBD or CDAT-CBD intein fusion protein, E.coli T7 express™ (NEB) cells were transformed with pTYB2-NDAT or CDAT-pTYB12 respectively and colonies were selected on LB agar plate containing 50 µg/ml of carbenecillin. The transformed bacterial colony was inoculated in LB medium containing 50 µg/ml of carbenecillin and grown to an $O.D_{600}$ of 0.8 at 37°C. Fusion protein expression was induced with 0.5 mM isopropyl β-D-1-thiogalactopyranoside (IPTG) for 16 h at 16°C. The bacterial culture was centrifuged at 5000 × g for 10 min at 4°C to harvest cells. The bacterial pellet was resuspended with ice cold lysis buffer (50 mM Tris, 150 mM NaCl, 0.05% Triton X-100 and one Complete Mini® protease inhibitor Cocktail tablet) and the suspension was subjected to French press (16000lb/ $inch^2$) to prepare a crude extract. The crude extract was centrifuged at 20,000 × g for 30 min to separate the soluble supernatant fraction from cell debris.

The soluble fraction of lysate was passed through a 2 ml bed volume of chitin column resin that composed of chitin coated agarose beads (NEB).

Stringent washings were performed with 20 bed volumes of column buffer (50 mM Tris, 500 mM NaCl, 1 mM EDTA) to enrich the fusion protein on column. The target proteins NDAT or CDAT were released from fusion tags by incubating the column with 3 bed volumes of the cleavage buffer (50 mM of DTT in column buffer) for 40 h at 4°C. Following the incubation, the elution fractions were collected and resolved by SDS-PAGE followed by commassie staining or immunoblot to verify the on column cleavage of target proteins. The eluted NDAT or CDAT fragment was dialyzed against 20 mM MOPS to remove DTT.

In Vitro Phosphorylation Assays

PKC Classical Isoforms

1.5 µg of purified NDAT or 7.5 µg of histones was incubated in a reaction mixture consisting of 20 mM MOPS pH 7.4, DOPS (40 µg/ml), DAG (7.6 µg/ml), 5 mM $MgCl_2$, 300 µM $CaCl_2$, 40 µM ATP and 0.22 U of PKC isoforms (α, βI, βII, and γ). These reactions were initiated by adding 12 µCi of [γ-^{32}P] ATP and incubated at 30°C for 30 min. 100 mM EDTA was used to terminate reactions. Histones were used as a positive control to test the kinase specificity.

CaMK II

1.5 µg of purified NDAT was incubated in a reaction mixture consisting of 20 mM MOPS pH 7.4, 2.4 µM calmodulin, 5 mM $MgCl_2$, 300 µM $CaCl_2$, 40 µM ATP and 100 U of CaMK II. These reactions were initiated by adding 12 µCi of [γ-^{32}P] ATP and incubated at 30°C for 30 min. 100 mM EDTA was used to terminate this reaction. Myelin basic protein was used as a positive control to test the kinase specificity.

PKA

1.5 µg of purified NDAT was incubated in a reaction mixture consisting of 20 mM MOPS pH 7.4, 5 mM $MgCl_2$, 300 µM $CaCl_2$, 40 µM ATP and 1250 U of PKA. These reactions were initiated by adding 12 µCi of [γ-^{32}P] ATP and incubated at 30°C for 30 min. 100 mM EDTA was used to terminate the reaction. Histones were used as a positive control to test the kinase specificity.

PKG

1.5 µg of purified NDAT was incubated in a reaction mixture consisting of 20 mM MOPS pH 7.4, 10 µM 8-Br cGMP, 5 mM $MgCl_2$, 300 µM $CaCl_2$, 40 µM ATP and 5000 U of PKG. These reactions were initiated by adding 12 µCi of [γ-^{32}P] ATP and incubated at 30°C for 30 min. 100 mM EDTA was used to terminate the reaction. Histones were used as a positive control to test the kinase specificity.

ERK1/2, Akt, Cdk-5, p38, and GSK-3β

1.5 µg of purified NDAT or CDAT was incubated in a reaction mixture consisting of 20 mM MOPS pH 7.4, 5 mM $MgCl_2$, 300 µM $CaCl_2$, 40 µM ATP and 10,000 U of GSK-3β or 100 U of activated ERK1 or ERK2. These reactions were initiated by adding 12 µCi of [γ-^{32}P] ATP and incubated at 30°C for 30 min. 100 mM EDTA was used to terminate the reactions. Myelin basic protein was used as a positive control to test the kinase specificity.

CK II

1.5 µg of purified NDAT was incubated in a reaction mixture consisting of 20 mM MOPS pH 7.4, KCl, 5 mM $MgCl_2$, 300 µM $CaCl_2$, 40 µM ATP and 1000U

casein kinase II. These reactions were initiated by adding 12 µCi of [γ-^{32}P] ATP and incubated at 30°C for 30 min. 100 mM EDTA was used to terminate the reactions. Calmodulin (CaM) was used as a positive control to test the kinase specificity.

In Vitro Dephosphorylation Assays

In vitro phosphcrylated NDAT samples were subjected to immunoprecipitation using rabbit polyclonal antibody 16 generated against rDAT N-terminal amino acids 42-59 followed by dephosphorylation as described below.

PP1 and PP2A

In vitro dephosphorylation assay was performed using immunoprecipitated complexes in a reaction mixture consisting of 20 mM MOPS pH 7.4, 200 µM $MnCl_2$, 5 mM DTT, 100 µM EDTA, 0.2% BSA and 2.5 U of protein phosphatase 1 or 0.02U of PP2A. Parallel experiments were perfor. ed with *in vivo* [^{32}P] metabolically labeled rDAT.

PP 2B

In vitro dephosphorylation assay was performed on immunoprecipitated complexes in a reaction mixture consisting of 20 mM MOPS pH 7.4, 200 µM $MnCl_2$, 5 mM DTT, 0.2% BSA and 500U of PP2B at 30°C for 2 h. The assays were supplemented with 1 µM calmodulin and 1 mM $CaCl_2$ 5 min before initiating the reaction.

Cell Surface Biotinylation

LLC-PK_1 cells expressing rDATs plated in 6 well plates and grown until they attained 70-80% confluence. Cells were washed twice with KRH and treated

with vehicle or test compounds (PMA, GBR 12909) at 37°C for 30 min, then were washed twice with ice-cold PBS containing 0.1 mM $CaCl_2$ and 1 mM $MgCl_2$ (PBS/Ca/Mg) and treated with EZ-Link® Sulfo-NHS-LC-Biotin (1 mg/ml in PBS/Ca/Mg) two times on ice for 35 min each. The reaction was quenched by incubating the cells twice for 20 min with 1 ml of 100 mM glycine in PBS/Ca/Mg at 4°C. Cells were washed with 1ml of PBS/Ca/Mg and lysed with RIPA buffer containing protease inhibitor for 30 min on ice with constant shaking. The lysates were centrifuged at 20,000 × *g* for 20 min at 4°C and equal amounts of protein were used for affinity binding with 50 µl of 50% Immobilized Neutravidin beads (Pierce) for 1h at room temperature to separate biotinylated and non-biotinylated proteins. The unbound non-biotinylated fractions were collected and beads were washed three times with RIPA buffer. Biotinylated proteins were eluted from the beads with 50 µl Laemmli sample buffer for 3 min at 95°C. Samples were subjected to SDS-PAGE, followed by transfer to PVDF membranes and immunoblotting for DAT using a highly specific DAT monoclonal antibody [89].

In Situ Proteolysis

Striatal membrane suspensions labeled with ^{32}P were treated with 10 µg/ml of endoproteinase asp-N for 60 min, at 22°C. Following proteolysis, membranes were centrifuged at 10,000 × g for 10 min at 4°C and supernatants were transferred to fresh tubes. The sedimented membranes were washed with 1ml of KBB and solubilized with 0.5% SDS sample buffer (50 mg/ml). To remove the insoluble material, samples were centrifuged at 20000 × g for 30 min. The

soluble fraction was subjected to immunoprecipitation with DAT polyclonal antibody 16 followed by electrophoresis and autoradiography.

Immunoprecipitation, Electrophoresis and Autoradiography

$^{32}PO_4$-labeled cell lysates or *in vitro* phosphorylated reaction mixtures were immunoprecipitated with rabbit polyclonal antiserum 16 generated against rDAT N-terminal amino acids 42–59 [63]. For peptide blocking experiments, diluted antiserum was preincubated with 50 µg/ml peptide 16 prior to addition of the sample. Immunoprecipitates were eluted with Laemli sample buffer (62.5 mM Tris-HCl, pH 6.8, 20% glycerol, 2% SDS, 5% β-mercaptoethanol, and 0.01% bromophenol blue) and were electrophoresed on 4-20% or 10-20% gradient SDS polyacrylamide gels with high or low range Rainbow molecular mass standards. The electrophoresed gels were dried and subjected to autoradiography using Kodak Biomax X-ray or Hyperfilm MP film. In all metabolic labeling experiments, a parallel set of cells were photoaffinity labeled with the cocaine analog [^{125}I] RTI82 [90] and their lysates were subjected to immunoprecipitation and electrophoresis to confirm the extraction and electrophoretic mobility of ^{32}P labeled DAT. Molecular Analyst software (Bio-Rad) was used to scan and quantify the autoradiograph regions of 100-110 kDa containing $^{32}PO_4$-labeled DAT [64, 85]. Phosphorylation intensities of treated samples were expressed as percent of the basal phosphorylation level, which was defined as 100% ± SE of triplicate values.

Electroelution and Dialysis

Phosphorylated and immunoprecipitated striatal DATs or NDATs were separated on 4-20% or 10-20% gradient tris-glycine gels by SDS-PAGE. The gels were dried at 80°C and at 25psi for 4-6 h and exposed to Hyperfilm MP for 12-24 h. By comparing the autoradiographic image, the labeled bands at ~80 kDa or ~7 kDa correspond to striatal DAT or NDAT respectively were excised from gels and rehydrated with SDS-PAGE running buffer. The rehydrated gel slices were subjected to electroelution using 3.5 kDa membrane cut-off at 10 mA/ tube for 6 h. The electroelutes were dialyzed using SlideA-Lyzer™ (Pierce) 10 kDa or 2 kDa cut-off cassettes against distilled water with at least three changes over 24 h. The dialysate was concentrated to ~100 µl and subjected to acetone precipitation of proteins.

Acetone Precipitation of Proteins

Three-four volumes of -20°C stored acetone was added to phosphorylated rDATs or NDATs followed by thorough mixing. The samples were stored at -20°C for at least 2 h and then centrifuged at 15000 × g for 10 min at 4°C. The supernatant was discarded and the protein pellets were air dried for 15 min at room temperature. Acetone precipitated protein pellets were used for phosphoaminoacid analysis.

Phosphoamino Acid Analysis

Phosphoamino acid analysis was performed using the method of Boyle *et al.* (1991) [91]. Metabolically labeled striatal DATs or *in vitro* phosphorylated NDAT samples were immunoprecipitated with polyclonal antiserum 16, and

electrophoresed on 10-20% gradient gels. After drying and autoradiography, the region of the gel containing phosphorylated striatal DAT or NDAT was excised, and the protein was eluted in to SDS-PAGE running buffer. Eluted samples were dialyzed against distilled water. Phosphorylated DATs or NDATs were precipitated from dialysate using standard acetone mediated protein precipitation procedures. The precipitated DAT or NDAT samples were acid hydrolyzed using 5.7M HCl for 1 h at 110°C. Unlabeled phosphoamino acid standards (Ser(P), Thr(P), and Tyr(P)) (1 mg/ml) were dissolved in pH 1.9 buffer (acetic acid 7.8%, formic acid 2.5%) at 1:15 dilution and added to the unknowns. Samples were spotted onto cellulose thin layer plates and electrophoresed using a Hunter thin layer electrophoresis unit at 1.5 kV for 35 min at pH 1.9 (acetic acid 7.8%, formic acid 2.5%) in the first dimension and at 1.3 kV for 20 min at pH 3.5 (pyridine 0.5%, acetic acid 5%) in the second dimension. Standards were visualized with ninhydrin, and the plates were subjected to autoradiography for 1-3 weeks.

Immunoblot Analysis

Cell lysates or immunoprecipitated DATs were electrophoresed on 4-20% or 10-20% gradient Tris-glycine SDS polyacrylamide gels at 150 volts and 30 mA for 1 h to separate the proteins. Following electrophoresis, proteins were electrophoretically transferred to 0.45 µm polyvinylidene difluoride (PVDF) membranes. Membranes were washed two times with distilled water and blocked with 3% BSA prepared in 10 mM phosphate-buffered saline (PBS), pH 7.4 overnight. Membranes were probed with a highly specific DAT monoclonal antibody diluted 1:1000 in 3% BSA, 10 mM PBS, pH 7.4 for 1 h at room

temperature. Blots were washed 3 times with 0.1% tween, 10 mM PBS, pH 7.4 and then incubated for 1 h at room temperature with goat anti-rabbit IgG-linked alkaline phosphatase conjugate diluted 1:5000 in a 3% BSA, 10 mM PBS solution. After extensive washing, blots were developed using alkaline phosphatase chemiluminiscent substrate Immun-Star™ (Bio-Rad) or colorimetric substrate 5-bromo-4-chloro-3-indolyl phosphate/nitro blue tetrazolium (NBT/BCIP) for 5-15 min. Colorimetrically developed blots were dried, scanned and quantified with Molecular Analyst software (Bio-Rad). Blots developed with chemiluminiscent substrates were visualized and images captured using a Lumi-Imager (Mannheim Boehringer). Immunoreactive band intensities were determined using LumiAnalyst software and data were analyzed with Prism 3 software.

Statistical Calculations and Graphs

Normalized phosphorylation values or [^{3}H] DA uptake values from multiple experiments were averaged for statistical analysis by analysis of variance (ANOVA) or student t-test and graphed using Prism 3.0 software (Graphpad Software, Sandiego CA).

CHAPTER III

RESULTS

Effects of Uptake Blockers on DAT Phosphorylation

Cocaine and β-CFT Treatment

To examine the effects of uptake blockers on DAT phosphorylation, rDAT expressing LLC-PK_1 cells were metabolically labeled with ^{32}P and treated with vehicle or 1 μM PMA in the presence or absence of 10 μM (−)-cocaine. $^{32}PO_4$ incorporated DATs were immunoprecipitated and analyzed by SDS-PAGE followed by autoradiography (Figure. 5, left). The cells treated with vehicle displayed a basal level of constitutive phosphorylation on DATs (100 ± 3%) that is defined as 100% for comparison with the phosphorylation levels obtained under experimental conditions. Phosphorylation was stimulated to approximately two-fold by PMA (215 ± 9% of basal, $p < 0.001$), as previously reported [64, 85]. The addition of cocaine during the 30 min vehicle or PMA treatment had no discernable effect on the level of either constitutive phosphorylation (98 ± 12% of basal; $p > 0.05$ relative to basal) or PMA-stimulated DAT phosphorylation (177 ± 24% of basal; $p < 0.01$ relative to basal, $p > 0.05$ relative to PMA). As similar set of studies were performed using high affinity cocaine analog β-CFT and the results are shown in Figure. 5, right. In these experiments PMA stimulated DAT phosphorylation levels were 184 ± 22% of basal ($p < 0.01$ relative to basal), while 1 μM β-CFT alone had no effect on constitutive

Figure 5. Cocaine and β-CFT Do not Affect Basal or PMA-Stimulated DAT Phosphorylation. rDAT LLC-PK_1 cells were metabolically labeled with ^{32}P and treated with or without 10 μM (−)-cocaine, 1 μM β-CFT or 1 μM PMA as indicated for 30 min followed by immunoprecipitation, SDS-PAGE and autoradiography of DAT. Upper panel: autoradiographs of representative experiments; lanes correspond to treatments indicated directly below on histogram. Lower panel: summary of DAT phosphorylation levels relative to basal (means ± SE of four independent experiments for cocaine and three independent experiments for β-CFT, performed in triplicate). *$p < 0.05$ relative to basal; **$p < 0.01$ relative to basal; ***$p < 0.001$ relative to basal; ANOVA

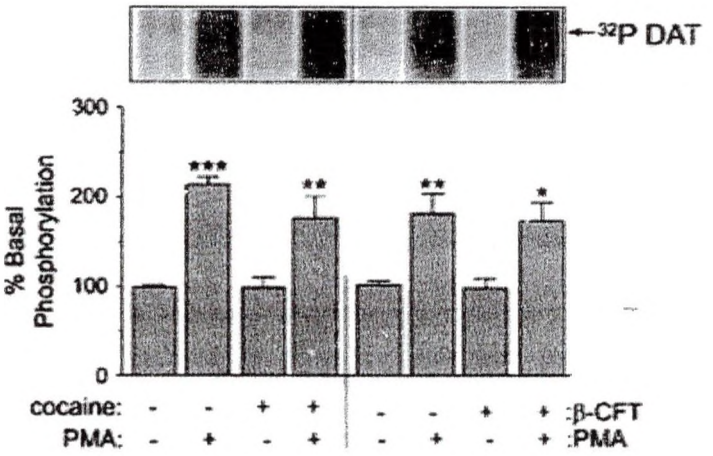

Figure 5. Cocaine and β-CFT Do not Affect Basal or PMA-Stimulated DAT Phosphorylation.

Gorentla, B.K. and R.A. Vaughan. Neuropharmacology, 2005 **49**(6):p. 759-68.

phosphorylation (100 ± 10%, $p > 0.05$ relative to basal) or PMA-stimulated phosphorylation (174 ± 21% of basal; $p < 0.05$ relative to basal, $p > 0.05$ relative to PMA).

Shorter PMA treatment times were performed using the same combinations of drug and PMA treatments for 5 and 10 min (Figure. 6) to determine if cocaine effects are transient. In these experiments PMA-stimulated DAT phosphorylation to 178 ± 9% and 284 ± 33% of basal by 5 and 10 min respectively ($p < 0.05$ and $p < 0.001$ relative to basal). Addition of cocaine during 5 or 10 min vehicle or PMA treatments did not show any difference in the levels of constitutive phosphorylation (99 ± 8% and 108 ± 8% of basal, both $p > 0.05$ relative to basal) or PMA-stimulated phosphorylation respectively (210 ± 36% and 301 ± 25% of basal at 5 min and 10 min, $p < 0.01$ and $p < 0.001$ relative to basal; both $p > 0.05$ relative to matching PMA treatment time).

Mazindol, MPH or GBR 12909 Treatments

We then extended the above studies to different classes of DA uptake blockers by examining the effects of mazindol, MPH, and GBR 12909. Mazindol (Mazanor®) is a drug used clinically to treat obesity, which has been classified as an appetite suppressant and has been shown to exhibit similar behavioral and pharmacological effects as cocaine. Cells treated with Mazindol produced a similar DAT phosphorylation profile as cocaine produced in this study. In these experiments constitutive and PMA stimulated phosphorylation values were 100 ± 5% and 257 ± 34%, respectively (PMA value $p < 0.01$ relative to basal). The addition of 1 µM mazindol did not affect constitutive phosphorylation

Figure 6. Cocaine Does not Affect Basal or PMA-Stimulated DAT Phosphorylation at Shorter Time Points. rDAT LLC-PK1 cells were metabolically labeled with ^{32}P and treated with or without 10 μM (−)-cocaine or 1 μM PMA for 5 or 10 min as indicated, followed by immunoprecipitation, SDS-PAGE and autoradiography of DAT. DAT phosphorylation levels were quantified by densitometry and results shown are the means ± SE of two independent experiments performed in triplicate. *$p < 0.05$ relative to basal; **$p < 0.01$ relative to basal; ***$p < 0.001$ relative to basal; ANOVA.

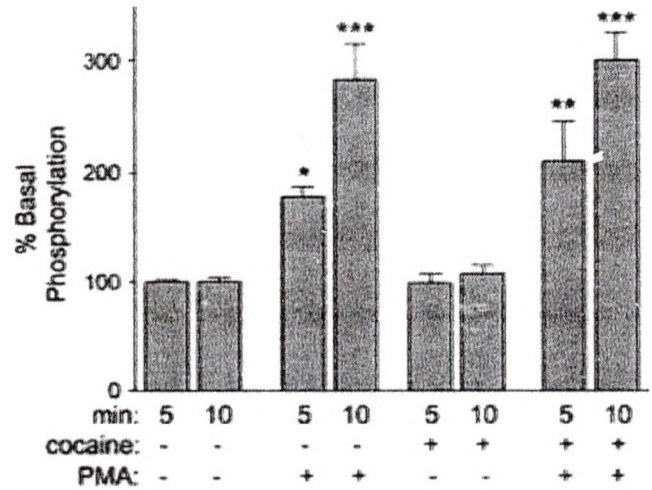

Figure 6. Cocaine Does not Affect Basal or PMA-stimulated DAT Phosphorylation at Shorter Time Points.

Gorentla, B.K. and R.A. Vaughan. Neuropharmacology, 2005 **49**(6):p. 759-68.

Figure 7 Mazindol and Methylphenidate Do not Affect Basal or PMA-Stimulated DAT Phosphorylation. rDAT LLC-PK_1 cells were metabolically labeled with ^{32}P and treated with or without 1 µM mazindol (left) or 10 µM MPH (right) in the presence or absence of 1 µM PMA for 30 min followed by immunoprecipitation, SDS-PAGE and autoradiography of DAT. Upper panels: autoradiographs of representative experiments; lanes correspond to treatments indicated directly below on histogram. Lower panel: summary of DAT phosphorylation levels relative to basal (means ± SE of three independent experiments for both compounds, performed in triplicate). *$p < 0.05$ relative to basal; **$p < 0.01$ relative to basal; ANOVA.

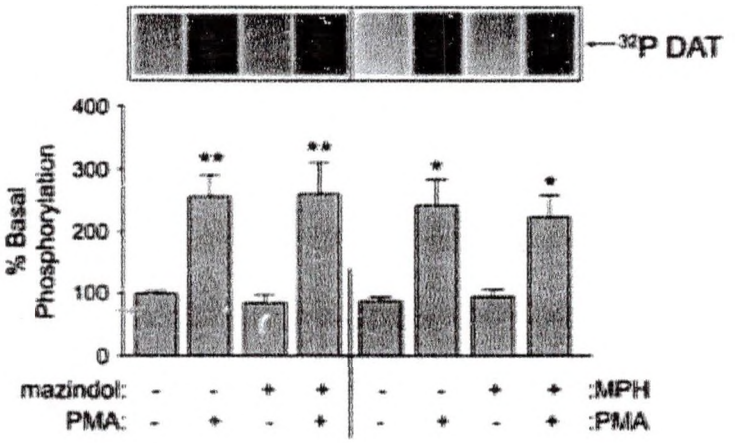

Figure 7. Mazindol and Methylphenidate Do not Affect Basal or PMA-Stimulated DAT Phosphorylation.

Gorentla, B.K. and R.A. Vaughan. Neuropharmacology, 2005 **49**(6):p. 759-68.

(85 ± 14% of basal; $p > 0.05$ relative to basal) or PMA-stimulated phosphorylation (279 ± 49% of basal, $p < 0.01$ relative to basal, $p > 0.05$ relative to PMA) (Figure. 7, left).

MPH (Ritalin®), a clinical drug used in the treatment of ADHD did not affect basal or PMA-stimulated DAT phosphorylation (Figure. 7, right) like cocaine, β-CFT and mazindol. The constitutive and PMA stimulated values were 100 ± 7% and 275 ± 48% of basal, respectively (PMA $p < 0.05$ relative to basal). Inclusion of 10 μM MPH had no effect on the constitutive phosphorylation (109 ± 15% of basal; $p > 0.05$ relative to basal), and PMA stimulated phosphorylation (253 ± 40% of basal; $p < 0.05$ relative to basal; $p > 0.05$ relative to PMA).

Treatment of cells with GBR 12909, a selective inhibitor for DA uptake displayed a different phosphorylation profile. The phosphorylation intensities of constitutive and PMA-stimulated samples were 101 ± 6% and 186 ± 7% of basal, respectively (PMA value $p < 0.001$ relative to basal). The treatment of 1 μM GBR 12909 had no effect on constitutive phosphorylation (111 ± 9% of basal, $p > 0.05$ relative to basal), but suppressed the PMA stimulated phosphorylation by up to 50% (147 ± 5% of basal; $p < 0.001$ relative to basal, $p < 0.01$ relative to PMA) (Figure. 8).

Effects of Uptake Blockers on DA Transport

Cocaine Treatment

Uptake blockers were used to examine their ability to affect transport activity or modulate PMA-stimulated DA transport down regulation. Drugs were added to cells in combination with vehicle or PMA and incubated for 30 min at

Figure 8. GBR 12909 Suppresses PMA-Stimulated DAT Phosphorylation. rDAT LLC- PK_1 cells were metabolically labeled with ^{32}P and treated with or without 1 µM GBR 12909 or 1 µM PMA for 30 min followed by immunoprecipitation, SDS-PAGE and autoradiography of DAT. Upper panel: autoradiograph of representative experiment; lanes correspond to treatments indicated directly below on histogram. Lower panel: summary of DAT phosphorylation levels relative to basal (means ± SE of three independent experiments, performed in triplicate). $^{***}p < 0.001$ relative to basal; $^{\#\#}p < 0.01$ relative to PMA; ANOVA.

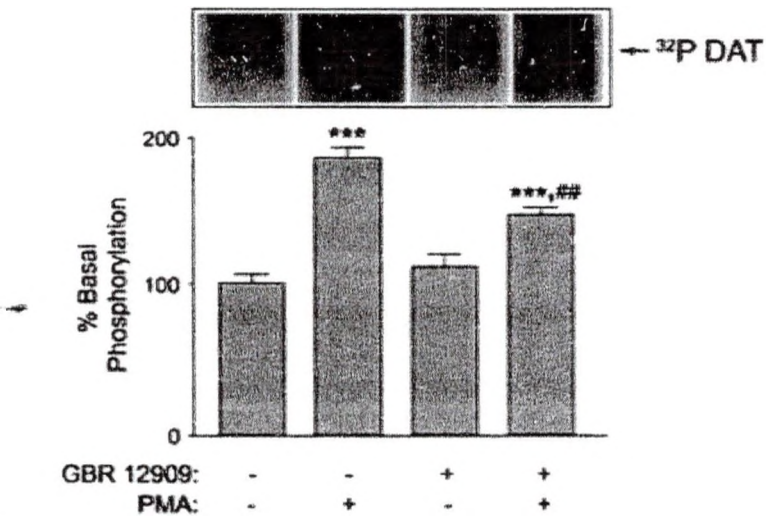

Figure 8. GBR 12909 Suppresses PMA-Stimulated DAT Phosphorylation.

Gorentla, B.K. and R.A. Vaughan. Neuropharmacology, 2005 **49**(6):p. 759-68.

37°C. To remove the test compounds, cells were washed thoroughly and subjected to [^{3}H] DA uptake. The [^{3}H] DA uptake obtained with vehicle treatment is considered the control which is defined as 100 % and is used to normalize the DA uptake values of other treatments. Pretreatment of cells with vehicle or cocaine did not affect the DA transport activity or PMA-induced transport down regulation (Figure 9A, top). The cells treated with 1 μM PMA decreased the DA transport values to 67 ± 3% of control ($p < 0.001$) resulting in PMA induced down regulation. Cells pretreated with 10 μM cocaine or cocaine plus PMA did not affect either control transport activity (96 ± 5% of control, $p > 0.05$ relative to control), or PMA induced down regulation (68 ± 3%, $p < 0.001$ relative to control; $p > 0.05$ relative to PMA).

MPH or Mazindol Treatment

DA uptake assays were extended to study the effect of MPH and mazindol on DA transport activity or PMA induced transport down regulation in a similar manner as cocaine treatments. The cells pretreated with MPH do not show a difference from control transport activity (93 ± 2% of control, $p > 0.05$ relative to control) (Figure 9B). The uptake values of PMA-induced down regulation (62 ± 3% of control; $p < 0.001$ relative to control), were not different from a combination treatment with MPH and PMA (63 ± 4% of control; $p < 0.001$ relative to control, $p > 0.05$ relative to PMA). MPH pretreatment did not influence transport activity or PMA induced transport down regulation.

Mazindol pretreatment decreased the subsequent [^{3}H] DA uptake even after extensive washings (78 ± 2% of control; $p < 0.001$ relative to control)

Figure 9. Effects of Cocaine, Methylphenidate and Mazindol on DA Transport Activity and PMA-Induced Down-Regulation of DA Transport Activity. rDAT LLC-PK_1 cells were treated as indicated with (A). vehicle, 1 µM PMA or 10 µM cocaine, (B). vehicle, 1 µM PMA or 10 µM MPH, or (C). vehicle, 1 µM PMA or 1 µM mazindol for 30 min followed by washing to remove drugs and assay for [^{3}H]DA transport. Results shown are means ± SE of three independent experiments for cocaine and two independent experiments for MPH and mazindol, performed in triplicate. $^{**}p < 0.01$ relative to control; $^{***}p < 0.001$ relative to control, $^{\#}p < 0.05$ relative to PMA, $^{@@@}p < 0.001$ relative to mazindol; ANOVA.

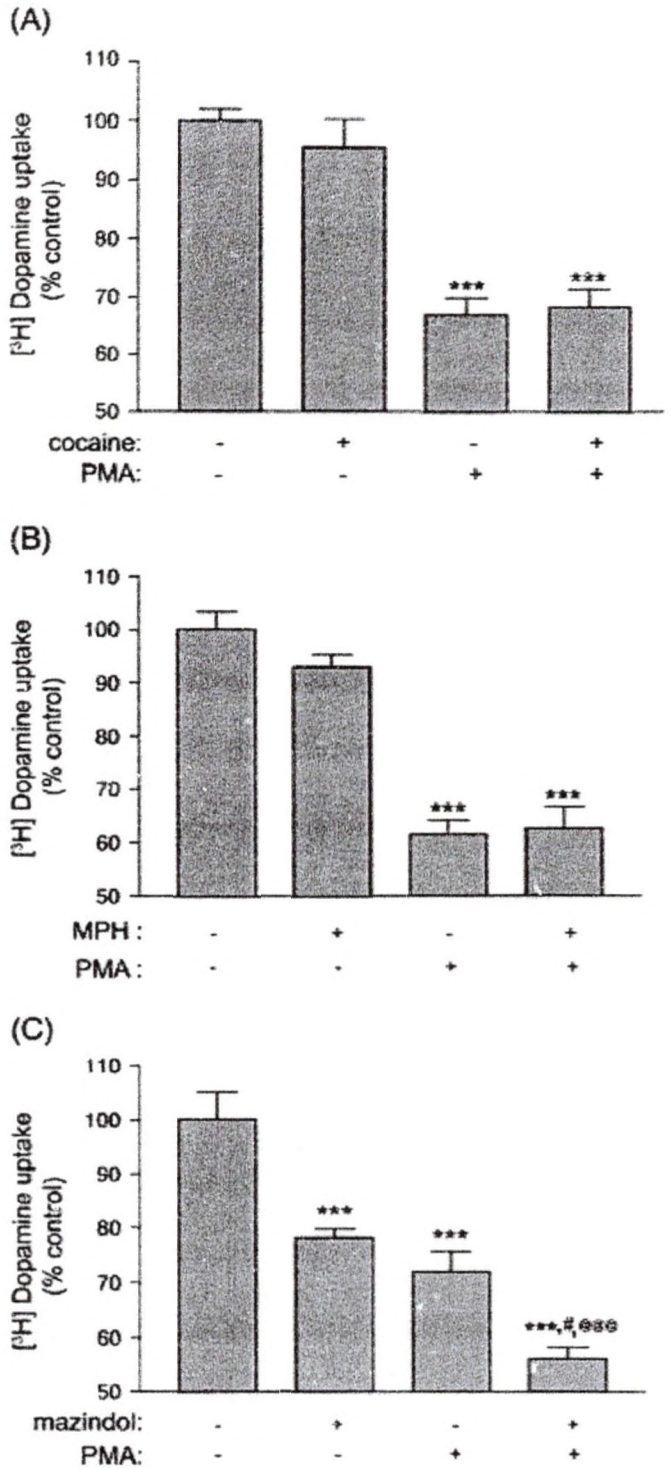

Figure 9. Effects of Cocaine, Methylphenidate and Mazindol on DA Transport Activity and PMA-Induced Down-Regulation of DA Transport Activity.

Gorentla, B.K. and R.A. Vaughan. Neuropharmacology, 2005 **49**(6):p. 759-68.

(Figure. 9C). To study this decrease in uptake values, we performed [^{3}H] CFT ligand binding assays (not shown). Binding assays showed a 30% loss in [^{3}H] CFT binding suggesting that the decrease of [^{3}H] DA uptake may be due to the presence of residual drug in the cell preparation. PMA treatment showed transport down regulation to 72 ± 4% of control ($p < 0.001$ relative to control), but co-treatment with mazindol further decreased the PMA-induced transport down regulation (56 ± 2% of control; $p < 0.001$ relative to control, $p < 0.05$ relative to PMA, $p < 0.001$ relative to mazindol). This increase in PMA-induced transport down regulation could be due to presence of residual drug that also decreased [^{3}H] CFT binding. Although it is possible that this decreased [^{3}H] DA uptake may also be due to the modulation of transport physiology by mazindol, our results show that mazindol does not subvert the effects of PMA.

GBR 12909 Blocks the Internalization of DAT

In an attempt to study the effect of GBR 12909 on DA transport activity we performed [^{3}H] DA uptake assays. Lack of binding reversibility of GBR 12909 following washings resulted in 10% or less DA uptake values compared to control. In this experiment, [^{3}H] DA uptake was minimal because of irreversible binding of GBR 12909, so we examined if this drug affects the cell surface distribution of DAT by using cell surface biotinylation. The control represents the amount of surface DAT on cells during vehicle treatment and is defined as 100% to compare with other treatments. Treatment of cells with PMA decreased the surface DAT levels to 67 ± 2% of control ($p < 0.05$) (Figure 10) suggesting that DAT undergoes internalization and these values are comparable with previous

Figure 10. GBR 12909 Blocks PMA-Induced DAT Internalization. rDAT LLC-PK_1 cells were treated with the indicated combinations of vehicle, 10 μM PMA and 10 μM GBR 12909 for 30 min followed by cell surface biotinylation and separation of biotinylated and non-biotinylated proteins. (A) Representative DAT immunoblot from the biotinylated fraction of cell lysates. (B) Summary of biotinylation levels (means ± SE of three independent experiments). *$p < 0.05$ relative to control; **$p < 0.01$ relative to control; ANOVA.

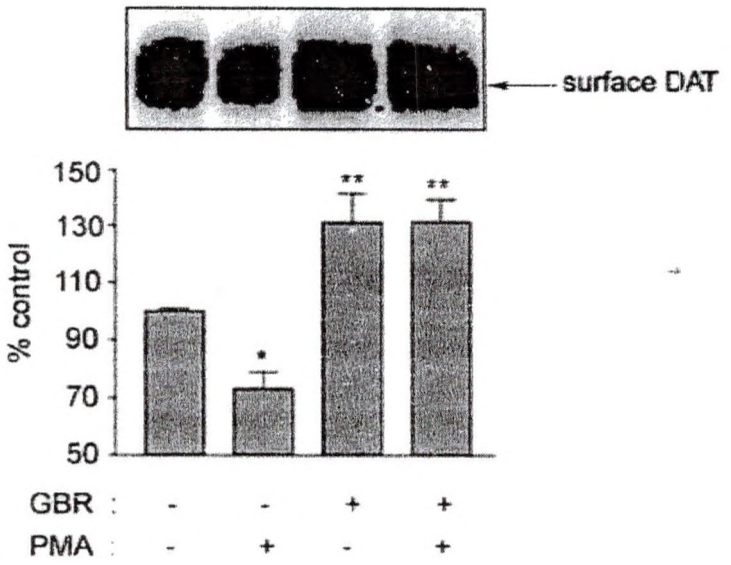

Figure 10. GBR 12909 Blocks PMA-Induced DAT Internalization.

studies. The co-treatment of GBR 12909 and PMA increased the surface expression of DAT suggesting that GBR 12909 blocks the PMA induced internalization of DAT. GBR 12909 treatment increased the surface expression of DAT to 130 ± 8% of the control ($p < 0.01$). These results provide preliminary evidence that binding of GBR 12909 can affect DAT phosphorylation and DAT endocytosis.

Effect of DA on DAT Phosphorylation

We have investigated the effects of DA on DAT phosphorylation by treating ^{32}P labeled cells with DA in the presence or absence of PMA (Figure. 11). Addition of 10 μM DA did not affect DAT constitutive phosphorylation (90 ± 8% of basal, $p > 0.05$ relative to basal) or PMA stimulated phosphorylation (PMA value 198 ± 18% of basal, $p < 0.01$ relative to basal; PMA plus DA value 233 ± 28% of basal, $p < 0.001$ relative to basal, $p > 0.05$ relative to PMA). In contrast, DAT substrates AMPH or METH induce DAT phosphorylation [85] and 5-HT or other SERT substrates suppress PMA-induced SERT phosphorylation [92].

Effects of DA on DA Transport

DAT has been shown to undergo functional transport down regulation with the pretreatment of DA in both synaptosomes and rDAT expressing HEK cells [81]. However, treatment of Madine-Darby canine kidney cells (MDCK) [93] with DA did not affect normal DA transport activity. Here we examined if rDAT expressing LLC-PK_1 cells undergo DA-induced down regulation. The cells pretreated with 1–10 μM DA showed transport down regulation in a dose dependent manner up to 30-40% (Figure 12A). We have also verified that PMA-

Figure 11. DA Does not Affect Basal or PMA-Stimulated DAT Phosphorylation. rDAT LLC-PK_1 cells were metabolically labeled with $^{32}PO_4$ and treated with or without 10 µM DA or 1 µM PMA for 30 min, followed by immunoprecipitation, SDS-PAGE and autoradiography of DAT. Upper panel: autoradiograph of a representative experiment, lanes correspond to treatments are indicated directly below the histogram. Lower panel: summary of DAT phosphorylation levels relative to basal (means ± SE of two independent experiments, performed in triplicate). *$p < 0.05$ relative to basal; **$p < 0.01$ relative to basal; ***$p < 0.001$ relative to basal; ANOVA.

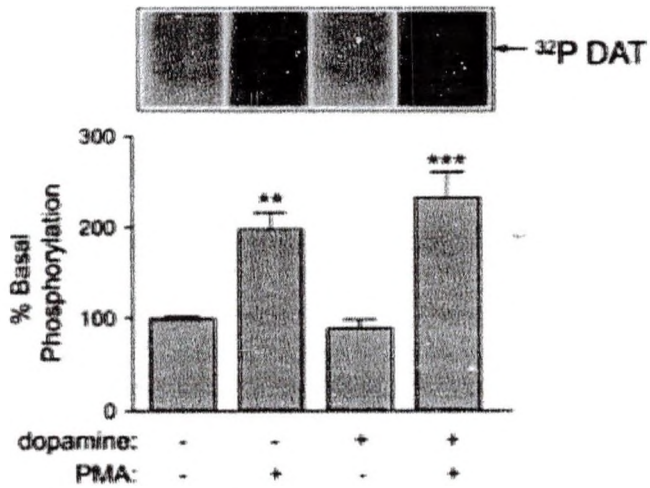

Figure 11. DA Does not Affect Basal or PMA-Stimulated DAT Phosphorylation.

Gorentla, B.K. and R.A. Vaughan. Neuropharmacology, 2005 **49**(6):p. 759-68.

Figure 12. DA and PMA Dose Response Curves for DA Transport Down-Regulation. rDAT LLC-PK_1 cells were treated with the indicated doses of DA (A) or PMA (B), or (C). 10 µM DA with or without 10 µM cocaine, for 30 min followed by washing and assay for [^{3}H]DA transport. Values shown are means ± SE of two (A and B) or three (C) independent experiments performed in triplicate for each compound. $^*p < 0.05$ relative to control; $^{**}p < 0.01$ relative to control; $^{***}p < 0.001$, relative to control; $^{\#}p < 0.05$ relative to DA, ANOVA.

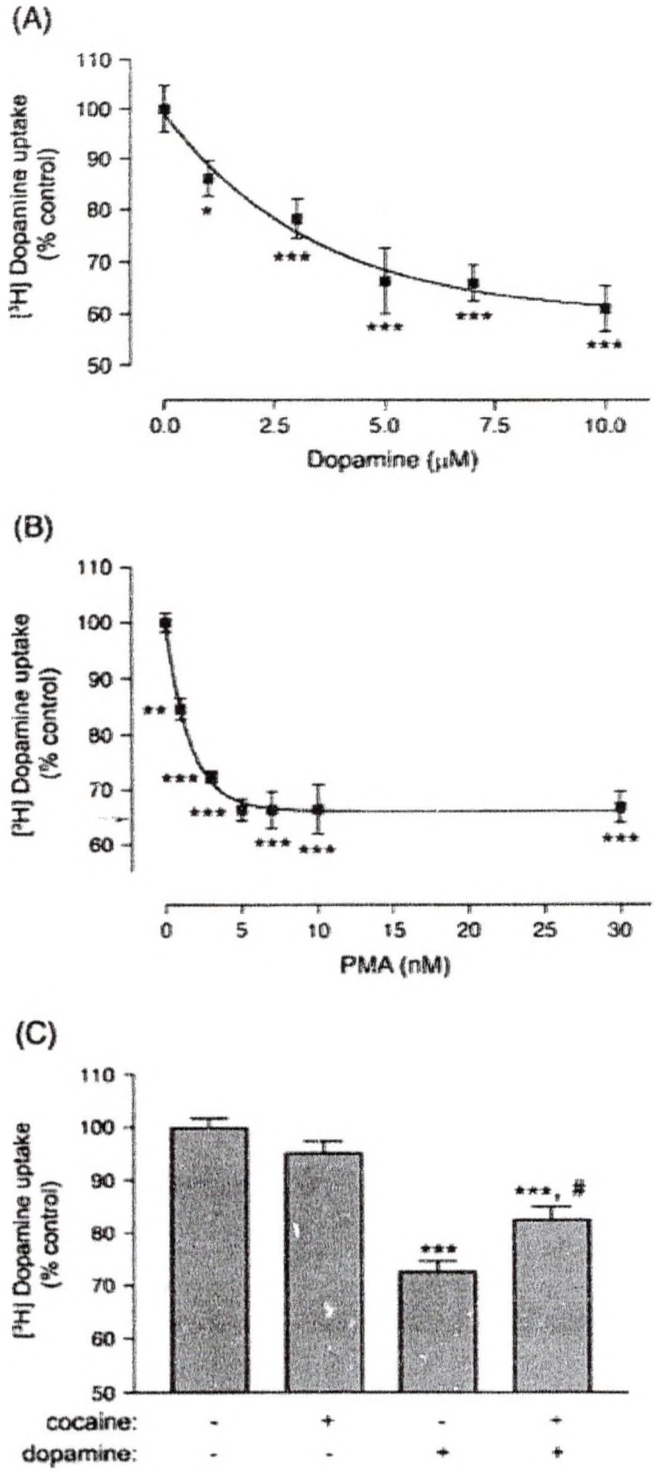

Figure 12. DA and PMA Dose Response Curves for DA Transport Down-Regulation.

Gorentla, B.K. and R.A. Vaughan. Neuropharmacology, 2005 **49**(6):p. 759-68.

induced transport down regulation occurs in a dose dependent manner,which started at nanomolar concentrations (Figure 12B). We co-treated the cells with 10 μM of DA and cocaine and assayed for [^{3}H] DA uptake to examine if transport is required for DA induced down regulation. Cocaine significantly attenuated the DA induced down regulation in cells suggesting that this event requires active transport (Figure 12C). Previous studies have demonstrated that LLC-PK$_1$ cells express DA receptors and are known to activate the PKC dependent pathways [94], that can lead to transport down regulation. To test this possibility, we preincubated the cells with DA and D1 or D2 antagonists such as SCH 23390 or sulpride to block the activation of DA receptors and subsequently assayed for [^{3}H] DA uptake. The presence of DA antagonists did not block DA induced transport down regulation (not shown) indicating that this process is not operating through dopamine receptor signaling.

DA-Induced Transport Down-Regulation Occurs Through PKC-Dependent Mechanisms

We examined the combined effects of DA and PMA on transport activity to determine if they produce maximal levels of down regulation. In these experiments, we co-treated the cells with high or intermediate concentrations of DA and PMA. The individual pretreatments at higher concentration such as 15 μM DA or 1 μM PMA induced transport down-regulation to 76 ± 6% or 64 ± 3% of control, respectively ($p < 0.01$ and $p < 0.001$ relative to control) (Figure. 13A). When cells were co-treated with DA and PMA at the above concentrations no further decrease in transport activity was evident (61 ± 2% of control, $p < 0.001$

Figure 13. DA-Induced Transport Down-Regulation is not Additive with PMA and is PKC Dependent. rDAT LLC-PK_1 cells were treated as indicated with (A) vehicle, 1 µM PMA or 15 µM DA for 30 min, (B) vehicle, 0.3 nM PMA or 10 µM DA for 30 min, or (C) vehicle or 10 µM BIM 30 min followed by vehicle or 20 µM DA for an additional 30 min. Cells were washed to remove pretreatment drugs followed by assay for [^{3}H]DA transport. Values shown are means ± SE of three independent experiments, performed in triplicate. $^*p < 0.05$ relative to control; $^{**}p < 0.01$ relative to control; $^{***}p < 0.001$, relative to control, $^{\#\#}p < 0.01$ relative to BIM plus DA; ANOVA.

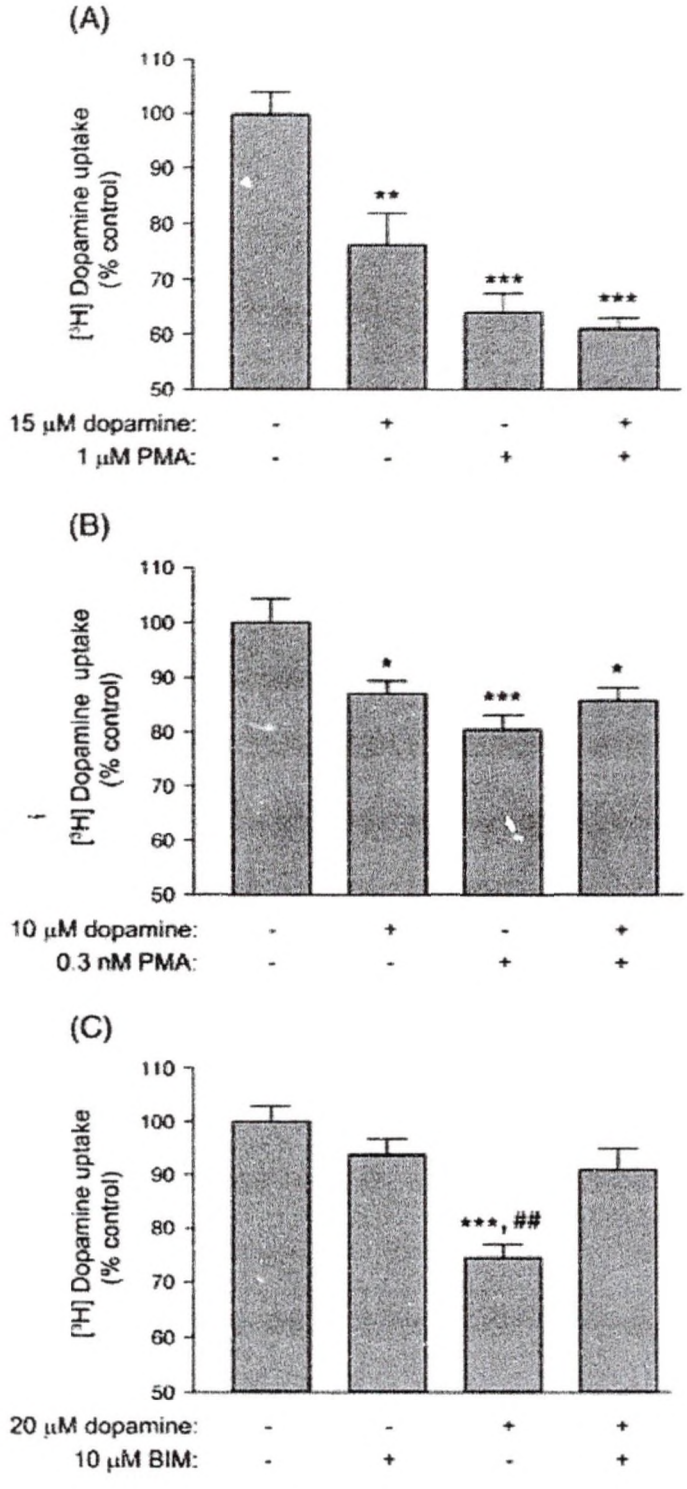

Figure 13. DA-Induced Transport Down-Regulation is not Additive with PMA and is PKC Dependent.

Gorentla, B.K. and R.A. Vaughan. Neuropharmacology, 2005 **49**(6):p. 759-68.

relative to control, $p > 0.05$ relative to DA only or PMA only) suggesting that each of these compounds achieved a maximal level of down regulation at this concentration and maximal effects could not be exceeded by the addition of the other compound. Therefore, it is possible that cells may exert additive effects when compounds are applied in intermediate concentrations. Cells incubated with intermediate concentrations, i.e. 10 µM DA or 0.3 nM PMA induced transport down regulation to sub-maximal levels (DA value, 87 ± 2% of control, $p < 0.05$ relative to control; PMA value, 80 ± 3% of control, $p < 0.001$ relative to control) (Figure. 13B). When co-treated, at these concentrations, higher levels of down regulation were not observed compared to individual treatments (86 ± 2% of control, $p < 0.05$ relative to control, $p > 0.05$ relative to DA only or PMA only). So an additive effect was not seen with co-treatment of DA and PMA even at intermediate concentrations suggesting that these individual down regulatory processes occur through a common mechanism.

To examine this possibility we incubated the cells with DA after PKC inhibitor bisindoylmaleimide I (BIM) pretreatment and assayed for [^{3}H] DA uptake (Figure.13C). DA uptake values with 20 µM DA or 10 µM BIM individual treatments were 74 ± 2% of control ($p < 0.001$ relative to control) or 94 ± 3% of control ($p > 0.05$ relative to control) respectively. When used in combination with DA, BIM effectively blocked DA-induced down regulation (91 ± 4% of control; $p > 0.05$ relative to control, $p > 0.05$ relative to BIM, and $p < 0.01$ relative to DA) suggesting that DA induced down regulation requires PKC. At a 10 µM concentration, BIM can block the activity of PKA while also inhibiting PKC.

However, previous results [63, 85] have shown that the treatment with the specific PKA inhibitor H89 did not affect the DA transport activity. Therefore, it is unlikely that inhibition of PKA by BIM accounts for blockade of DA induced down regulation. Together these results suggest that DA induced down regulation occurs by a PKC-dependent mechanism.

Purification and Immunochemical Characterization of NDAT

We have purified NDAT from precursor NDAT-CBD fusion protein that was expressed in T7 express bacteria. We have used standard methods to separate and purify NDAT from a crude lysate. Fractions of all the manipulations during the purification process were collected and analyzed using SDS-PAGE followed by commassie staining or immunoblot (Figure 14A). About 95% of the expressed NDAT-CBD fusion protein was found in the soluble fraction of crude extract (data not shown). The crude lysate from IPTG induced bacterial cultures showed a strong protein band at 62 kDa on commassie-stained gel (Figure 14A, lane 2, arrow a), while un-induced bacterial culture lysate did not display such a band in the corresponding region (lane 1) suggesting IPTG induced the expression of the fusion protein. To purify the NDAT-CBD fusion protein we passed the IPTG induced lysate through a chitin column and followed by stringent washes. Following washings we initiated the cleavage of NDAT-CBD fusion protein by incubating the column with 50 mM DTT for 40 h at 4°C.

The E1 and E2 elution fractions were collected from the chitin column, which showed a single NDAT protein band on commassie stained gel at 7 kDa with 95% purity (lanes 5, 6, arrow b). These fractions were immunobloted with a

DAT-specific antibody that recognizes the N-terminal tail of DAT. Immunoblot analysis showed immunoreactivity at ~7 kDa in lanes 7 and 8 that is comparable with commassie stained bands in lanes 5 and 6. Additionally, we found immunoreactive protein bands which represent uncleaved NDAT fusion protein. These results suggest that the expressed NDAT represents the N-terminal cytosolic tail of DAT.

Further, we immunochemically characterized the purified NDAT by immunoprecipitation and immunoblot analysis. NDATs were specifically immunoprecipitated by poly clonal antibody 16B that recognizes the N-terminal aminoacids 42-59 (lane 2, Figure 14B). The inclusion of immunizing peptide competitively blocked the immunoprecipitation of NDAT as shown in lane 3. The pre-immune serum did not immunoprecipitate NDAT (lane 4). These results were consistent with the immunoprecipitation profile of full length rDAT (upper panel, Figure 14B) suggesting that recombinantly expressed NDAT is indeed the N-terminal tail of full length DAT. We have achieved a final yield of 2-5 mg of NDAT per liter of culture.

Multiple Protein Kinases Directly Phosphorylate NDAT *In Vitro*

In an attempt to screen the protein kinase(s) that phosphorylate the N-terminus of DAT, we performed *in vitro* phosphorylation assays with recombinantly expressed NDAT with various purified serine/threonine kinases. The role of PKC has been well documented in DAT phosphorylation and regulation [63, 95]. Therefore, we first started with PKCα to determine if it is able to phosphorylate NDAT *in vitro*. The *in vitro* phosphorylation was initiated with

Figure 14. (A) Column Purification and SDS–PAGE Analysis of NDAT. Expression of NDAT fusion protein was induced with 0.5 mM IPTG at 16°C for 16 h. Total E.coli crude lysate was passed through chitin affinity column to purify NDAT-CBD fusion protein (an arrow on top left representing 'a'). After washing the column, NDAT (bottom left arrow showing 'b') was cleaved from fusion tag on column using buffer containing 50mM DTT. All the samples were analyzed by SDS-PAGE followed by commassie staining (left) or immunoblot (right). Lane 1, uninduced total lysate. Lane 2, total lysate of cells induced with IPTG that was used as input of the chitin column. Lane 3, column flow through. Lane 4, represents column washing. Lanes 5-6 represents elution fractions E1 and E2. Lanes 7-8 represents immunoblot analysis of E1 and E2 respectively.
(B) Immunochemical Characterization of NDAT: NDAT or rDAT was immunoprecipitated with DAT poly 16 antibodies (Ab16), poly 16 antibody preabsorbed peptide 16 (p16), or with preimmune serum (PI). The immune complexes were analyzed by SDS-PAGE followed by western blot. Upper panel shows the immunochemical reactivity of rDAT compared with NDAT in lower panel.

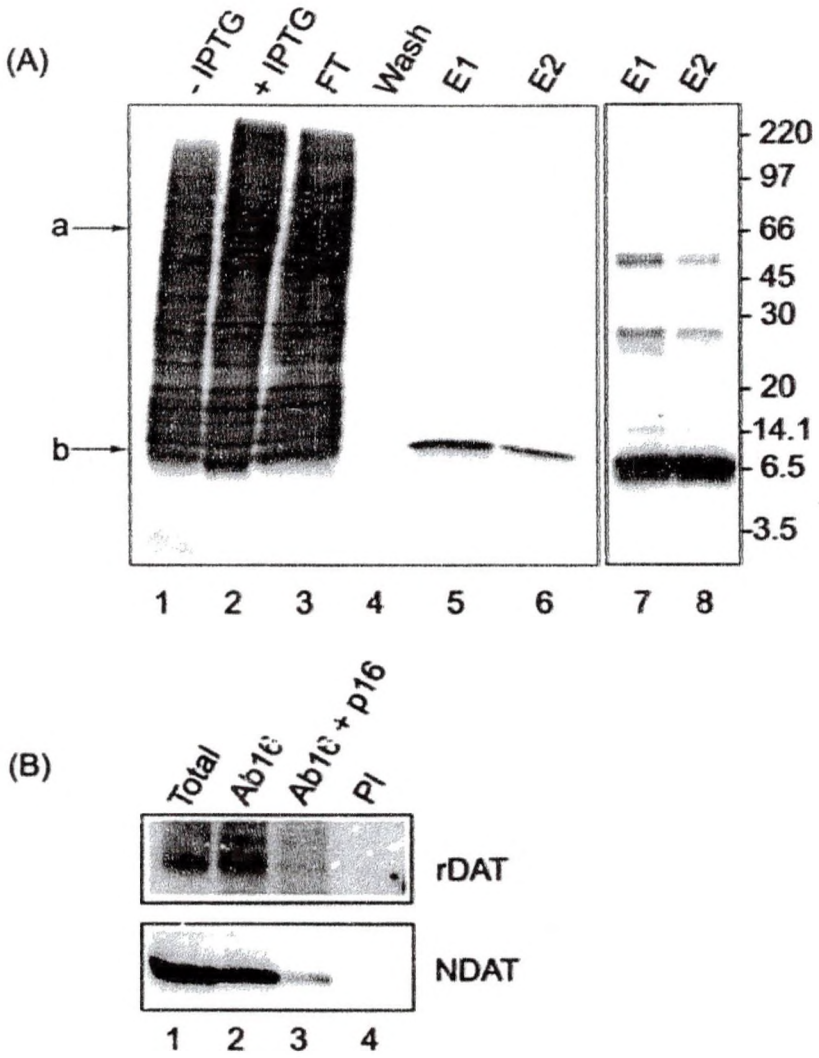

Figure 14. (A) Column Purification and SDS–PAGE Analysis of NDAT, (B) Immunochemical Characterization of NDAT.

purified PKCα and incubated for 30 min at 30°C. Reactions were terminated with the addition of EDTA and NDATs were subjected to immunoprecipitation, SDS-PAGE and autoradiography or immunoblot (Figure 15). The results showed that PKCα phosphorylates NDAT *in vitro* (lane 1) while the addition of EDTA completely blocked NDAT phosphorylation suggesting that PKCα specifically phosphorylated NDAT (lane 2). Other reactions that received only NDAT or only PKCα did not show any phosphorylated band and represent negative controls (lane 3, 4) to show that the NDAT preparation or the purified kinase do not contain any contaminating proteins that may lead to misinterpretation of NDAT phosphorylation. The presence of equal amounts of NDAT in these reactions was demonstrated by immunoblot analysis (bottom panel).

We extended these studies to other protein kinases to detect if these kinases phosphorylate NDAT *in vitro*. Figure 16A shows the *in vitro* phosphorylation of NDAT by PKC isoforms (α, βI, βII, and γ), CaMK IIα, ERK1/2, PKA, PKG, CKII and GSK-3β. All the tested protein kinases phosphorylated NDAT and were easily detectable with equal specific activities of these protein kinases; however GSK-3β did not phosphorylate the NDAT. Surprisingly, ERK1/2 isoforms phosphorylated NDAT to greater extent than any other protein kinase. These results suggest that multiple protein kinases may directly phosphorylate the N-terminal tail of DAT *in vivo*. Additionally, immunoblot analysis of ERK phosphorylated NDAT displayed a discrete upward shift in electrophoretic mobility compared to unphosphorylated NDAT or NDATs that were phosphorylated by other kinases (bottom panel, Figure 16A). This result

Figure 15. PKCα Phosphorylates NDAT *In Vitro.* NDAT was phosphorylated *in vitro* by incubation with PKCα at 30°C for 30 min in the presence of 20 mM MOPS, pH 7.4, buffer containing 5 mM $MgCl_2$, 300 μM $CaCl_2$, DOPS (40 μg/ml), DAG (1.6 μg/ml), 40 μM ATP and 12 μCi of [γ-^{32}P] ATP. Following the reaction samples were analyzed by immunoprecipitation followed by autoradiography (upper panel) or immunoblot (lower panel). Lane 1, represents the reaction mix that contains NDAT and PKCα. Lane 2, sample that received EDTA. Lane 3- 4, samples that did not receive either NDAT or PKCα.

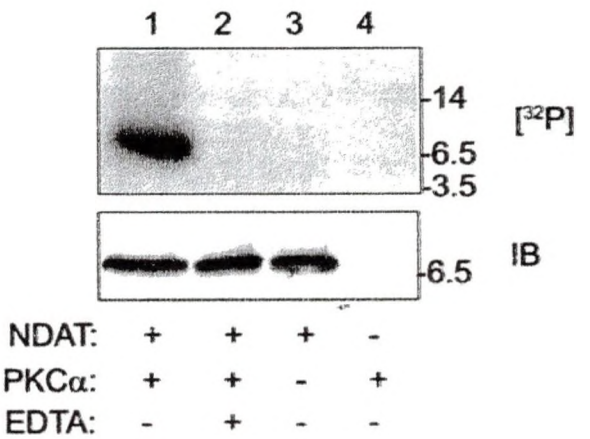

Figure 15. PKCα Phosphorylates the NDAT *In Vitro*.

suggests that ERK mediated phosphorylation may promote different conformation for NDAT.

ERKs are classified as proline-directed serine/threonine kinases, which specifically phosphorylates on S/T that immediately precedes a proline (S/T-P) [96, 97]. Such sites are also present in the distal region of NDAT, which are amenable for phosphorylation by other proline directed protein kinases including p38α kinase, JNK2, and Cdk 5. Although there is no evidence for these protein kinases to regulate DA transport activity *in vivo*, it is possible that they may play a role in N-terminal phosphorylation of DAT that is involved in DA efflux. Therefore we tested if these protein kinase(s) are involved in NDAT phosphorylation. Additionally we have also tested the ability of Akt1 to phosphorylate NDAT.

Varied levels of phosphorylation were achieved on NDATs when incubated with different protein kinases of equal specific activity (Figure 16B). The phosphorylation levels achieved on NDAT by these protein kinases were represented as ERK = p38α kinase > JNK2 > Cdk > Akt1. Additionally, p38α kinase and JNK2α2 phosphorylated NDATs have an electrophoretic shift on immunoblot that matches the migration of ERK1-phosphorylated NDAT. However, Cdk5 and Akt 1 phosphorylated NDATs did not show this shift on the immunoblot. These results suggest that ERK1, p38 and JNK2 may share the same phosphorylation site on NDAT.

Because of the demonstrated regulatory roles of ERK1 and PKCα in DAT phosphorylation and /or DAT function, we focused further studies on PKCα and/or ERK.

Figure16. Multiple Kinases Phosphorylate NDAT *In Vitro*. NDAT was phosphorylated *in vitro* by incubating with different protein kinases (A) PKCα, βI, βII, γ, ERK1/2, CaMK II, PKA, PKG, GSK-3β, and CKII (B) ERK1, p38 kinase, JNK2, Cdk5, and Akt1 at 30°C for 30 min in the presence of 20 mM MOPS, pH 7.4, buffer containing 5 mM $MgCl_2$, 300 μM $CaCl_2$, 40 μM ATP and 12 μCi of [γ-^{32}P] ATP. Following the reaction, samples were analyzed by immunoprecipitation followed by autoradiography (upper panel) or immunoblot (lower panel). The lanes correspond to protein kinase treatments that are indicated directly above the autoradiograph.

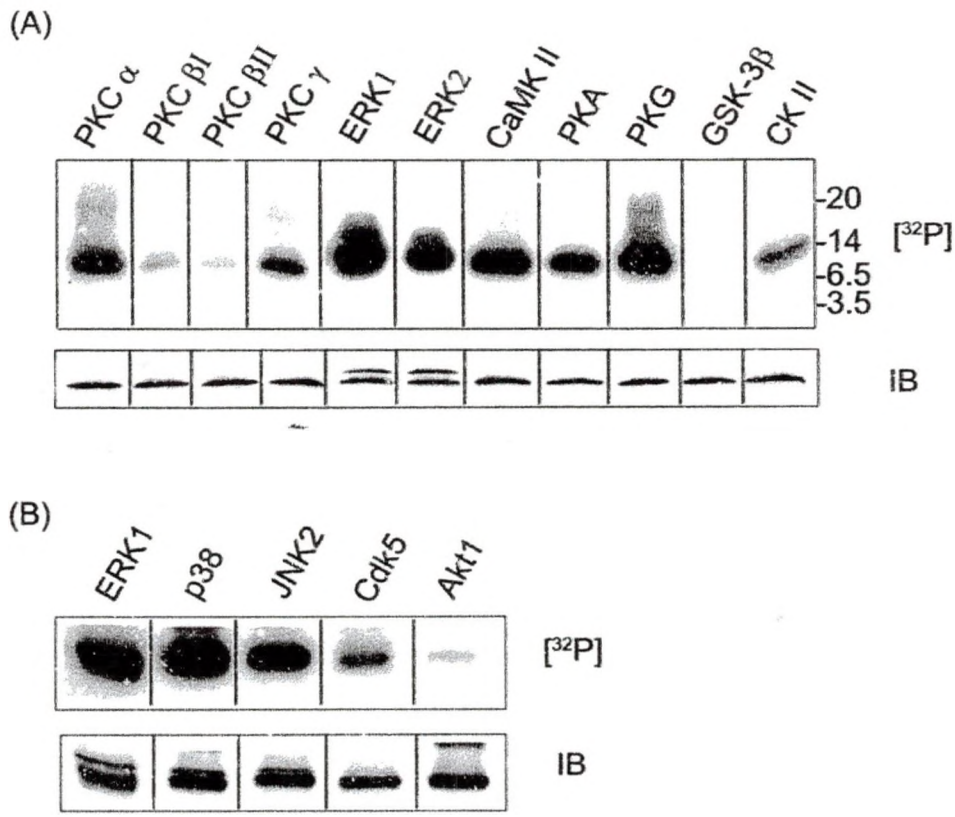

Figure 16. Multiple Kinases Phosphorylate the NDAT *In Vitro*.

In Vitro Dephosphorylation of NDAT

The application of protein phosphatase inhibitors in cell lines [63] or treatment of cell homogenates with purified protein phosphatases [72] have demonstrated the role of protein phosphatases on DAT phosphorylation and DA transport activity. Here we attempted to dephosphorylate *in vitro* phosphorylated NDATs by using *in vitro* dephosphorylation assays with exogenous protein phosphatases. We initiated the *in vitro* dephosphorylation reaction by adding purified protein phosphatases PP1, PP2A or PP2B to the reaction mixtures consisting of PKCα or ERK1 phosphorylated NDATs or ^{32}P labeled rDATs. Following the reaction, the reaction products were separated by SDS-PAGE and detected by autoradiography. The phosphorylation levels in control samples that did not receive protein phosphatase were defined as 100% for comparison with phosphorylation levels obtained following treatments. The results show that PKCα-phosphorylated NDAT was completely or partially dephosphorylated by PP1 or PP2B respectively. However, PP2A was not able to dephosphorylate the PKC phosphorylated NDAT (Figure 17B). A similar dephosphorylation profile was found with $^{32}PO_4$ labeled rDAT samples suggesting that PP1 and/or PP2B may regulate the PKC mediated phosphorylation of DAT *in vivo* (Figure 17A). Treatment with PP1 displayed a significant amount of dephosphorylation in PKCα phosphorylated NDAT (20.2 ± 9.6 % of control; $p< 0.001$ and $p< 0.01$ relative control and PP2A respectively) and in $^{32}PO_4$ labeled rDAT (12.3 ± 5.7 % of control; $p< 0.001$ and $p< 0.05$ relative control and PP2A respectively) with treatment of PP1. PP2B was able to dephosphorylate PKCα-phosphorylated

Figure 17. *In Vitro* Dephosphorylation of NDAT. (A) ^{32}P metabolically labeled rDAT samples or (B) PKCα or (C) ERK1 *in vitro* phosphorylated NDAT samples were subjected to immunoprecipitation using rabbit polyclonal antibody 16. The immunoprecipitated complexes subjected to dephosphorylation in a reaction mixture consisting of 20 mM MOPS pH 7.4, 200 µM $MnCl_2$, 5 mM DTT, 100 µM EDTA, 0.2% BSA and PP1 or PP2A or PP2B at 30°C for 2 h. PP2B assays were supplemented with 1 µM calmodulin and 1 mM $CaCl_2$, 5 min before initiation of the reaction. Following the reaction, the samples were analyzed on SDS-PAGE followed by immunoblot (upper panel) or autoradiography (middle panel). The lanes correspond to treatments indicated directly below on histogram. Summary of NDAT or rDAT phosphorylation levels relative to control (means ± SE of three independent experiments). *$p < 0.05$ relative to control; **$p < 0.01$ relative to control; ***$p < 0.001$ relative to control; ANOVA.

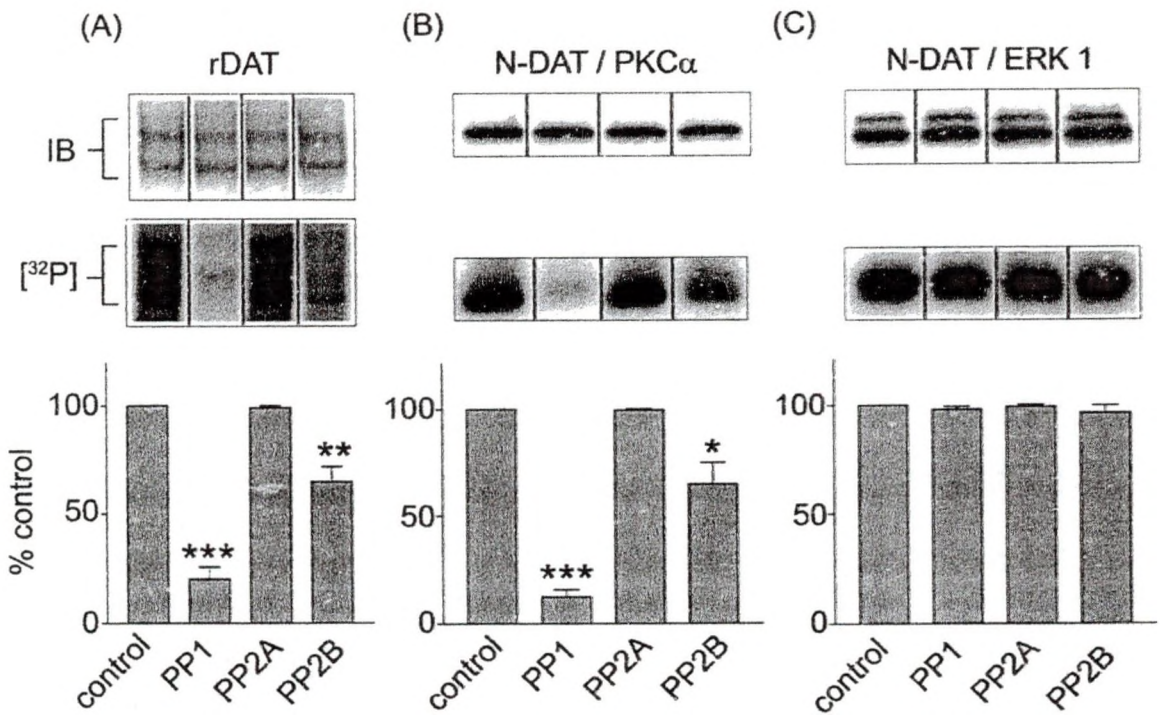

Figure 17. *In Vitro* Dephosphorylation of NDAT.

Figure 18. Phosphoamino Acid Analysis of (A) PKC α and (B) ERK Phosphorylated NDAT. PKC α or ERK1 phosphorylated NDATs were purified by immunoprecipitation and gel electrophoresis. Autoradiographs displayed the phosphorylation pattern demonstrated in Fig. 2A. DAT bands were excised, eluted, and subjected to acid hydrolysis. Cerenkov counting of the hydrolysates showed counts/min of 500 and 800 in the PKC α and ERK1 samples, respectively. Aliquots of the hydrolysates were mixed with phosphoamino acid standards, and amino acids were separated by two-dimensional electrophoresis on thin layer cellulose plates. Plates were subjected to autoradiography, and phosphoamino acid standards were visualized with ninhydrin (dotted circles). X, origin; S, phosphoserine; T, phosphothreonine; Y, phosphotyrosine.

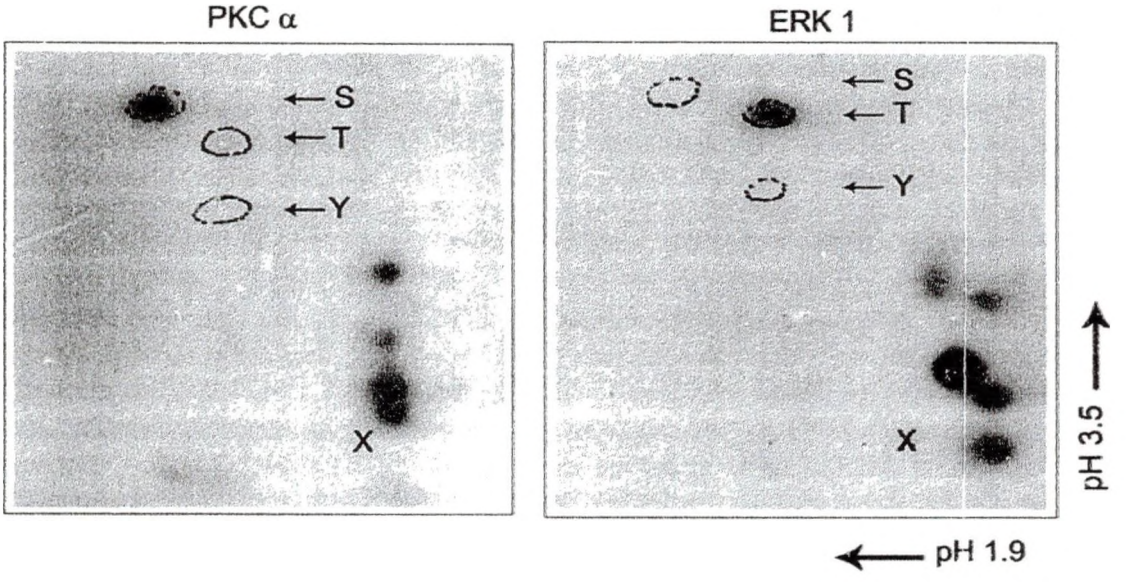

Figure 18. Phosphoamino Acid Analysis of (A) PKC α and (B) ERK Phosphorylated NDAT.

NDAT to 50% of control (64.5 ± 18.0 % of control; $p< 0.05$) which is consistent with rDAT (64.8 ± 12.3% of control; $p< 0.01$).

We extended these studies to examine if ERK-phosphorylated NDATs undergo dephosphorylation. None of the tested protein phosphatases were able to dephosphorylate ERK phosphorylated NDAT or alter the upward shift in electrophoretic mobility (Figure 17C). Taken together, these studies suggest that multiple protein phosphatases may regulate DAT dephosphorylation and different sites display differential sensitivity for DAT dephosphorylation.

Phosphoamino Acid Analysis of NDAT

From previous studies it is known that Ser and Thr residues are involved in DAT phosphorylaton *in vivo* [65]. To identify the amino acid residues involved in NDAT phosphorylation, we performed phosphoamino acid analysis of phosphorylated NDATs. Following the *in vitro* phosphorylation of NDAT by PKCα or ERK1, the products were purified by immunoprecipitation and gel electrophoresis. The purified products were electro-eluted from gel pieces and hydrolyzed in 6N HCl and the hydrolysate was electrophoresed on two-dimensional thin layer plates along with phosphoamino acid standards. After electrophoresis, ninhydrin was applied to the TLC plates to identify the free phosphoamino acid spots and the plates were exposed to film for autoradiography. The results showed that PKCα phosphorylates NDAT only on Ser(s) (Figure 18, left), and ERK1 phosphorylates exclusively on Thr(s) (Figure 18, right). The combination of these two results were consistent with the presence of phospho-S and phospho-T in the phosphoamino acid analysis of full

length DAT [65] suggesting that PKCα and ERK1 may directly phosphorylate the N-terminal tail of DAT *in vivo* on these residues.

MAPKs Phosphorylate NDAT on T53

To further characterize the ERK phosphorylation, we mutated NDAT Thr(s) (T43, T46, T53, and T62) individually to Ala by site directed mutagenesis. Standard procedures were used to express and purify the mutant NDATs. The purified mutant NDATs were subjected to *in vitro* phosphorylation and was analyzed by SDS-PAGE followed by autoradiography. Figure 19A displays that ERK1 did not phosphorylate the T53A mutant NDAT, while other mutants were phosphorylated to comparable levels as wild type NDAT. Similarly, p38 kinase and JNK2 did not phosphorylate the T53A mutant (not shown) suggesting that T53 is a MAPKs phosphorylation site *in vitro*. Additionally, we did not observe an upward shift in electrophoretic mobility with the T53A mutant on immunoblots as was found with wild type and other mutants (bottom panel). Interestingly, T53 is located in an ERK consensus recognition motif (P-X-S/T-P) suggesting that T53 is an optimal site for ERK phosphorylation *in vivo*. However, ERK can also phosphorylate at a minimal consensus sequence that contains S/T preceded by proline (X-S/T-P). Such a minimal sequence is also present on the C-terminal cytosolic tail of rat DAT at T593 in addition to N-terminus T53. It is also possible that the phosphorylation at T593 can contribute to the presence of T phosphorylation in full length DAT [65]. To test this possibility we recombinantly expressed rat DAT C-terminal tail domain and examined if it undergoes ERK mediated phosphorylation *in vitro*. The *in vitro* phosphorylation results showed

Figure 19. (A) ERK 1 Phosphorylates NDAT *In Vitro* on T53. Equal proteins of Wt or T to A mutant NDATs were phosphorylated *in vitro* by incubating with ERK1 at 30°C for 30 min in the presence of 20 mM MOPS, pH 7.4, buffer containing 5 mM MgC_2, 300 µM $CaCl_2$, 40 µM ATP and 12 µCi of [γ-^{32}P] ATP. Following the reaction samples were analyzed by immunoprecipitation followed by autoradiography (upper panel) or immunoblot (lower panel). Lane 1, represents the reaction mixture that had NDAT and PKCα. Lane 2, sample that received EDTA. Lane 3- 4, samples that do not receive either NDAT or PKCα. The type of NDAT mutants are indicated directly above the autoradiograph. (B) ERK 1 Does not Phosphorylate CDAT *In Vitro*. Equal amounts of NDAT or CDAT were phosphorylated *in vitro* by incubating with PKCα or ERK1 at 30°C for 30 min as described in methods. Following the reaction samples were analyzed by immunoprecipitation followed by autoradiography (upper panel) or immunoblot (lower panel). The lanes correspond to treatment were indicated directly above the autoradiograph.

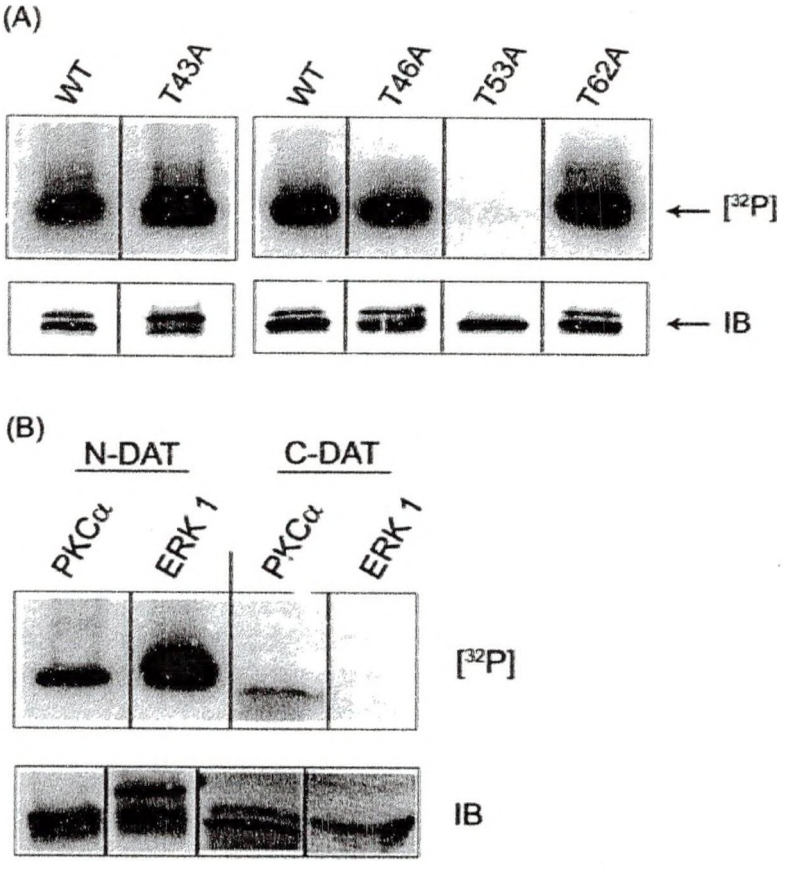

Figure 19. (A) ERK 1 Phosphorylates NDAT *In Vitro* on T53. (B) ERK 1 Does not Phosphorylate CDAT *In Vitro*.

that ERK1 did not phosphorylate C-DAT (Figure 19B) suggesting ERK1 may not phosphorylate the C terminal tail of DAT *in vivo* even though it has a minimal consensus sequence.

N-terminal tail threonine(s) are involved in DAT phosphorylation *in vivo*

DAT contains multiple Ts on cytosolic tail domains, intracellular loops and TMs. Our mutational analysis showed that T53 is a MAPK phosphorylation site *in vitro*; however it is not known if T53 undergoes phosphorylation on full length DAT *in vivo*.

Here we attempted to localize the threonine phosphorylation on native DAT using *in situ* proteolysis with Asp-N followed by phosphoamino acid analysis. Asp-N treatment was previously shown to proteolytically cleave DAT at D174 and yield an intact 19 kDa N-terminal peptide (Asp-N fragment) [89]. For this experiment, we metabolically labeled rat striatal tissue in presence of OA/OAG and performed *in situ* protelolysis of striatal membranes with endoproteinase Asp-N as described in the methods. Following proteolysis, we solubilized the membranes and purified DATs and Asp-N fragments by immunoprecipitation using polyclonal 16B antibody that recognizes the DAT N-terminal cytosolic tail. Immunoprecipitates were subjected to electrophoresis and autoradiography. Asp-N cleavage of DAT resulted in the production of a 19kDa phosphorylated Asp-N fragment (Figure 20A, right) consistent with our previous studies [89].

We subjected the full length DAT and Asp-N fragment to standard phosphoamino acid analysis followed by autoradiography. The results showed the presence of phospho-T along with phospho-S in both the full length DAT (left)

Figure 20. Threonine Phosphorylation was Found on the N-terminal Region of DAT. (A) *In Situ* Proteolysis of DAT. Membranes from striatal slices labeled with $^{32}PO_4$ and treated with 10 μM OA plus 10 μM OAG were subjected to proteolysis with 10 μg/ml of endoproteinase Asp-N for 1 h at 22°C. The membranes were sedimented, solubilized, immunoprecipitated with poly clonal 16 antibodies, and analyzed by electrophoresis and autoradiography on an 8-16% Tris-Tricine gel. The arrow on the right denotes the position of immunoprecipitated phosphopeptide fragments at ~19 kDa. (B) Phosphoamino Acid Analysis of Full Length DAT and Asp-N Fragments. ^{32}P metabolically labeled full length DATs or Asp-N fragments were purified by immunoprecipitation and gel electrophoresis. Autoradiographs displaying the phosphorylation pattern are demonstrated in Fig. 20A. DAT bands were excised, eluted, and subjected to acid hydrolysis. Cerenkov counting of the hydrolysates showed counts/min of 250 and 100 in the full length DAT and Asp-N fragment samples, respectively. Aliquots of the hydrolysates were mixed with phosphoamino acid standards, and amino acids were separated by two-dimensional electrophoresis on thin layer cellulose plates. Plates were subjected to autoradiography, and phosphoamino acid standards were visualized with ninhydrin (dotted circles). X, origin; S, phosphoserine; T, phosphothreonine; Y, phosphotyrosine.

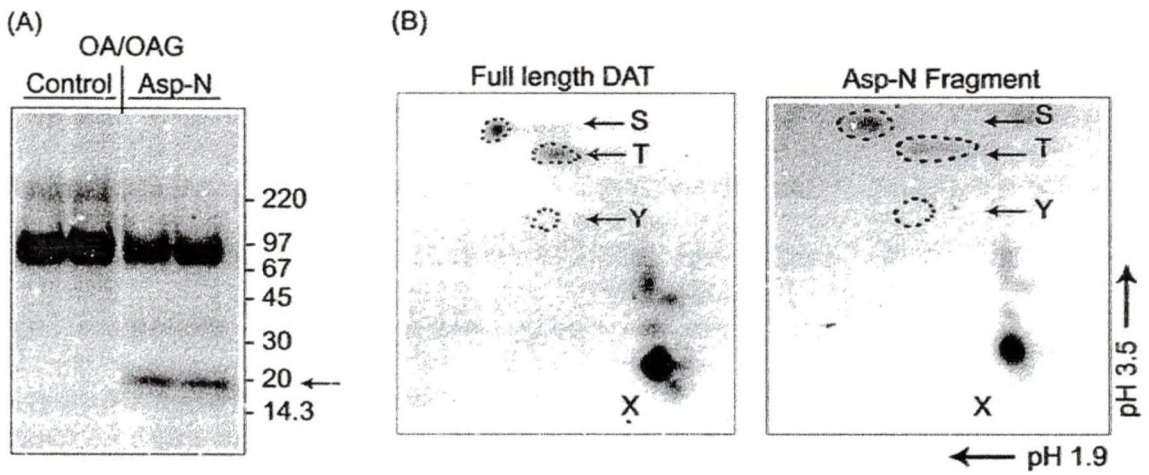

Figure 20. Threonine Phosphorylation was Found on N-terminal Region of DAT. (A) *In Situ* Proteolysis of DAT. (B) Phosphoamino Acid Analysis of Full Length DAT and Asp-N Fragment.

and the Asp-N fragment (right) (Figure 20B).We also performed control experiments in parallel to verify that phospho-T was indeed coming from DAT but not from contaminating proteins. For this experiment we subjected DATs to immunoprecipitation with either polyclonal 16B or pre-immune serum followed by phosphoamino acid analysis. The phosphoamino acid analysis of DATs that were immunoprecipitated with polyclonal 16B showed the presence of phospho-S and phospho-T, whereas pre-immune immunoprecipitated samples did not show any phosphorylation signals (not shown). This result strongly argues that phospho-T was coming from DAT, and not from any contaminant.

The 19 kDa Asp-N fragment representing the N-terminal cytosolic tail, TMs 1-3, EL1, IL1 and proximal portion of EL2 contains T residues. Because protein kinase accessible Thr(s) (T43, T46, T53, and T62) are present only on the N-terminal cytosolic tail, it is very likely that phospho-T may be derived from one of these four threonines. Collectively, these results suggests that T53 is a putative DAT phosphorylation site *in vivo*.

Effects of MEK Inhibitors or MEK Mutants on DA Transport Activity

We independently investigated if ERKs can regulate DA transport activity in cell lines by treating with pharmacological inhibitors of MEK or by transient transfection of mutant MEK constructs.

For these studies, we inhibited MEK activity with PD98059 which suppresses phosphorylation of ERK. We incubated rDAT-expressing LLC-PK_1 cells with vehicle or PD98059 or PMA for 30 min at 37°C. Following treatments cells were subjected to [^{3}H] DA uptake. Treatment of cells with 50 μM PD98059

decreased DA transport values to 63 ± 2.4% of control ($p<0.001$) (Figure 21A) that is consistent with previous studies [70]. Cells treated with 1 µM PMA showed decreased DA transport values of 72.7 ± 2.1% of control ($p<0.001$) consistent with previous findings [64]. In addition we analyzed the levels of phospho-ERK in cell lysates of this experiment using western blot analysis. Consistent with previous reports [70], phosphorylated forms of ERK were markedly decreased with the treatment of PD98059 compared to control (as shown in Figure 21B, right).

Mansour et al., (1994) have shown that transient transfection of constitutively active MEK mutant S218E-S222D (MEK-CA) resulted in increased levels of phosphorylated p44 and p42 forms of MAPK relative to those transfected with the wild-type mutant [98]. We examined the effects of MEK mutants on DA transport. For these studies, we transiently transfected rDAT-expressing LLC-PK_1 cells with His-taged wild-type MEK or MEK-CA or a kinase-dead mutant K97M (MEK-KO) and incubated the cells for 36 h. One set of MEK-WT transfected cells were treated with PD98059. Following transfection and/or treatments, cells were subjected to [^{3}H] DA uptake. We verified the success of transfection by western blot analysis using anti-His specific antibody. Western blot results showed that cells transfected with Wt or mutant MEKs constructs expressed equal amount of Wt or mutant MEK protein (not shown). The cell lysates from this experiment were analyzed for phospho-ERK levels. Phospho-ERK levels (Figure 21 B, upper panel) and [^{3}H] DA uptake values (Figure 21 B, bottom panel) of MEK-WT or MEK-CA transfected cells were not significantly

Figure 21. Effects of MEK Inhibitor or MEK Mutants on DA Transport Activity. (A) rDAT LLC- PK_1 cells were treated as indicated with vehicle, 50 μM PD98059, or 1 μM PMA for 30 min followed by [^{3}H] DA transport assay. (B) rDAT LLC- PK_1 cells were transfected as indicated with MEK-WT, MEK-CA, or MEK-KO and subjected to immunoblot (upper panel) or [^{3}H] DA transport assay (bottom panel) after 36 h. Uptake values shown are means ± SE of three (A) or eight bottom (B) independent experiments, performed in triplicate. ***p <0.001 relative to control, **p < 0.001 relative to control; ANOVA.

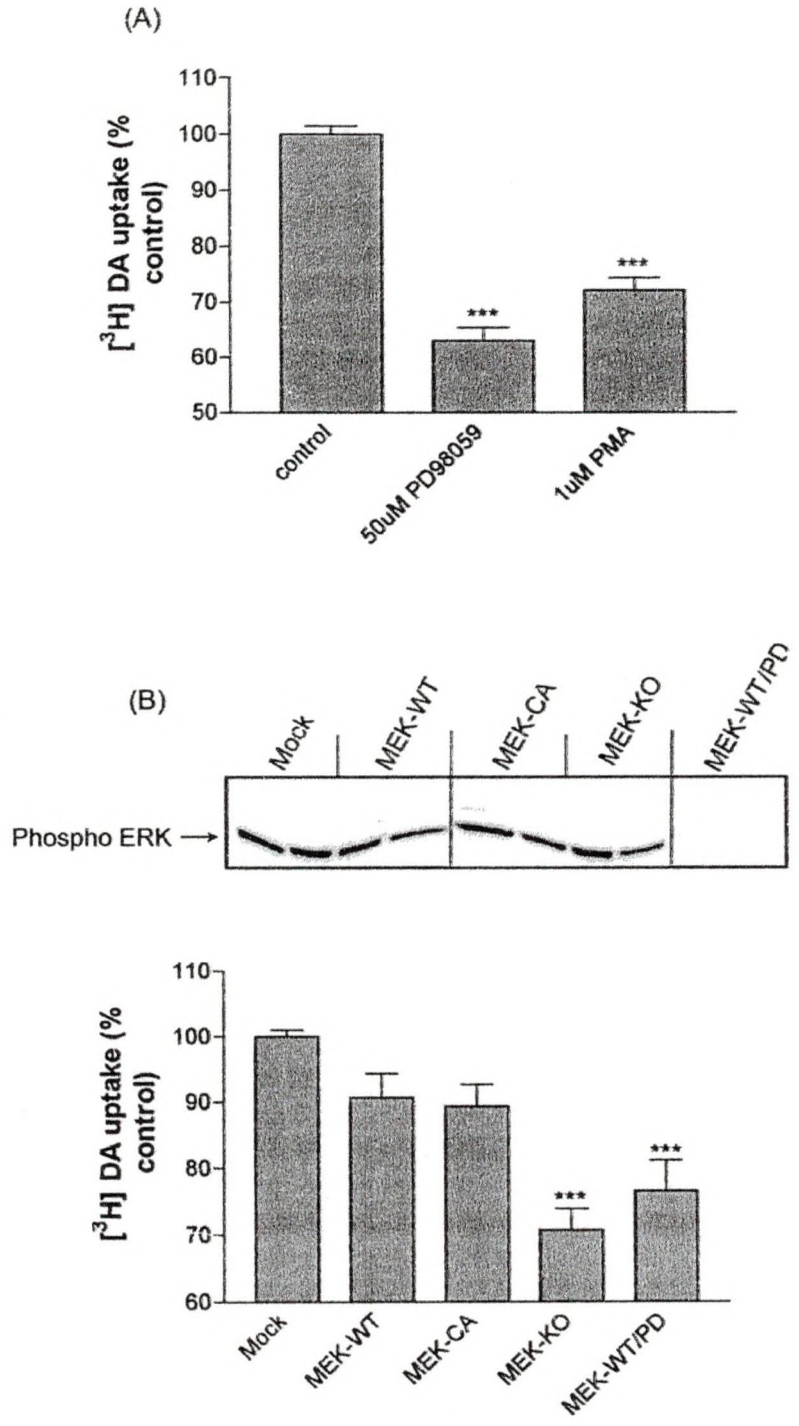

Figure 21. Effects of MEK Inhibitors or MEK Mutants on DA Transport Activity.

different from mock transfection ($p>0.05$ relative to control, n=8). Cells transfected with MEK-KO showed a significant level of transport down regulation (76.6 ± 4.5 % of control; $p<0.001$) compared to control, while not affecting the phospho-ERK levels. However, the cells that were treated with MEK inhibitor showed a decrease in transport (70.8 ± 3 % of control; $p<0.001$) and phospho-ERK levels consistent with previous studies [70, 98]. In this study, phospho-ERK levels do not show correlation with the type of transfected MEK constructs. Therefore, we were not able to make a conclusion regarding the effects of ERKs on DA transport activity in this experiment.

Effects of BDNF or MEK Inhibitor on DAT Phosphorylation

We attempted to examine if ERK activation or inhibition affects the DAT phosphorylation. For these studies, we used brain-derived growth factor (BDNF) to activate the MAPK kinase pathway that results in the activation of ERKs. To inhibit the activation of ERKs we used MEK inhibitor PD98059. Therefore, we metabolically labeled rat striatal slices with $^{32}PO_4$ and then treated with vehicle or 1 µM OA or 200ng/mg BDNF or 50µM PD98059. $^{32}PO_4$ incorporated DATs were immunoprecipitated and analyzed by SDS-PAGE followed by autoradiography (Figure. 22, left). In addition, we analyzed the levels of phospho-ERK in crude lysates using immunoblot analysis. Tissues treated with vehicle displayed a basal level of constitutive phosphorylation on DATs (100 ± 3.6%), while the OA treatment leads to a 2-3 fold increase in DAT phosphorylation (264 ± 7% of control; $p<0.001$) compared to vehicle as previously reported [63, 65]. Treatment with PD98059 marginally decreased DAT phosphorylation to 83 ± 5.4 % of

Figure 22: Effects of BDNF or MEK Inhibitor on DAT Phosphorylation. (A) Rat striatal slices labeled with $^{32}PO_4$ were treated with vehicle, 10 μM OA, 50 μM PD98059 or 200 ng/ml BDNF, followed by immunoprecipitation, SDS-PAGE, and autoradiography (upper panel). The bottom panel represents immunoblot analysis of crude striatal lysates for phospho-ERK (bottom panel). Equal amounts of sample from treated and untreated tissue were subjected to immunoprecipitation, electrophoresis, and autoradiography or immunoblot. Molecular mass standards for all gels are shown in kDa. (B) Quantitation of DAT phosphorylation. The data from three independent experiments are normalized, averaged, and expressed as the ratio of $^{32}PO_4$ incorporation relative to the basal sample ± S.E. ***$p < 0.001$ relative to control, **$p < 0.001$ relative to control; ANOVA.

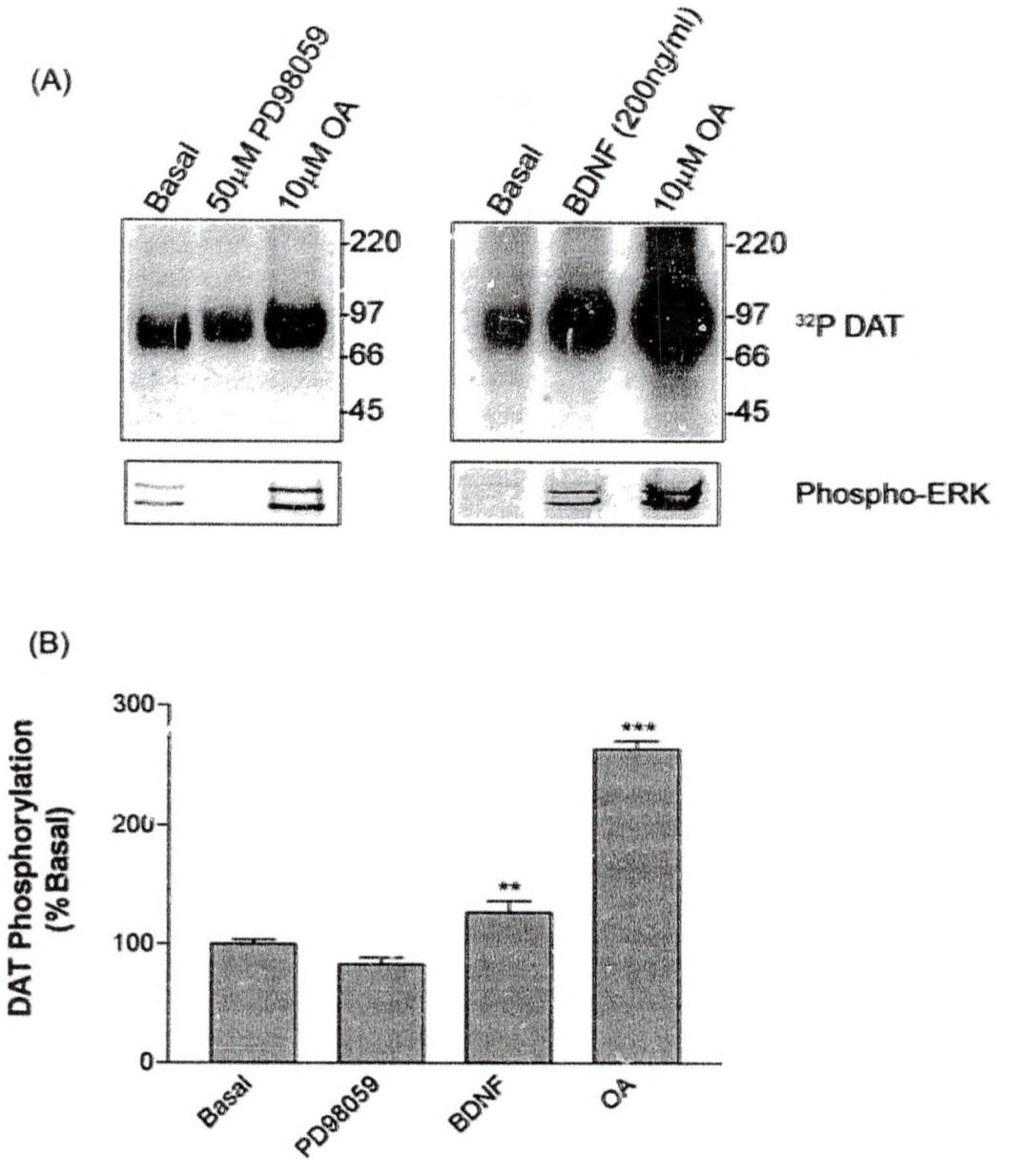

Figure 22: Effect of BDNF and MEK Inhibitor on DAT Phosphorylation

control and these values are statistically insignificant compared with control (Figure. 22, left). The addition of BDNF increased basal DAT phosphorylation levels to 126.9 ± 9.6% of control (Figure. 22, right) ($p<0.01$). In addition, the immunoblot results showed that BDNF or PD98059 treatments increased or decreased the phospho-ERK levels respectively. These results are consistent with previous reports [99].

CHAPTER IV

DISCUSSION

Differential Effects of DA and Psychoactive Drugs on DAT Phosphorylation and Regulation.

This study investigated the acute effects of multiple DA uptake blockers on basal and PKC-stimulated DAT phosphorylation and transport regulation. To our knowledge this is the first such study to examine β-CFT, mazindol, or MPH with respect to most of these properties. Our results show that (−)-cocaine, β-CFT, mazindol, or MPH do not affect the levels of basal and PMA stimulated DAT phosphorylation in rDAT LLC-PK_1 cells. In contrast, Cowell *et al* (2000) have reported that cocaine suppressed PMA stimulated phosphorylation in striatal synaptosomes [88]. These investigators used a cocaine plus PMA treatment time of 45 s, presenting the possibility that cocaine might affect an early phase of PMA-induced DAT phosphorylation or specific cocaine inducible processes in brain that are not present in cell lines. If cocaine suppresses PMA-stimulated phosphorylation only at shorter PMA treatment times, our results suggest that these effects are transient and rapidly become masked or reversed by sustained activation of PKC. Such a possibility is supported by the biphasic regulation of SERT transport activity and phosphorylation by PKC with distinct effects observed at shorter (1–5 min) and longer (30 min) PMA treatment times [100]. If the different results of the DAT studies are related to cocaine-induced processes

cocaine users, acute presence of drug would not directly affect these or related activities. Radiotracer analogs of β-CFT are widely used in clinical and experimental *in vivo* imaging studies [103] image and quantify transporter availability with positron emission tomography (PET) or single-photon emission computed tomography (SPECT). The results of these studies indicate little potential for cocaine-based imaging agents to directly produce effects on subcellular location or binding capacity of DAT that might complicate image interpretation.

We also examined the acute effects of other classes of DA uptake inhibitors that are in current clinical and preclinical use. Like cocaine, neither mazindol nor MPH affected basal or PMA-stimulated DAT phosphorylation. MPH and mazindol pretreatment were also without effect on DA transport, as previously found for MPH [83], and MPH and possibly mazindol did not affect PMA-induced transport down-regulation. Thus there is no evidence from *in vitro* studies to suggest that these physiological processes would be acutely affected in patients using these drugs. Both of these drugs induce self-administration and other cocaine-like behaviors [47, 48], which may potentially relate to the similar lack of effects on DAT phosphorylation and regulation.

We have also examined the acute effects of GBR 12909, a potent DA noncompetitive inhibitor designed to treat cocaine abuse. GBR 12909 did not affect basal DAT phosphorylation, but it strongly suppressed PMA-stimulated phosphorylation and cell surface biotinylation. These results indicate that GBR

12909 prevents PMA-induced down-regulation and may induce upregulation of the DAT surface expression.

Although the GBR compound acts as a DA uptake blocker similar to cocaine, the pharmacological properties of this drug are not clearly properly understood. The basis for differential effects of GBR 12909 has been hypothesized to involve ligand binding kinetics and/or binding sites [104, 105]. Unlike cocaine displacement, GBR compounds were not displaced due to their higher hydrophobicity and therefore they cannot be removed from cells or membranes in wash-out procedures. Hydrophobic partitioning of GBR in the membrane may generate a continually available reservoir of ligand that results in pseudo-irreversible binding to DAT and long-term blockade of DA transport activity [53]. Such long-lasting binding to DAT may affect its phosphorylation or endocytosis properties, which in turn may play a role in drug-induced behavior.

The suppression of PMA-stimulated phosphorylation by GBR 12909 may be due to its non-specific effect on membranes. So GBR compounds alter the ability of DAT to interact with kinases, phosphatases, or endocytic proteins. This could also explain the unaffected basal phosphorylation during GBR treatment. Increasing evidence indicates that cocaine or GBR 12909 binding sites are at least partially distinct [104, 106]. Irreversible GBR analogs bind to DAT in transmembrane domains 1 or 2 [90], suggesting the potential for binding to induce a DAT conformation that affects phosphorylation of the adjacent N-terminal tail [65]. The suppression of PMA-induced phosphorylation and endocytosis by GBR compounds suggests that this class of compounds could

attenuate functions controlled by PKC. GBR has been demonstrated to block AMPH-induced DA efflux [88], but the potential functional significance of acute GBR inhibition of this function is not obvious.

Further, we examined the effects of substrate DA on DAT phosphorylation and DA transport activity. DA concentrations from 1-20 μM show significant dose dependent down regulation in transport activity. The extent of DA-induced down regulation is consistent with previous findings [81]. However DA did not affect either basal or PMA stimulated DAT phosphorylation. In contrast, psychostimulant substrates AMPH or METH induce DAT phosphorylation while affecting transport down regulation [66, 85]. One caveat for absence of DA effect on DAT phosphorylation is that a low level of phosphorylation induced by DA treatment may be masked by the overall signal or may be missed if the samples were dephosphorylated during processing [72]. Additional studies are needed to clarify these issues. These results are related to the necessity for DAT phosphorylation to permit efflux [40] and the differential ability of AMPH but not DA to induce substrate channels in DAT [27].

Pretreatment with DA or PMA at sub-maximal or maximal concentrations produced down-regulation responses that are not different from down regulatory responses produced by co-treatments at respective concentrations. If these two compounds exert their effects independently, it is expected that co-treatment of DA and PMA will produce a much stronger additive effect. However, this did not occur at sub-maximal and maximal concentrations suggesting that DA- or PKC-induced down regulation mechanisms occur via a common pathway. Additionally,

blockade of DA-induced transport down regulation by BIM supports this idea and these results were consistent with AMPH or METH induced down regulatory mechanisms [83, 85]. Based on these studies, it is possible that pathways related to substrate or PKC induced effects can merge *in vivo* and do not produce additivity.

The mechanistic role of DA in the activation of PKC-dependent DAT regulatory pathways is not known. Transport may change local ion concentrations that may modulate kinases or phosphatases that act on transport-dependent DAT conformations or affect DA transport-associated DAT-protein interactions. A SNARE-dependent protein, Syntaxin 1 has been reported to interact with N-terminal tails of GAT1 [78, 80] and regulate substrate-induced down regulation, through interaction with N-terminal tails. Similar types of DAT regulatory mechanisms have been proposed to be involved in DA induced transport down regulation [73].

Our findings that application of DA did not result in interference of PKC-induced DAT phosphorylation or down-regulation contrast significantly with the finding that substrates inhibit these properties of SERT [92]. Similarly GAT1 GABA transporters show upregulation of function in the presence of substrate [107], whereas DATs are down-regulated under comparable conditions. Thus for SERT and GAT1, substrates induce homeostatic mechanisms that maintain or increase transmitter clearance, while the opposite occurs for DAT. Down-regulation of DAT by DA requires concentrations that are significantly above the transport K_m, suggesting that the response occurs primarily under conditions of

extreme transport demand. Transport-induced down-regulation of DAT may represent a neuroprotective mechanism that functions when substrate levels are high to limit translocation and cytoplasmic accumulation of DA and its neurotoxic metabolites such as 6-hydroxydopamine that can activate apoptotic responses (Luo et al., 1999). Individual variabilities in these molecular mechanisms may thus to contribute to selective vulnerabilities to Parkinson's disease or other dopaminergic pathologies.

Regulation of DAT and related neurotransmitter transporters is proving to be a complex process involving multiple functions of these proteins, their subcellular distribution, and trafficking. The results presented here further contribute to the elucidation of these processes and indicate the potential for therapeutic and abused DAT drugs to exert some of their effects by modulation of DAT phosphorylation and/or regulation of surface expression in addition to their pharmacological actions.

MAPKs Phosphorylate the N-terminal Tail of DAT *In Vitro*

In this study, we have shown that multiple protein kinases phosphorylate NDAT and MAPKs specifically phosphorylate at T53 *in vitro* which may potentially be involved *in vivo* phosphorylation of DAT. To our knowledge, this is the first study to show the *in vitro* phosphorylation of a recombinantly expressed N-terminus of DAT.

Evidence of *in vitro* phosphorylation of NDAT is consistent with the presence of phosphorylation on the N-terminal tail of the DAT *in vivo* [65]. The results of these studies are comparable with *in vivo* assays, which may reflect the physiological conditions. Established studies have shown that PKC activators such as PMA or OAG increase DAT phosphorylation in both LLC-PK_1 cells and striatal slices indicating that PKC is involved in DAT phosphorylation [63, 65]. The *in vitro* phosphorylation of NDAT by purified PKC is consistent with the idea that PKC may directly phosphorylate DAT *in vivo*.

Additionally, CaMK II, PKA, PKG, CdK5, Akt1, MAPKs including ERK1/2, p38, and JNK2 phosphorylated NDAT indicating the potential for one or more these kinases to phosphorylate DAT *in vivo*. However, there is no evidence to support the role of multiple protein kinases in DAT phosphorylation *in vivo*. Treatment of synaptosomes with forskolin had no affect on DAT phosphorylation suggesting that PKA may not be involved in DAT phosphorylation [63]. The roles of other protein kinases in DAT phosphorylation are not known. More *in vivo* experiments are needed to examine if multiple protein kinases are involved in this process.

phosphatases *in vivo [72]*. In contrast, none of the tested protein phosphatases were able to dephosphorylate ERK-phosphorylated NDATs. Based on a shift in electrophoretic mobility and resistance to phosphatase treatment it may be presumed that ERK1 phosphorylated NDAT may have attained a different structure that may be inaccessible for the tested protein phosphatases.

Further, the resistance of ERK-phosphorylated NDAT for dephosphorylation may be explained by comparing with following caveat. The proline-directed serine/threonine phosphorylation of Tau protein regulates microtubule association by keeping the protein in a favorable cis-confirmation that is not accessible to protein phosphatases such as PP2A [108, 109]. This allows the protein to significantly retain phosphorylation for a greater duration by checking spontaneous dephosphorylation. Biologically, this conformation can be converted into a trans-conformation by peptidyl–prolyl cis/trans isomerase enzyme (Pin1), which is then susceptible to protein dephosphorylation and accessible for protein phosphatases [108]. We speculate a similar type conformational change may have occurred in ERK phosphorylated NDAT leading to inaccessibility by protein phosphatases that result in resistance to dephosphorylation. This distinct conformation and inaccessibility to protein phosphatases may be implicated in a role for DAT-protein interactions. The identification of interaction between PP2A and DAT [75] supports a potential mechanistic relationship between PP2A and proline-directed threonine phosphorylation.

Our mutational analysis of NDAT followed by *in vitro* phosphorylation showed that T53 is a MAPK phosphorylation site for NDAT *in vitro*. Even though T53 is located in favored consensus recognition motif for ERK phosphorylation (P-X-S/T-P), minimal consensus sequence is enough to phosphorylate S/T preceded by proline (S/T-P) [110, 111]. Such sequences are present in C-terminal tail of rat DAT (T593) in addition to T53. The lack of phosphorylation of T593 in CDAT and phosphorylation of T53 of NDAT by ERK suggests phospho-T observed with full length DAT phosphoamino acid analysis may be from T53.

Further, to localize the T phosphorylation we proteolyzed the full-length striatal DAT with endoproteinase Asp-N that specifically cleaves the peptide bond on the N-terminal side of D residues. The predicted cleavage site for Asp-N is D174 located on EL2 of DAT results in a 19 kDa phosphopeptide that showed phospho-T with phosphoamino acid analysis suggesting that threonine phosphorylation occurs on the N-terminal cytosolic tail. Further, the identification of an *in vitro* phosphorylation site at T53 and localization of phospho-T in Asp-N fragment suggests that T53 may be an *in vivo* phosphorylation site.

These results cannot rule out the possibility that phosphorylation may occur in other portions of DAT. DAT contains potential phosphorylation sites on IL2, which are highly conserved throughout the cocaine sensitive neurotransmitter transporters and has been shown to undergo phosphorylation in both NET and SERT [112, 113]. SERT and NET undergo phosphorylation on T276 and T258 respectively which are present on IL2 of these transporters. The corresponding residue for DAT is T260 in IL2 of DAT, which is also located in a

PKC/PKA/PKG consensus recognition motif. Based on these studies, it ispossible that T260 may also be involved in DAT phosphorylation.

Our independent study to assess the effect of ERKs on DA transport activity was consistent with previous results. Moron *et al* (2003) have shown that treatment of cells or synaptosomes with MEK inhibitor PD98059, decreased DA transport activity and DAT surface expression [70]. The application of PD98059 showed decrease in transport activity while suppressing the activation of ERKs suggesting that activation of ERKs regulates DA transport activity. The general scheme of ERK activation involves three sequentially activated kinases. The ERK family of MAPKs is activated by different kinds of stimuli including growth factors, cytokines, and ligands of heterotrimeric G protein coupled receptors. These diverse external stimuli activate the proto-oncogenic small G protein, Ras which in turn activates the protein kinase cascade that includes Raf → MEK (ERK kinase) → ERK [114]. Activity of ERKs is regulated by phosphorylation and dephosphorylation. Dephosphorylated ERKs are inactive, but once activated by MEK-mediated phosphorylation, ERKs then regulate the target proteins such as phospholipases, transcription factors, and cytoskeletal proteins through direct phosphorylation. Increasing evidence suggests that ERKs are also involved in phosphorylation and regulation of membrane proteins including receptors, channels, and connexins [115-117]. Hence, the regulation of these protein forms the basis for controlling various processes including cell growth, morphogenesis, synaptic plasticity, and learning.

Therefore to evaluate the role of ERKs on DA transport activity, we transiently transfected the LLC-PK_1 cells with MEK-CA or MEK-KO. The transfection of a MEK-CA mutant should result in the activation of ERKs constitutively even in the absence of growth factor [98], which results in increased levels of phospho-ERK. The MEK-KO mutant is a kinase-dead mutant and transfection with this mutant should produce a dominant negative effect in the activation of ERKs that in turn results in decreased levels of phospho-ERK. Transient expression of MEK-CA showed an increase in DA transport and phospho-ERK levels in rDAT expressing HEK cells. (Moron et al 2003). However, our results showed that there was no change in the levels of phospho-ERK following the transient expression, which made it impossible to relate it with DA transport in this study. The presence of inappropriate expression patterns in phospho-ERK levels in this experiment can be speculated as cell type specific effects and this result is not consistent with previous results [70, 98]. Further, evidence for ERKs role in the regulation of DA transport has come from growth factor stimulation studies. Recently, Hoover et al (2006) have shown that application of BDNF leads to activation of ERKs and an increase in DA transport in synaptosomes [99].

Based on NDAT phosphorylation studies, it can be speculated that ERKs may promote DAT phosphorylation *in vivo*. To examine this possibility we performed the ^{32}P metabolic labeling of striatal slices in the presence of BDNF and PD98059. Treatment with BDNF significantly increased basal DAT phosphorylation and phospho-ERK levels. Additionally, the application of MEK

inhibitor PD98059, showed a marginal decrease in basal DAT phosphorylation and phospho-ERK levels. The role of ERKs on DAT properties have been less studied. Lin *et al* (2003) have reported that ERK inhibitors such as U0126 decreased basal DAT phosphorylation indicating that ERKs may regulate the constitutive phosphorylation of DAT [68]. Taken together, these results suggest that the activation of ERKs play a role in DAT phosphorylation. The marginal effects of these compounds on DAT phosphorylation may be due to inaccessibility of these compounds to the striatal tissues. Metabolic labeling of synaptosomes may circumvent the observed partial effects of these compounds.

Collectively these results suggest that ERKs may play a role in DAT phosphorylation and DAT regulation. Also these studies may increase the current understanding of the role of DAT phosphorylation in DAT function. *In vivo* verification of putative T53 phosphorylation site is highly warranted before pursuing functional aspects of DAT. The best way to accomplish this can be mass spectrometric analysis of native DATs.

APPENDICES

APPENDIX A

Rat DAT cDNA sequence in pcDNA 3.0 is shown below. The coding sequence is underlined between the untranslated sequences.

Eco RI

5`.....[redacted]CCGCAGGAGTCAGTCGAAGAAGAAAGAAGCAGAGTTCCTTG
GGCTCCGGTCTACCCATGAGTAAGAGCAAATGCTCCGTGGGACCAATGTCT
TCAGTGGTGGCCCCGGCTAAAGAGTCCAATGCTGTGGGCCCCAGAGAGGT
GGAGCTCATCCTGGTCAAGGAGCAGAACGGAGTGCAGCTGACCAACTCCA
CCCTCATCAACCCGCCACAGACACCAGTGGAGGCTCAAGAGCGGGAGACC
TGGAGCAAGAAAATTGATTTCCTGCTATCAGTCATCGGCTTTGCTGTGGACC
TGGCCAATGTCTGGAGGTTTCCCTACCTGTGCTACAAAAATGGTGGAGGTG
CCTTCCTGGTGCCCTACCTGCTCTTCATGGTTATTGCTGGGATGCCCCTCTT
CTACATGGAGCTGGCTCTCGGACAGTTCAACAGAGAAGGAGCTGCTGGTGT
CTGGAAGATCTGTCCTGTCCTGAAAGGTGTGGGCTTCACTGTTATCCTCATC
TCTTTCTACGTGGGCTTCTTCTACAATGTCATCATCGCATGGGCACTGCACT
ACTTCTTCTCCTCCTTCACCATGGACCTCCCATGGATCCACTGCAACAACAC
CTGGAATAGCCCCAACTGCTCCGATGCCCATGCCAGCAACTCTAGCGACGG
CCTGGGCCTCAATGACACCTTTGGGACCACACCCGCTGCTGAGTACTTTGA
GCGTGGCGTGCTGCACCTTCACCAGAGCCGTGGCATTGATGACCTGGGCC
CTCCACGGTGGCAGCTCACAGCCTGCCTGGTGCTGGTCATTGTTCTGCTCT
ACTTCAGCCTATGGAAGGGAGTAAAGACCTCAGGGAAGGTGGTGTGGATCA
CAGCTACCATGCCCTATGTGGTCCTCACAGCCCTGCTCCTGCGTGGAGTTA
CCCTTCCTGGAGCCATGGATGGCATCAGAGCATACCTCAGTGTGGACTTCT
ACCGACTCTGTGAGGCATCTGTGTGGATCGATGCTGCCACCCAGGTGTGCT
TCTCCCTCGGCGTTGGGTTTGGAGTGCTGATTGCCTTCTCCAGTTACAATAA
ATTCACCAATAACTGCTATAGAGACGCAATCATCACCACCTCCATTAACTCC
CTGACAAGCTTCTCCTCTGGCTTCGTCGTCTTCTCCTTCCTGGGGTATATGG
CACAGAAGCACAATGTGCCCATCAGAGATGTGGCCACAGATGGACCTGGG
CTCATCTTCATCATCTATCCTGAGGCGATCGCCACACTCCCGCTGTCTTCTG
CCTGGGCTGCTGTCTTCTTCCTCATGCTGCTCACTCTGGGTATCGACAGTG
CAATGGGGGGCATGGAGTCAGTGATCACTGGGCTCGTCGATGAGTTCCAG
CTGCTACATCGGCATCGAGAGCTCTTCACTCTTGGCATTGTCCTGGCTACTT
TCCTGCTGTCTCTCTTCTGCGTCACCAACGGTGGCATCTACGTCTTCACACT
GCTGGACCACTTTGCAGCTGGCACATCTATCCTCTTTGGCGTGCTCATTGAA
GCCATTGGGGTGGCCTGGTTCTACGGCGTCCAGCAATTCAGTGATGACATC
AAGCAAATGACAGGGCAGCGACCCAACCTGTACTGGCGGCTATGCTGGAA
GCTGGTCAGCCCCTGCTTCCTCCTGTATGTGGTCGTGGTCAGCATTGTGAC
CTTCAGACCCCCACACTATGGGGCCTACATCTTCCCAGACTGGGCCAATGC
CCTGGGCTGGATCATCGCCACATCCTCCATGGCCATGGTGCCCATTTATGC

GACCTACAAGTTCTGCAGCCTGCCGGGGTCCTTCCGGGAGAAACTGGCCT
ATGCCATCACACCTGAGAAAGACCATCAGCTAGTGGACAGAGGGGAGGTG
CGCCAATTCACGCTGCGTCACTGGCTGTTGCTGTAAAGTGGAAGGAGACAG
CTGCCAGCTGGGCCACCTCACAACAGCGGGGACAGGGAGATCGCAAAGGA
AACCCACGAGTCAAGAAAGGAAGGAGGGCCACTTCCATGCTTCTCCTTTGT
CGTACGGAAAAATAATCGAAGCATGGGCTTCAACCTTTGACTGTTCACACCC
AAATCATTGCCACAAAGAAGCCTCTGTCTGTGTATGGCTGTAAAAACATACA
CCTCTACACAGTGAGGTCAACAATGTCCCTGTCCCTACTGGGTGGGAAAAC
CCTAGCTGGTATCCTGTCCCTGCAAGGCTGACTCCCCCATCTGTGGTCACT
CTGGGAGAACAGGTCATACTGCCCCCT[redacted].....3`

Eco RI

APPENDIX B

The cloned pTYB2-NDAT sequence showing the rat DAT N-terminal cytosolic tail cDNA sequence is shown below. Underlined sequence represents the restriction sites, yellow highlighted sequence shows primer binding sites in the pTYB2 plasmid and sequence in red letters represents cDNA sequence representing the cleaved NDAT protein.

T7 universal primer

pTYB2 5`..... .....CGGGGATCTCGATCCCGCGAAATTAATACGACTCACTAT
AGGGGAATTGTGAGCGGATAACAATTCCCCTCTAGAAATAATTTTGTTTAAC

Nde I

TTTAAGAAGGAGATATACATATGAGTAAGAGCAAATGCTCCGTGGGACCAAT
GTCTTCAGTGGTGGCCCCGGCTAAAGAGTCCAATGCTGTGGGCCCCAGAG
AGGTGGAGCTCATCCTGGTCAAGGAGCAGAACGGAGTGCAGCTGACCAAC
TCCACCCTCATCAACCCGCCACAGACACCAGTGGAGGCTCAAGAGCGGGA

Sma I

GACCTGGAGCAAGCCCGGGTGCTTTGCCAAGGGTACCAATGTTTTAATGGC
GGATGGGTCTATTGAATGTATTGAAAACATTGAGGTTGGTAATAAGGTCATG
GGT .....3´

Intein reverse sequencing primer

APPENDIX C

The cloned pTYB12-CDAT sequence showing the rat DAT C-terminal cytosolic tail cDNA sequence is shown below. Underlined sequence represents the restriction sites, yellow highlighted sequence shows primer binding sites in the pTYB12 plasmid and sequence in red letters represents cDNA sequence representing the cleaved CDAT protein.

pTYB12 Intein Forward Primer → (117 bp) .....

Bsm I

5′...GGATCCCAGGTTGTTGTACAGAATGCTTTCTGCAGCCTGCCGGGGTCCT
TCCGGGAGAAACTGGCCTATGCCATCACACCTGAGAAAGACCATCAGCTAG
TGGACAGAGGGGAGGTGCGCCAATTCACGCTGCGTCACTGGCTGTTGCTG
TAACTCGAGCCCGGGTGACTGCAG...3′

Xho I

(58 bp) ←T7 Terminator Reverse Primer

APPENDIX D

Primary protein sequence of NDAT and CDAT

NDAT:
MSKSKCSVGPMSSVVAPAKESNAVGPREVELILVKEQNGVQLTNSTLINPPQTP
VEAQERETWSK

CDAT:
FCSLPGSFREKLAYAITPEKDHQLVDRGEVRQFTLRHWLLL

APPENDIX E

Site directed mutagenesis primers

The sequences of oligonucleotide primers used for Quick Change® site directed mutagenesis. The substituted codons are highlighted in red.

Name	Sequence
T43A	
Forward	AACGGAGTGCAGCTGGCCAACTCCACCCTCATC
Reverse	GATGAGGGTGGAGTTGGCCAGCTGCACTCCGTT
T46A	
Forward	CAGCTGACCAACTCCGCCCTCATCAACCCGCCA
Reverse	TGGCGGGTTGATGAGGGCGGAGTTGGTCAGCTG
T53A	
Forward	CTCATCAACCCGCCACAGGCACCAGTGGAGGCTCAAGAG
Reverse	CTCTTGAGCCTCCACTGGTGCCTGTGGCGGGTTGATGAG
T62A	
Forward	GCTCAAGAGCGGGAGGCCTGGAGCAAGCCCGGG
Reverse	CCCGGGCTTGCTCCAGGCCTCCCGCTCTTGAGC

REFERENCES

1. Sudhof, T.C., *The synaptic vesicle cycle: a cascade of protein-protein interactions.* Nature, 1995. **375**(6533): p. 645-53.

2. Sudhof, T.C., *The synaptic vesicle cycle.* Annu Rev Neurosci, 2004. **27**: p. 509-47.

3. Jahn, R., T. Lang, and T.C. Sudhof, *Membrane fusion.* Cell, 2003. **112**(4): p. 519-33.

4. Amara, S.G. and M.J. Kuhar, *Neurotransmitter transporters: recent progress.* Annu Rev Neurosci, 1993. **16**: p. 73-93.

5. Lindvall, O., A. Bjorklund, and G. Skagerberg, *Selective histochemical demonstration of dopamine terminal systems in rat di- and telencephalon: new evidence for dopaminergic innervation of hypothalamic neurosecretory nuclei.* Brain Res, 1984. **306**(1-2): p. 19-30.

6. Axelrod, J. and I.J. Kopin, *The uptake, storage, release and metabolism of noradrenaline in sympathetic nerves.* Prog Brain Res, 1969. **31**: p. 21-32.

7. Iversen, L.L., *The Uptake of Noradrenaline by the Isolated Perfused Rat Heart.* Br J Pharmacol Chemother, 1963. **21**: p. 523-37.

8. Eisenfeld, A.J., J. Axelrod, and L. Krakoff, *Inhibition of the extraneuronal accumulation and metabolism of norepinephrine by adrenergic blocking agents.* J Pharmacol Exp Ther, 1967. **156**(1): p. 107-13.

9. Iversen, L.L., B. Jarrott, and M.A. Simmonds, *Differences in the uptake, storage and metabolism of (+)- and (-)-noradrenaline.* Br J Pharmacol, 1971. **43**(4): p. 845-55.

10. Bannon, M.J., et al., *Expression of a human cocaine-sensitive dopamine transporter in Xenopus laevis oocytes.* J Neurochem, 1990. **54**(2): p. 706-8.

11. Guastella, J., et al., *Cloning and expression of a rat brain GABA transporter.* Science, 1990. **249**(4974): p. 1303-6.

12. Pacholczyk, T., R.D. Blakely, and S.G. Amara, *Expression cloning of a cocaine- and antidepressant-sensitive human noradrenaline transporter.* Nature, 1991. **350**(6316): p. 350-4.

13. Shimada, S., et al., *Cloning and expression of a cocaine-sensitive dopamine transporter complementary DNA.* Science, 1991. **254**(5031): p. 576-8.

14. Giros, B., et al., *Cloning, pharmacological characterization, and chromosome assignment of the human dopamine transporter.* Mol Pharmacol, 1992. **42**(3): p. 383-90.

15. Ramamoorthy, S., et al., *Antidepressant- and cocaine-sensitive human serotonin transporter: molecular cloning, expression, and chromosomal localization.* Proc Natl Acad Sci U S A, 1993. **90**(6): p. 2542-6.

16. Chen, N.H., M.E. Reith, and M.W. Quick, *Synaptic uptake and beyond: the sodium- and chloride-dependent neurotransmitter transporter family SLC6.* Pflugers Arch, 2004. **447**(5): p. 519-31.

17. Rudnick, G. and J. Clark, *From synapse to vesicle: the reuptake and storage of biogenic amine neurotransmitters.* Biochim Biophys Acta, 1993. **1144**(3): p. 249-63.

18. Zahniser, N.R. and S. Doolen, *Chronic and acute regulation of Na+/Cl- -dependent neurotransmitter transporters: drugs, substrates, presynaptic receptors, and signaling systems.* Pharmacol Ther, 2001. **92**(1): p. 21-55.

19. Li, L.B., et al., *The role of N-glycosylation in function and surface trafficking of the human dopamine transporter.* J Biol Chem, 2004. **279**(20): p. 21012-20.

20. Giros, B. and M.G. Caron, *Molecular characterization of the dopamine transporter.* Trends Pharmacol Sci, 1993. **14**(2): p. 43-9.

21. Mortensen, O.V. and S.G. Amara, *Dynamic regulation of the dopamine transporter.* Eur J Pharmacol, 2003. **479**(1-3): p. 159-70.

22. Butcher, S.P., et al., *Amphetamine-induced dopamine release in the rat striatum: an in vivo microdialysis study.* J Neurochem, 1988. **50**(2): p. 346-55.

23. Yamashita, A., et al., *Crystal structure of a bacterial homologue of Na+/Cl- -dependent neurotransmitter transporters.* Nature, 2005. **437**(7056): p. 215-23.

24. Sonders, M.S. and S.G. Amara, *Channels in transporters.* Curr Opin Neurobiol, 1996. **6**(3): p. 294-302.

25. Sonders, M.S., et al., *Multiple ionic conductances of the human dopamine transporter: the actions of dopamine and psychostimulants.* J Neurosci, 1997. **17**(3): p. 960-74.

26. Ingram, S.L., B.M. Prasad, and S.G. Amara, *Dopamine transporter-mediated conductances increase excitability of midbrain dopamine neurons.* Nat Neurosci, 2002. **5**(10): p. 971-8.

27. Kahlig, K.M., et al., *Amphetamine induces dopamine efflux through a dopamine transporter channel.* Proc Natl Acad Sci U S A, 2005. **102**(9): p. 3495-500.

28. Kahlig, K.M., et al., *Regulation of dopamine transporter trafficking by intracellular amphetamine.* Mol Pharmacol, 2006. **70**(2): p. 542-8.

29. Torres, G.E., et al., *Oligomerization and trafficking of the human dopamine transporter. Mutational analysis identifies critical domains important for the functional expression of the transporter.* J Biol Chem, 2003. **278**(4): p. 2731-9.

30. Sorkina, T., et al., *Oligomerization of dopamine transporters visualized in living cells by fluorescence resonance energy transfer microscopy.* J Biol Chem, 2003. **278**(30): p. 28274-83.

31. Hastrup, H., N. Sen, and J.A. Javitch, *The human dopamine transporter forms a tetramer in the plasma membrane: cross-linking of a cysteine in the fourth transmembrane segment is sensitive to cocaine analogs.* J Biol Chem, 2003. **278**(46): p. 45045-8.

32. Hastrup, H., A. Karlin, and J.A. Javitch, *Symmetrical dimer of the human dopamine transporter revealed by cross-linking Cys-306 at the extracellular end of the sixth transmembrane segment.* Proc Natl Acad Sci U S A, 2001. **98**(18): p. 10055-60.

33. Chen, N. and M.E. Reith, *Substrates dissociate dopamine transporter oligomers.* J Neurochem, 2008. **105**(3): p. 910-20.

34. Sulzer, D., et al., *Amphetamine redistributes dopamine from synaptic vesicles to the cytosol and promotes reverse transport.* J Neurosci, 1995. **15**(5 Pt 2): p. 4102-8.

35. Sulzer, D., N.T. Maidment, and S. Rayport, *Amphetamine and other weak bases act to promote reverse transport of dopamine in ventral midbrain neurons.* J Neurochem, 1993. **60**(2): p. 527-35.

36. Raiteri, M., et al., *Release of dopamine from striatal synaptosomes.* Ann Ist Super Sanita, 1978. **14**(1): p. 97-110.

37. Sulzer, D. and S. Rayport, *Amphetamine and other psychostimulants reduce pH gradients in midbrain dopaminergic neurons and chromaffin granules: a mechanism of action.* Neuron, 1990. **5**(6): p. 797-808.

38. Fischer, J.F. and A.K. Cho, *Chemical release of dopamine from striatal homogenates: evidence for an exchange diffusion model.* J Pharmacol Exp Ther, 1979. **208**(2): p. 203-9.

39. Jones, S.R., et al., *Dopamine neuronal transport kinetics and effects of amphetamine.* J Neurochem, 1999. **73**(6): p. 2406-14.

40. Khoshbouei, H., et al., *N-terminal phosphorylation of the dopamine transporter is required for amphetamine-induced efflux.* PLoS Biol, 2004. **2**(3): p. E78.

41. Bannon, M.J., *The dopamine transporter: role in neurotoxicity and human disease.* Toxicol Appl Pharmacol, 2005. **204**(3): p. 355-60.

42. Blum, D., et al., *Molecular pathways involved in the neurotoxicity of 6-OHDA, dopamine and MPTP: contribution to the apoptotic theory in Parkinson's disease.* Prog Neurobiol, 2001. **65**(2): p. 135-72.

43. Javitch, J.A. and S.H. Snyder, *Uptake of MPP(+) by dopamine neurons explains selectivity of parkinsonism-inducing neurotoxin, MPTP.* Eur J Pharmacol, 1984. **106**(2): p. 455-6.

44. Javitch, J.A., et al., *Parkinsonism-inducing neurotoxin, N-methyl-4-phenyl-1,2,3,6 -tetrahydropyridine: uptake of the metabolite N-methyl-4-phenylpyridine by dopamine neurons explains selective toxicity.* Proc Natl Acad Sci U S A, 1985. **82**(7): p. 2173-7.

45. Nicklas, W.J., et al., *Mitochondrial mechanisms of neurotoxicity.* Ann N Y Acad Sci, 1992. **648**: p. 28-36.

46. Kuhar, M.J., M.C. Ritz, and J.W. Boja, *The dopamine hypothesis of the reinforcing properties of cocaine.* Trends Neurosci, 1991. **14**(7): p. 299-302.

47. Ritz, M.C., et al., *Cocaine receptors on dopamine transporters are related to self-administration of cocaine.* Science, 1987. **237**(4819): p. 1219-23.

48. Bergman, J., et al., *Effects of cocaine and related drugs in nonhuman primates. III. Self-administration by squirrel monkeys.* J Pharmacol Exp Ther, 1989. **251**(1): p. 150-5.

49. Andersen, P.H., *The dopamine inhibitor GBR 12909: selectivity and molecular mechanism of action.* Eur J Pharmacol, 1989. **166**(3): p. 493-504.

50. Tella, S.R., B. Ladenheim, and J.L. Cadet, *Differential regulation of dopamine transporter after chronic self-administration of bupropion and nomifensine.* J Pharmacol Exp Ther, 1997. **281**(1): p. 508-13.

51. Rothman, R.B., et al., *GBR12909 antagonizes the ability of cocaine to elevate extracellular levels of dopamine.* Pharmacol Biochem Behav, 1991. **40**(2): p. 387-97.

52. Sogaard, U., et al., *A tolerance study of single and multiple dosing of the selective dopamine uptake inhibitor GBR 12909 in healthy subjects.* Int Clin Psychopharmacol, 1990. **5**(4): p. 237-51.

53. Baumann, M.H., et al., *Preclinical evaluation of GBR12909 decanoate as a long-acting medication for methamphetamine dependence.* Ann N Y Acad Sci, 2002. **965**: p. 92-108.

54. Preti, A., *Vanoxerine National Institute on Drug Abuse.* Curr Opin Investig Drugs, 2000. **1**(2): p. 241-51.

55. Koe, B.K., *Molecular geometry of inhibitors of the uptake of catecholamines and serotonin in synaptosomal preparations of rat brain.* J Pharmacol Exp Ther, 1976. **199**(3): p. 649-61.

56. Chait, L.D., E.H. Uhlenhuth, and C.E. Johanson, *Reinforcing and subjective effects of several anorectics in normal human volunteers.* J Pharmacol Exp Ther, 1987. **242**(3): p. 777-83.

57. Dutta, A.K., et al., *Dopamine transporter as target for drug development of cocaine dependence medications.* Eur J Pharmacol, 2003. **479**(1-3): p. 93-106.

58. Fone, K.C. and D.J. Nutt, *Stimulants: use and abuse in the treatment of attention deficit hyperactivity disorder.* Curr Opin Pharmacol, 2005. **5**(1): p. 87-93.

59. Volkow, N.D., et al., *Dopamine transporter occupancies in the human brain induced by therapeutic doses of oral methylphenidate.* Am J Psychiatry, 1998. **155**(10): p. 1325-31.

60. Melikian, H.E., *Neurotransmitter transporter trafficking: endocytosis, recycling, and regulation.* Pharmacol Ther, 2004. **104**(1): p. 17-27.

61. Doolen, S. and N.R. Zahniser, *Conventional protein kinase C isoforms regulate human dopamine transporter activity in Xenopus oocytes.* FEBS Lett, 2002. **516**(1-3): p. 187-90.

62. Vaughan, R.A., *Phosphorylation and regulation of psychostimulant-sensitive neurotransmitter transporters.* J Pharmacol Exp Ther, 2004. **310**(1): p. 1-7.

63. Vaughan, R.A., et al., *Protein kinase C-mediated phosphorylation and functional regulation of dopamine transporters in striatal synaptosomes.* J Biol Chem, 1997. **272**(24): p. 15541-6.

64. Huff, R.A., et al., *Phorbol esters increase dopamine transporter phosphorylation and decrease transport Vmax.* J Neurochem, 1997. **68**(1): p. 225-32.

65. Foster, J.D., B. Pananusorn, and R.A. Vaughan, *Dopamine transporters are phosphorylated on N-terminal serines in rat striatum.* J Biol Chem, 2002. **277**(28): p. 25178-86.

66. Granas, C., et al., *N-terminal truncation of the dopamine transporter abolishes phorbol ester- and substance P receptor-stimulated phosphorylation without impairing transporter internalization.* J Biol Chem, 2003. **278**(7): p. 4990-5000.

67. Page, G., et al., *The up-regulation of the striatal dopamine transporter's activity by cAMP is PKA-, CaMK II- and phosphatase-dependent.* Neurochem Int, 2004. **45**(5): p. 627-32.

68. Fog, J.U., et al., *Calmodulin kinase II interacts with the dopamine transporter C terminus to regulate amphetamine-induced reverse transport.* Neuron, 2006. **51**(4): p. 417-29.

69. Carvelli, L., et al., *PI 3-kinase regulation of dopamine uptake.* J Neurochem, 2002. **81**(4): p. 859-69.

70. Moron, J.A., et al., *Mitogen-activated protein kinase regulates dopamine transporter surface expression and dopamine transport capacity.* J Neurosci, 2003. **23**(24): p. 8480-8.

71. Lin, Z., et al., *Phosphatidylinositol 3-kinase, protein kinase C, and MEK1/2 kinase regulation of dopamine transporters (DAT) require N-terminal DAT phosphoacceptor sites.* J Biol Chem, 2003. **278**(22): p. 20162-70.

72. Foster, J.D., et al., *Dopamine transporters are dephosphorylated in striatal homogenates and in vitro by protein phosphatase 1.* Brain Res Mol Brain Res, 2003. **110**(1): p. 100-8.

73. Lee, K.H., et al., *Syntaxin 1A and receptor for activated C kinase interact with the N-terminal region of human dopamine transporter.* Neurochem Res, 2004. **29**(7): p. 1405-9.

74. Johnson, L.A., et al., *Regulation of amphetamine-stimulated dopamine efflux by protein kinase C beta.* J Biol Chem, 2005. **280**(12): p. 10914-9.

75. Bauman, A.L., et al., *Cocaine and antidepressant-sensitive biogenic amine transporters exist in regulated complexes with protein phosphatase 2A.* J Neurosci, 2000. **20**(20): p. 7571-8.

76. Carneiro, A.M. and R.D. Blakely, *Serotonin-, protein kinase C-, and Hic-5-associated redistribution of the platelet serotonin transporter.* J Biol Chem, 2006. **281**(34): p. 24769-80.

77. Ohno, K., et al., *The neuronal glycine transporter 2 interacts with the PDZ domain protein syntenin-1.* Mol Cell Neurosci, 2004. **26**(4): p. 518-29.

78. Sung, U., et al., *A regulated interaction of syntaxin 1A with the antidepressant-sensitive norepinephrine transporter establishes catecholamine clearance capacity.* J Neurosci, 2003. **23**(5): p. 1697-709.

79. Deken, S.L., et al., *Transport rates of GABA transporters: regulation by the N-terminal domain and syntaxin 1A.* Nat Neurosci, 2000. **3**(10): p. 998-1003.

80. Quick, M.W., *Substrates regulate gamma-aminobutyric acid transporters in a syntaxin 1A-dependent manner.* Proc Natl Acad Sci U S A, 2002. **99**(8): p. 5686-91.

81. Chi, L. and M.E. Reith, *Substrate-induced trafficking of the dopamine transporter in heterologously expressing cells and in rat striatal synaptosomal preparations.* J Pharmacol Exp Ther, 2003. **307**(2): p. 729-36.

82. Saunders, C., et al., *Amphetamine-induced loss of human dopamine transporter activity: an internalization-dependent and cocaine-sensitive mechanism.* Proc Natl Acad Sci U S A, 2000. **97**(12): p. 6850-5.

83. Sandoval, V., et al., *Methamphetamine-induced rapid and reversible changes in dopamine transporter function: an in vitro model.* J Neurosci, 2001. **21**(4): p. 1413-9.

84. Kantor, L. and M.E. Gnegy, *Protein kinase C inhibitors block amphetamine-mediated dopamine release in rat striatal slices.* J Pharmacol Exp Ther, 1998. **284**(2): p. 592-8.

85. Cervinski, M.A., J.D. Foster, and R.A. Vaughan, *Psychoactive substrates stimulate dopamine transporter phosphorylation and down-regulation by cocaine-sensitive and protein kinase C-dependent mechanisms.* J Biol Chem, 2005. **280**(49): p. 40442-9.

86. Kantor, L., G.H. Hewlett, and M.E. Gnegy, *Enhanced amphetamine- and K+-mediated dopamine release in rat striatum after repeated amphetamine: differential requirements for Ca2+- and calmodulin-dependent phosphorylation and synaptic vesicles.* J Neurosci, 1999. **19**(10): p. 3801-8.

87. Daws, L.C., et al., *Cocaine increases dopamine uptake and cell surface expression of dopamine transporters.* Biochem Biophys Res Commun, 2002. **290**(5): p. 1545-50.

88. Cowell, R.M., et al., *Dopamine transporter antagonists block phorbol ester-induced dopamine release and dopamine transporter phosphorylation in striatal synaptosomes.* Eur J Pharmacol, 2000. **389**(1): p. 59-65.

89. Gaffaney, J.D. and R.A. Vaughan, *Uptake inhibitors but not substrates induce protease resistance in extracellular loop two of the dopamine transporter.* Mol Pharmacol, 2004. **65**(3): p. 692-701.

90. Vaughan, R.A. and M.J. Kuhar, *Dopamine transporter ligand binding domains. Structural and functional properties revealed by limited proteolysis.* J Biol Chem, 1996. **271**(35): p. 21672-80.

91. Boyle, W.J., P. van der Geer, and T. Hunter, *Phosphopeptide mapping and phosphoamino acid analysis by two-dimensional separation on thin-layer cellulose plates.* Methods Enzymol, 1991. **201**: p. 110-49.

92. Ramamoorthy, S. and R.D. Blakely, *Phosphorylation and sequestration of serotonin transporters differentially modulated by psychostimulants.* Science, 1999. **285**(5428): p. 763-6.

93. Daniels, G.M. and S.G. Amara, *Regulated trafficking of the human dopamine transporter. Clathrin-mediated internalization and lysosomal*

degradation in response to phorbol esters. J Biol Chem, 1999. **274**(50): p. 35794-801.

94. Nowicki, S., et al., *Dopamine-induced translocation of protein kinase C isoforms visualized in renal epithelial cells.* Am J Physiol Cell Physiol, 2000. **279**(6): p. C1812-8.

95. Melikian, H.E. and K.M. Buckley, *Membrane trafficking regulates the activity of the human dopamine transporter.* J Neurosci, 1999. **19**(18): p. 7699-710.

96. Blume-Jensen, P. and T. Hunter, *Oncogenic kinase signalling.* Nature, 2001. **411**(6835): p. 355-65.

97. Lu, K.P., *Pinning down cell signaling, cancer and Alzheimer's disease.* Trends Biochem Sci, 2004. **29**(4): p. 200-9.

98. Mansour, S.J., et al., *Transformation of mammalian cells by constitutively active MAP kinase kinase.* Science, 1994. **265**(5174): p. 966-70.

99. Hoover, B.R., et al., *Rapid regulation of dopamine transporters by tyrosine kinases in rat neuronal preparations.* J Neurochem, 2007. **101**(5): p. 1258-71.

100. Jayanthi, L.D., et al., *Evidence for biphasic effects of protein kinase C on serotonin transporter function, endocytosis, and phosphorylation.* Mol Pharmacol, 2005. **67**(6): p. 2077-87.

101. Loder, M.K. and H.E. Melikian, *The dopamine transporter constitutively internalizes and recycles in a protein kinase C-regulated manner in stably transfected PC12 cell lines.* J Biol Chem, 2003. **278**(24): p. 22168-74.

102. Vaughan, R.A., *Regulation of the dopamine transporters by phosphorylation and impact on cocaine action. Regulation of dopamine transporter by phosphorylation and impact on cocaine action.* Cerebral Signal Transduction: From First to Fourth Messengers, Humana Press, Totowa, NJ 2000: p. 375-400.

103. Laruelle, M., M. Slifstein, and Y. Huang, *Positron emission tomography: imaging and quantification of neurotransporter availability.* Methods, 2002. **27**(3): p. 287-99.

104. Ukairo, O.T., et al., *Recognition of benztropine by the dopamine transporter (DAT) differs from that of the classical dopamine uptake inhibitors cocaine, methylphenidate, and mazindol as a function of a DAT*

transmembrane 1 aspartic acid residue. J Pharmacol Exp Ther, 2005. **314**(2): p. 575-83.

105. Desai, R.I., et al., *Relationship between in vivo occupancy at the dopamine transporter and behavioral effects of cocaine, GBR 12909 [1-{2-[bis-(4-fluorophenyl)methoxy]ethyl}-4-(3-phenylpropyl)piperazine], and benztropine analogs.* J Pharmacol Exp Ther, 2005. **315**(1): p. 397-404.

106. Chen, N. and M.E. Reith, *Structure and function of the dopamine transporter.* Eur J Pharmacol, 2000. **405**(1-3): p. 329-39.

107. Bernstein, E.M. and M.W. Quick, *Regulation of gamma-aminobutyric acid (GABA) transporters by extracellular GABA.* J Biol Chem, 1999. **274**(2): p. 889-95.

108. Zhou, X.Z., et al., *Pin1-dependent prolyl isomerization regulates dephosphorylation of Cdc25C and tau proteins.* Mol Cell, 2000. **6**(4): p. 873-83.

109. Lu, P.J., et al., *The prolyl isomerase Pin1 restores the function of Alzheimer-associated phosphorylated tau protein.* Nature, 1999. **399**(6738): p. 784-8.

110. Davis, R.J., *The mitogen-activated protein kinase signal transduction pathway.* J Biol Chem, 1993. **268**(20): p. 14553-6.

111. Songyang, Z., et al., *A structural basis for substrate specificities of protein Ser/Thr kinases: primary sequence preference of casein kinases I and II, NIMA, phosphorylase kinase, calmodulin-dependent kinase II, CDK5, and Erk1.* Mol Cell Biol, 1996. **16**(11): p. 6486-93.

112. Jayanthi, L.D., et al., *Phosphorylation of the norepinephrine transporter at threonine 258 and serine 259 is linked to protein kinase C-mediated transporter internalization.* J Biol Chem, 2006. **281**(33): p. 23326-40.

113. Ramamoorthy, S., et al., *Phosphorylation of threonine residue 276 is required for acute regulation of serotonin transporter by cyclic GMP.* J Biol Chem, 2007. **282**(16): p. 11639-47.

114. Johnson, G.L. and R. Lapadat, *Mitogen-activated protein kinase pathways mediated by ERK, JNK, and p38 protein kinases.* Science, 2002. **298**(5600): p. 1911-2.

115. Caunt, C.J., et al., *Seven-transmembrane receptor signalling and ERK compartmentalization.* Trends Endocrinol Metab, 2006. **17**(7): p. 276-83.

116. Schrader, L.A., et al., *ERK/MAPK regulates the Kv4.2 potassium channel by direct phosphorylation of the pore-forming subunit.* Am J Physiol Cell Physiol, 2006. **290**(3): p. C852-61.

117. Warn-Cramer, B.J., et al., *Regulation of connexin-43 gap junctional intercellular communication by mitogen-activated protein kinase.* J Biol Chem, 1998. **273**(15): p. 9188-96.